



Room 14-0551  
77 Massachusetts Avenue  
Cambridge, MA 02139  
Ph: 617.253.5668 Fax: 617.253.1690  
Email: docs@mit.edu  
<http://libraries.mit.edu/docs>

## **DISCLAIMER OF QUALITY**

Due to the condition of the original material, there are unavoidable flaws in this reproduction. We have made every effort possible to provide you with the best copy available. If you are dissatisfied with this product and find it unusable, please contact Document Services as soon as possible.

Thank you.

**Some pages in the original document contain pictures, graphics, or text that is illegible.**

**RAPID DETERMINATION OF ANTIMICROBIAL SUSCEPTIBILITY  
USING GEL MICRODROPLETS AND FLOW CYTOMETRY**

*by*

Jonathan G. Bliss

B.S. Electrical Engineering, Northeastern University, 1979

M.S. Electrical Engineering, Massachusetts Institute of Technology, 1986

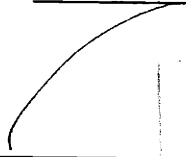
Submitted to the Department of  
Medical Engineering / Medical Physics  
Harvard - M.I.T. Division of Health Sciences & Technology  
in partial fulfillment of the requirements for degree of

Doctor of Philosophy


at the  
Massachusetts Institute of Technology  
October 22, 1990

© Massachusetts Institute of Technology, 1990. All rights reserved.


Signature of Author

  
\_\_\_\_\_  
*Harvard-MIT Division of Health Sciences & Technology*  
*October 22, 1990*

Certified by

  
\_\_\_\_\_  
*James C. Weaver*  
*Principal Research Scientist*  
*Harvard-MIT Division of Health Sciences & Technology*  
*Thesis Supervisor*

Accepted by

  
\_\_\_\_\_  
*Roger G. Mark*  
*Chairman, Departmental Graduate Committee*  
*Harvard-MIT Division of Health Sciences & Technology*

MASSACHUSETTS INSTITUTE OF TECHNOLOGY

NOV 08 1990

LIBRARIES

# RAPID DETERMINATION OF ANTIMICROBIAL SUSCEPTIBILITY USING GEL MICRODROPLETS AND FLOW CYTOMETRY

by

Jonathan G. Bliss

Submitted to the Department of Medical Engineering / Medical Physics  
on October 22, 1990, in partial fulfillment of  
requirements for the degree of Doctor of Philosophy in  
Medical Engineering

## Abstract:

This goal of this thesis is to develop and evaluate a new technology for antibiotic testing, based on culture of microorganisms in small (<50  $\mu\text{m}$  diameter) agarose particles called gel microdroplets (GMDs). Currently available clinical technologies are severely rate-limited by a requisite pre-culture step, which serves to isolate pure strains from the clinical specimen, but which typically takes 12 to 24 hours. The GMD-based method is unique in its potential to obviate the pre-culture step, and thus deliver timely results. The method, in many ways a miniaturization of standard, accepted methods, is as follows:

- GMDs are used to isolate and contain individual cells or colony-forming-units (CFUs) from a cell suspension. If the suspension is polymicrobial, GMD preparation serves to isolate pure strains, in a matter of minutes.
- Upon incubation, clonal growth leads to formation of a microcolony within each GMD occupied by a viable and growing CFU. In the presence of an antimicrobial agent, microcolony growth from susceptible CFUs is either partially or completely inhibited.
- Fluorescent staining of indicator biomaterials, combined with flow cytometric analysis, permits the rapid measurement of biomass in a large number of GMD microcolonies. Biomass measurement before and after incubation forms the basis of a GMD-based growth assay, and when performed in the presence of an antimicrobial agent, permits the quantitation of growth inhibition.

For susceptible organisms, a serial drug dilution method allows the determination of the minimum inhibitory concentration (MIC), *i.e.* the minimum drug level which completely inhibits growth over the incubation period. In the clinical setting, the MIC guides antibiotic therapy in the treatment of infection.

In this thesis, a model system consisting of the yeast *C.utilis*, and the antifungal agent, Amphotericin-B, was used to develop, demonstrate and assess the GMD-based method. The gold-standard method of broth macro-dilution was used to establish a reference MIC for the drug-organism pair, and optical density measurements were used as a quantitative reference method. Experimental results demonstrated the ability to measure growth of *C. utilis* microcolonies in GMDs, and to quantify growth inhibition in the presence of Amphotericin-B. From these results, a GMD-based MIC was determined, which was found to be in excellent agreement with the gold-standard MIC. Working from a pure culture, the result was obtained after 4 hours of incubation, *vs.* the 24 to 48 hours recommended for conventional methods. The time required to isolate pure strains was approximately 0.3 hours for the GMD method, *vs.* 24 to 48 hours (typical) for conventional plating of yeast.

## Acknowledgements

A number of years ago, I was fortunate enough to take an HST course titled "Medical Engineering Measurements". One day, the instructor introduced us to some rather non-traditional ideas for measuring biological activity, based on the concept of small volume elements. I was very intrigued with the ideas, and impressed by the enthusiasm with which they were described. Imagine my delight when, a few months later, that instructor asked if I was interested in helping to nurse those ideas into reality. The rest of the story, or at least part of it, is contained in the chapters of this thesis. I am forever indebted to "that instructor", Jim Weaver, for inviting me along on this adventure, and for his guidance, patience, and friendship over its duration.

I also thank my committee members, Professors William Siebert and Arnie Demain, for their guidance and support, as well as reading this document on short notice. Thankfully, our conversations were not limited to the research project at hand, but covered such topics as what to do if attacked by bears, and even scarier, what to expect in pursuing a scientific career in the 1990's and beyond.

I was fortunate to be accompanied on this adventure by three friends: Drs. Greg Williams, Gail Harrison, and Kevin Powell. Greg and Gail were somehow able to teach me hands-on microbiology, and were instrumental in the earliest proof-of-principle experiments underlying this thesis work. Gail also proofread the bulk of this thesis, identifying the order-of-magnitude errors while I wrestled with syntax. With Kevin, I shared many stimulating hours discussing flow cytometers, instrumentation, and data analysis software. I will remember with great fondness the heady times when, with the four of us working in the laboratory, so many proposed GMD methods went from concept to reality.

I am also happy to acknowledge the support and guidance of the faculty of the Harvard-MIT Division of Health Sciences and Technology. I especially thank the co-director, Professor Roger Mark, who encouraged me in most uncertain terms to finish this work.

Many thanks also to the staff and students at the Biomedical Engineering Center, especially Dr. Stephen Burns, who was "instrumental" in the design of the Data Acquisition System used for this thesis work, and well as Ken Szajda and Peter Roman, who aided immensely in its instantiation. Also, thanks to Steven Dyer, for his assistance in assembling the software and hardware used in producing this document. Thanks also to *emeritus* members of the BMEC, Paul Albrecht, Deb Burstein, and Joe Smith, for their unflagging moral support over the years, and for cheering me on during my thesis defense.

Financial support for this work was provided by the Army Research Office (Contract DAAG29-85-K-0241) and the National Institutes of Health (GM34077). The Ortho flow cytometer used was purchased under the DoD-University Research Instrumentation Program (Grant DAAG29-84-G-0066).

An undertaking such as this could not be completed without a support network. Mine was anchored by a loving God, manifested not only as Sustainer, but as Revealer and Revealed throughout these years. I am also eternally indebted to my family, and especially my parents Philip ('37) and Ruth Bliss, for their support in this endeavor, waiting patiently for the completion of my education. Even the staunchest Red Sox fans have not experienced "Well, there's always *next* year" to the extent my parents have. Moreover, the patient meticulousness and stubborn determination that I learned as a child from my parents has cer-



tainly contributed to my ability to complete this work. I also wish to thank Professors George Ball and Richard Dingle, and (imminently Dr.) Carrie Farrell, three friends who independently, convincingly, and with critical timing, uttered those three little words that doctoral students occasionally need to hear: "Don't quit now".

### Dedication

In my Master's thesis, I acknowledged "my friend Kristine, ... an endless source of love, hope and perhaps most importantly, perspective". That statement is no less true today than it was then, though it doesn't begin to express my love and respect for this remarkable person. With the quiet determination that is her trademark, she has endured my doctoral student life, and supported me in my efforts to bring it to a close. I hope that I am able, with time, to fully express my gratitude for her nurturing and healing ways, for keeping me whole. I suspect that getting her a dog or two would go a long way in this regard. For now, I can only offer this, my humble dedication: to my wife, Kristine.

### Biographical Notes

Born in New Britain, CT, December 30, 1956, and raised in Newington, CT.

Attended Northeastern University, Boston, MA. BS degree in Electrical Engineering, 1979. Awards include: Harold D. Hodgkinson Award (top senior), Laurence F. Cleveland Award (top EE senior), Tau Beta Pi (NU chapter president 1978-9).

1980-82: Research Associate, Division of Nuclear Medicine, Beth Israel Hospital, Boston

1983-85: Research Associate, MIT Artificial Intelligence Laboratory. Master's thesis, under Professor Tomaso Poggio: "Velocity-tuned Filters for Spatio-temporal Interpolation".

1986-90: Research Associate, MIT Biomedical Engineering Center for Clinical Instrumentation. Doctoral thesis under Dr. James C. Weaver.

Weaver, J., J.Bliss, K.Powell, G.Harrison, G.Williams "*Clonal Growth Measurements at the Single-Cell Level Using Flow Cytometry and Gel Microdroplets*" (submitted).

Williams, G., S.Threefoot, J.Lorenz, J.Bliss, J.Weaver, A. Demain (1987) "*Rapid Detection of E. Coli Immobilized in Gel Microdroplets*", Ann. NY Acad. Sci. 501, 350-353.

Bliss, J., G.Harrison, J.Mourant, K.Powell, J.Weaver (1988) "*Electroporation: The Population Distribution of Macromolecular Uptake and Shape Changes in Red Blood Cells Due to a Single 50μsecond Pulse*" Bioelectrochem. Bioenerget. 19, 57-71.

Weaver, J., J.Bliss, G.Harrison, J.Mourant, K.Powell (1987) "*Electroporation in Individual Cells: Measurements Using Light Scattering and Fluorescence by Flow Cytometry*", Proc. IEEE/EMB

Bliss, J. (1986) "*Velocity-Tuned Filters for Spatio-Temporal Interpolation*" Proc. IEEE Workshop on Motion.

Bliss, J., J.Parker, H.Royal, R.Uren, G.Kolodny (1982) "*All Digital Nuclear Medicine Department: Interprocessor Communications*" in Digital Imaging: Clinical Advances in Nuclear Medicine. Soc. Nuc. Med.

---

## TABLE OF CONTENTS

---

<b>Chapter 1 Introduction</b>	<b>11</b>
Section 1.1: Introduction to the Problem	12
Costs of Susceptibility Uncertainty	
Research Goals	
Section 1.2: The Clinical Scenario	16
1.2.1: Identification vs. Susceptibility	17
Section 1.3: Susceptibility Testing: Overview	18
1.3.1: Susceptibility Testing: Current Methods	20
1.3.2: Standard Protocols	20
Broth Macrodilution	
Broth Microdilution	
Agar Dilution	
Disc Diffusion Test	
Incubation Time	
Inoculation Density	
Preculture	
1.3.3: Susceptibility Testing for Antifungal Agents	26
1.3.4: Automated Methods for Susceptibility Testing	27
The Vitek System	
1.3.5: Future Methods for Susceptibility Testing	30
1.3.6: Summary	33
Section 1.4: GMD-based Growth Assay	34
1.4.1: Growth, and the Measurement Thereof	35
1.4.2: GMD-based Growth Assay: Expected Results	36
Biomass Distributions: Log Histograms	
Log Histograms and Exponential Growth	
Life Cycle of Cell Suspensions	
Section 1.5: Summary	45
 <b>Chapter 2 Description of Methods</b>	 <b>47</b>
Section 2.1: Gel Entrapment and Culture of Cells	47
2.1.1: Existing Technology: Gel Macrodroplets	48
2.1.2: A New Technology: Gel Microdroplets	49
2.1.3: Diffusion in Spherical Geometries	50
Culture in Droplets: Geometric Advantage	
Culture in Microdroplets: Size Advantage	
2.1.4: Gels and Their Properties	55

2.1.5: Review of Gels for Cell Immobilization .....	56
Comparison of Gels : Strength and Stability	
Comparison of Gels: Viability and Molecular Transport	
2.1.6: Immobilization Methods .....	66
Comparison of Methods	
2.1.7: Gel Microdroplets: Summary and Protocol Overview .....	69
Section 2.2: Flow Cytometry .....	71
2.2.1: Principles of Flow Cytometry .....	72
The Flow Cell	
Hydrodynamic Focusing	
Sample Illumination	
Flow Cuvette	
Sorting	
Physical Dimensions for the System Used	
2.2.2: Optical Subsystem .....	78
2.2.3: Electrical Subsystem .....	81
Section 2.4: Flow Cytometry and GMDs .....	82
2.4.1: Triggering on GMDs .....	84
2.4.2: GMD Flow Cytometry and Fluorescent Stains .....	85
2.4.3: Fluorescent Labels for Nucleic Acids: Propidium Iodide .....	90
2.4.4: Fluorescent Stain for Proteins: FITC .....	93
Section 2.5: Summary .....	94
<b>Chapter 3 Growth Experiments</b> .....	<b>96</b>
Optical Density as Reference Method	
Physical Basis for Optical Density Measurements	
Section 3.1: Macroscopic Growth Measurement: Optical Density .....	99
Protocol 3.1	
Results	
Section 3.2: Measurement of Growth by GMD-based Growth Assay .....	101
Protocol 3.2	
Results	
Section 3.3: Discussion .....	106
3.3.1: Comparison of Growth Assay Results .....	106
3.3.2: Microcolony Break-out .....	108
Specific Labeling of GMDs	
3.3.3: Cell Viability in GMDs .....	111
Section 3.4: Measurement of Growth Inhibition by Optical Density .....	114
Protocol 3.3	
Results	
Section 3.5: Measurement of Growth Inhibition by GMD Assay .....	117
Protocol 3.4	
Results	
Cell Viability Revisited	
Section 3.6: Discussion and Comparison of Assays .....	123
Section 3.7: Summary .....	125

<b>Chapter 4 Susceptibility Experiments</b>	127
Section 4.1: Macroscopic MIC determination: Turbidity	127
Protocol 4.1	
Results	
Protocol Variances	
Section 4.2: GMD-based MIC determination	132
Protocol 4.2	
Results	
Discussion	
4.2.1: The Dose-Response Curve: Deriving an MIC	136
Optical Density Dose-Response Curve: 4 Hours	
Optical Density Dose-Response Curve: Evolution	
The Effect of Inoculation Density	
Section 4.3: Summary	143
 <b>Chapter 5 Discussion &amp; Conclusion</b>	 145
Section 5.1: Statistical Inoculation	145
5.1.1: Cell Density From Occupation Statistics	148
5.1.2: Poisson Assumptions: Modified Poisson Statistics	149
Section 5.2: A Demonstration of Strain Isolation: Photomicroscopy	150
Method	
Plate 1	
Plate 2	
Plate 3	
Section 5.3: Sample Size Requirements for GMD Assays	156
5.3.1: A Glimpse of a Clinical Instrument	161
Incubation Time	
Test Result Reading Time	
Section 5.4: Conclusion	164
5.4.1: Towards a Clinically Useful Technology	165
 <b>Appendix A Protocol for GMD Preparation</b>	 169
Section A.1: Introduction	169
Section A.2: Overview of Protocol	170
Section A.3: Detailed GMD protocol	171
General Preparation	
Preparation of Gel	
Inoculation of Gel	
Formation and Gelation of Liquid Microdroplets	
Recovery of Gel Microdroplets	
Fixing Samples	
GMD sieving	
Section A.4: Materials	178
Sieve Apparatus	
Other Devices	

<b>Appendix B</b>	<b>DAS: The Data Acquisition System</b>	<b>180</b>
Section B.1:	Introduction	180
	DAS Functional Specification	
Section B.2:	Functional Description	182
B.2.1:	Pulse Feature Sampling	182
B.2.2:	Pulse Detection and Integrator Control	183
B.2.3:	Dual-threshold Trigger Scheme	185
B.2.4:	DAS Hardware Overview	187
B.2.5:	DAS Software Overview: AQ	188
Section B.3:	DAS Interface Details	188
B.3.1:	Trigger and Control Circuit	189
	Trigger Operation: Valid Pulse	
	Trigger Operation: Noise Pulse	
	System Dead-time	
	Propagation Delay	
B.3.2:	Integrate and Hold Circuit	195
	Components	
	Signals Received	
	Signals Generated	
	Integrator Operation: Valid Pulse	
	Integrator Operation: Noise Pulse	
	Integrator Performance	
	Integrator Droop	
	Sample and Hold	
	FET Reset Switch	
	FET Drive Circuit	
	Charge Dumping	
B.3.3:	Multiplex and Digital Converter Circuit	202
	Components	
	Signals Received	
	Signals Generated	
	Multiplexer and Digitizer Circuit: Operation	
	ADC Performance	
	DMA performance	
	Multiplexer Performance	
Section B.4:	DAS Software Overview	207
B.4.1:	Data Acquisition Module	208
B.4.2:	Data Display Module	208
B.4.3:	Data Storage Module	209
Section B.5:	DAS Software - Details	210
B.5.1:	AQ Top-level	210
B.5.2:	AQ Interaction with DMA	212
B.5.3:	AQ Source Code	214
B.5.4:	80186 Timer	218
<b>Appendix C</b>	<b>Media &amp; Apparatus</b>	<b>220</b>
<b>Appendix D</b>	<b>The Diffusion Equation</b>	<b>223</b>

---

## LIST OF FIGURES AND TABLES

---

<b>Chapter 1</b>	<b>Introduction</b>	11
	Figure 1.1 Schematic view of GMD-based growth assay	38
<b>Chapter 2</b>	<b>Description of Methods</b>	47
	Figure 2.1 Concentration profile evolution in spherical geometry	52
	Table 2.1 Diffusion times ( $T=r^2/D$ ) in 80 $\mu\text{m}$ GMD vs 1mm droplet	54
	Figure 2.2 The Agarobiose Dimer	57
	Figure 2.3 Agarobiose with sulfate ester	58
	Table 2.2 Properties of 2½ % agarose gels	59
	Table 2.3 Gel prices, dollars per kilogram.	60
	Figure 2.4 Ortho flow cell (schematic representation)	73
	Figure 2.5 Optical Subsystem of Ortho Cytofluorograph	79
	Figure 2.6 Flow cytometry of a GMD sample	83
	Figure 2.7 Diffusion of Free Dye Out of GMDs	88
<b>Chapter 3</b>	<b>Growth Experiments</b>	96
	Figure 3.1 Growth of <i>C. utilis</i> , by optical density measurements	101
	Figure 3.2 Growth of <i>C. utilis</i> in GMDs, by flow cytometry	104
	Figure 3.3 Growth of <i>C. utilis</i> in GMDs: mean log{RF} vs. time	106
	Figure 3.4 Sub-population estimation by curve-fitting	112
	Figure 3.5 Growth Inhibition of <i>C. utilis</i> by Amphotericin-B: Optical density	116
	Figure 3.6 Growth inhibition of <i>C. utilis</i> by Amphotericin-B : GMD assay	119
	Figure 3.7 <i>C. utilis</i> in GMDs, plus Amphotericin-B: mean log{RF} vs. time	121
<b>Chapter 4</b>	<b>Susceptibility Experiments</b>	127
	Figure 4.1 Susceptibility assay: optical density vs. visual scoring	130
	Figure 4.2 Susceptibility assay: GMD-based assay	134
	Figure 4.3 Dose-response curve for GMD-based MIC assay	137
	Figure 4.4 Dose-response curve for OD-based MIC assay, at 4 hours	138
	Figure 4.5 Evolution of Dose-response curve for OD-based MIC assay	140
<b>Appendix A</b>	<b>Protocol for GMD Preparation</b>	169
	Figure A.1 Schematic view of dispersion protocol for GMDs	171
	Figure A.2 Sieve device to recover GMDs (20 $\mu$ to 44 $\mu$ )	177

<b>Appendix B</b>	<b>DAS: The Data Acquisition System</b>	<b>180</b>
Figure B.1	Single-threshold triggering scheme	184
Figure B.2	Dual threshold triggering scheme	186
Figure B.3	Overview of DAS Hardware	187
Figure B.4	Functional schematic of DAS interface	189
Figure B.5	DAS Trigger and control circuit	190
Figure B.6	DAS integrate-and-hold circuit	195
Figure B.7	DAS multiplexer and digital converter circuit	202
Figure B.8	AQ top-level software control	211
Figure B.9	DAS interface to DMA controller	213
Figure B.10	AQ definitions for DMA controller use	215
Figure B.11	AQ code for initializing DMA controller	216
Figure B.12	AQ code for filling DMA buffer	217
Figure B.13	AQ source code for setting up 50 $\mu$ sec clock	219

*Chapter 1***Introduction**

---

As a child, my mother had polio. Thirty years later, as a child, I was vaccinated, or so I am told. In the 1950's, penicillin was a miracle drug that saved lives, and which represented the hope that modern medicine would free humanity from untimely death. In the 1980's over 40% of the antibiotics produced in this country went into livestock feed<sup>1</sup>. The miraculous has become mundane.

Nevertheless, infectious disease is still with us. Infections still kill, and increasingly, there is concern that the miracle may be short-lived. More than one author of science-fiction has considered the possibilities of biological warfare or of mutant, antibiotic-resistant escapees from some genetics experiment gone awry. The subtle irony is that no mad dictators or sloppy biotechnologists are needed to realize the underlying fear; evolution, time and plasmids may suffice<sup>2</sup>.

Broadly, the subject of this thesis is the treatment of infectious disease. More specifically, it deals with the clinician's need to choose a drug to treat a particular patient with a particular infection. Unfortunately, this has more to do with efficiency of health-care delivery than with freeing humanity from untimely death, but one has to start somewhere. Moreover, as a society, our attitude towards health-care in the foreseeable future seems to be to save lives when it is cost-effective to do so. Ultimately, the method developed in this thesis may both save a few lives, and save money. For at least one of these reasons, this thesis is appropriate for the times.



## Section 1.1: Introduction to the Problem

Optimal clinical management of infectious disease depends on efficient and rapid determination of an effective antimicrobial agent. Once the diagnosis of infection has been made, antibiotic therapy should begin immediately. Unfortunately, to date there has been no method available to the clinician to determine immediately, and with certainty, what drug is effective against a particular infective organism, and what dosage is required. Indeed, due to the length of time required to execute the laboratory tests, this information is unavailable to the clinician for at least 8 hours after the time a clinical specimen is taken; a more typical delay would be 16 to 24 hours, and for some organisms, the delay is several days.

Lacking susceptibility information, the initial choice of drug therapy is made on the basis of such factors as the patient's history, physical findings, Gram stain, clinical experience, and judgement. In some specific cases, very rapid methods, based for example on immunochemistry, may be able to provide essentially immediate information regarding the organism's identity, from which broad inferences about its susceptibility may be made. When susceptibility results finally arrive they are used to confirm or modify the clinician's initial choice. In most cases, the clinician is right. In other cases, the laboratory results disagree with the clinician's choice, but the patient recovers anyway, and the desired endpoint is reached.

### Costs of Susceptibility Uncertainty

However, there are several less satisfactory scenarios, many of which are related in some fashion to the problem of resistance. Specifically, the patient may endure such risks and costs as:

- treatment that is unnecessarily aggressive, or broad-spectrum. Given the uncertainty of the situation, the clinically (and legally) safest route is to treat aggressively, often with two or three wide-spectrum drugs, with the goal of killing or inhibiting every plausible infecting organism. When the

laboratory results arrive, the treatment can be more narrowly tuned accordingly. Frequently, this strategy works, though not always. Additionally, this strategy increases the risk of toxic side-effects, selection for resistant strains, as well as the cost of treatment.

- selection for resistant strains. It is acknowledged that aggressive, wide-spectrum treatment kills not only pathogens, but the non-pathogenic commensal organisms of normal human flora. The remaining organisms, which are resistant by definition, are left to flourish unfettered. This can negatively impact the patient's condition; certainly as important from a global perspective is the continual creation of reservoirs of resistant pathogens, which can then be spread to other patients by various means (*v.i.*). A classic example of this phenomenon is presented as the history of the appearance of resistance, largely in response to the introduction of new antibiotics, in Boston City Hospital over the period 1935-1975<sup>3</sup>.
- unnecessary exposure to drug side-effects. All antibiotics have side-effects, whose risks and severities vary among patients. Unfortunately, the risk of side effects must commonly be traded off with the risk of delivering an ineffective drug. For example, the drug vancomycin fell from favor many year ago due to its high risk of nephrotoxicity; however, it has enjoyed a resurgence in recent years because it is one of the few drugs effective against strains of *S.aureus* which have (recently) developed resistance to both penicillin and its synthetic derivatives such as methycillin. The penicillins are much cheaper and safer, but without knowing for sure that the infective organisms are susceptible, the only safe way to treat a serious *S.aureus* infection is with the riskier vancomycin.
- ineffective treatment. In some cases, the best guess is still incorrect, and the patient receives a drug to which the organism is not susceptible. This is usually evident within a few days, as the patient's condition declines.

- unnecessarily long hospital stay, while awaiting test results. Hospitals are terrible places to be, especially for sick patients. There is a recognized and major risk of nosocomial infection, *i.e.* an infection acquired while hospitalized. A typically cited incidence rate for nosocomial infection is 5 to 10% of hospitalized patients<sup>4</sup>. A common route of infection is *via* the medical staff, who circulate among numerous sick patients, and who make excellent carriers. Contributing to the problem is the common use of in-dwelling catheters and similar devices, which disrupt the body's normal defense mechanisms. Any factor which prolongs the length of hospital stay, including waiting for lab results, or initial treatment with an ineffective drug, increases the chances of nosocomial infection.
- superinfection with a more virulent organism, while hospitalized. As a special case of nosocomial infection, since most garden variety pathogens are killed or inhibited by widespread use of antibiotics in the hospital, there is a selection of resistant organisms. Thus, the patient may present with an easily treatable infection, but pick up a more virulent, resistant infection in the hospital. Again, the best defense is to shorten the hospital stay.
- increased cost to patient and third-party payer. Treatment with multiple, wide-spectrum, intravenous antibiotics can be expensive, especially if it involves the newer drugs, *e.g.* N-th generation cephalosporins, for which resistance is less likely. In addition, each day of hospital stay costs in the neighborhood of \$800, and \$1,000 or more for the intensive care unit. One result of the recent, aggressive attempts to manage health-care costs has been to shorten the length of stay, for exactly this reason.
- unnecessary treatment. One of the major symptoms of infection is fever; unfortunately, the majority of fevers are fevers 'of unknown origin' (FUOs), *i.e.* fevers for which no cause could be found, and especially for which all attempts to culture out an infective organism failed. Unfortunately, in patients who are immunocompromised, infection can be quickly fatal; thus almost any fever will induce

instant, aggressive treatment. In some patients, this might mean hospitalization, surgery to remove an in-dwelling catheter, and treatment with toxic drugs. Immunocompromised patients are also highly susceptible to fungal infections<sup>5</sup>, which are extremely serious; thus the treatment may include the antifungal agent Amphotericin-B, well-known for its toxic side-effects. For the immunocompromised patient who truly has an infection, such intervention can be life-saving; however, for the majority of patients, who are just having a fever, without infection, such intervention is expensive, risky, and aggravating.

### Research Goals

Motivated by the previous considerations, the ultimate goal of this work is to develop a new clinical technology that can provide susceptibility information to the clinician, at the time of initial choice, *i.e.* of antibiotic therapy. If successful, this effort would both improve the care the patient receives, and make it less costly. While the goal seems straightforward enough, it turns out to be technically quite challenging, for reasons that will become apparent momentarily.

The immediate goal, *i.e.* the goal of this thesis, is to develop and evaluate the basis of this new technology, the culture of microorganisms in small (<50  $\mu\text{m}$  diameter) agarose particles called gel microdroplets (GMDs), and the measurement of the microcolonies thus formed. As will be seen, this method is in many ways a hybrid miniaturization of conventional, accepted methods. Yet, by exploiting some simple physical principles, it may well be the enabling technology which makes the ultimate goal attainable.

In the remainder of this chapter, I will first present an overview of current manual and automated methods for susceptibility testing, as well as potential future methods; this will be followed by an introduction to gel microdroplet based methods. In Chapter 2, I will consider in some detail certain key aspects of GMDs and flow

cytometry. Chapters 3 and 4 will present results and discussion for the main experiments of this thesis. The experiments of Chapter 3 demonstrate the ability to culture microorganisms in GMDs, and measure the growth of microcolonies, using flow cytometry. In Chapter 4, a GMD-based susceptibility assay is demonstrated for a yeast-antifungal system. Finally, Chapter 5 will discuss some other pertinent issues, suggesting direction for further work, and conclude the thesis.

## Section 1.2: The clinical scenario

In this section, I will review the typical clinical scenario, primarily as a means of establishing a context for susceptibility testing. When a patient presents in an emergency ward with symptoms of infection, the typical work-up is as follows:

- On the basis of patient history and physical examination, the diagnosis of infection is placed on the top of the list of differential diagnoses.
- On the basis of patient history and physical examination, one or more clinical specimens *e.g.* urine, blood, stool, sputum, is taken and sent to the bacteriology laboratory.
- In the laboratory, the samples are examined microscopically, typically using the Gram stain, or other stains if the situation merits. On the basis of microscopy, a broad categorization is made, *e.g.* Gram-negative rod. This categorization limits the possibilities of identity, and suggests a list of possible antibiotic therapies.
- On the basis of patient history, physical examination, initial laboratory report, clinical judgement, *etc.*, the clinician prescribes an initial antibiotic regimen.
- Meanwhile, back in the laboratory, the clinical specimens are plated onto nutrient-agar plates, or possibly in nutrient broth. The goal is to isolate colonies, representing clonal growth from single organisms, in sufficient numbers for further testing. This testing has two objectives:

(i) to identify the organism, ideally to the species level, and (ii) to determine the organism's susceptibility, *i.e.* to identify one or more drugs, and dosages, which either kill or inhibit growth of the organism. These tests are guided, in particular narrowed in scope, by the initial identity categorization.

- The results of the identification and susceptibility tests are available to the physician as soon as possible, but after a delay that is at least 'overnight', and is more typically 1 to 3 days. On the basis of these results, the antibiotic regimen may be changed.

### 1.2.1: Identification *vs.* Susceptibility

In some cases, knowing an organism's species identity gives its susceptibility as well. Historically, from a clinical perspective, this has been assumed to be true until a resistant strain of the species is identified, or until circumstantial evidence suggests otherwise.

For example, as of 1985, the published, standard recommendations for susceptibility testing state that "routine susceptibility tests are not needed when resistance to the antimicrobial agent of choice, *e.g.* that of *S.pyogenes* to penicillin, has not been described"<sup>6</sup>. Such policies are guided by considerations of cost and efficiency; there is the recognized risk that the first described case may be the patient currently being treated, and that the resistance may only be suspected by the patient's failure to respond to the drug regimen used. Such a policy also requires a certain vigilance, *i.e.* constant contact with the literature, to be aware of newly identified resistance. Of course, changing a testing policy requires a health-care management decision, where the relative risks and costs of missing a rare resistant organism are weighed against the cost of expanded routine testing.

The standard method for identification is to incubate a standard inoculum of the isolated organism (*v.i.*) in the presence of different carbohydrate sources, different enzymatic substrates, *etc.*, and include some indicator substance to signal a positive

response, such as a pH-sensitive dye. These methods tend to require on order of 24 hours, though in some cases useful results can be obtained in as little as 5 hours; unfortunately, the isolation step adds at least an overnight delay to the total testing time (*v.i.*). They are also readily amenable to automation, contributing to their attractiveness. One automated method, the Vitek (*v.i.*), can return identification results in as little as 4 hours, depending on the species. Of course, even in these cases, the pre-culture step delays the result by at least 12 hours. In a few cases, identity can be rapidly determined with either immunological methods, *e.g.* agglutination tests, or with DNA-probes (*v.i.*). In the future, further development of clinical applications for these technologies are anticipated.

The methods developed and discussed in this thesis are not concerned with identification, although there is reason to believe that many of the tests of identity could be miniaturized and adapted to GMD technology. In particular, it is expected that fluorescently-labeled DNA-probes<sup>7</sup> and monoclonal antibodies will be crucial to the application of GMD methods to mixed-species clinical specimens, by providing an 'identity' signal which can be simultaneously measured with the growth signal derived from the GMD growth assay.

My personal view, shared by some<sup>8</sup>, is that from an economic and legal perspective, as well as from the perspective of the patient's welfare, obtaining susceptibility information should have the highest priority. Identity information *is* important; *e.g.* it is critical to know what pathogens are showing up in the hospital and community, but a few days' delay in obtaining that information is tolerable.

### Section 1.3: Susceptibility Testing: Overview

In this section, I will review the goals and current methods of antimicrobial susceptibility testing. My purpose is to define the problem and the desired results, so that we can assess whether GMD-based methods are suitable to the task. I will also list

some of the well-recognized shortcomings of current methods, with the expectation of asking whether the GMD method is able to provide superior performance.

In the most common clinical scenario, the result of susceptibility testing is essentially binary. The question to be answered is: does a candidate drug inhibit growth of a particular organism at the concentrations which are typically achieved in the patient, given a standard drug dose schedule, *e.g.* as specified by the manufacturer. A variant of this question admits the possibility of using maximum safe dosages, or includes pertinent factors such as the high drug levels found in urine due to the concentrating effect of the kidneys. These questions are addressed by methods which deliver categorical results *i.e.* which place the organism in one of a small number of categories:

- susceptible: the organism is inhibited by typical drug levels.
- moderately susceptible: the organism is susceptible, but requires the maximum safe dosage.
- conditionally susceptible: the organism is susceptible, but only if the infection is located in a place where the drug is concentrated, *e.g.* the urinary bladder.
- resistant: the organism is not inhibited by any drug level that is safe and attainable.

The primary example of this approach is the disk diffusion test (*v.i.*). Newer methods, which at some point do derive more quantitative results, incorporate some mechanism, typically a computer program, for translating the result into a category. In a sense, an absolute MIC is less useful on a routine basis, because it requires, at minimum, knowing and remembering the typical and attainable serum drug levels for each of the antibiotics.



### 1.3.1: Susceptibility Testing: Current Methods

In this section, I will review the three general, currently used methods for susceptibility testing. In summary form, they are:

- disk diffusion: the organism is cultured on nutrient agar, onto which disks, impregnated with a standard amount of a candidate drug, are placed. The drug diffuses out of the disk creating a local drug concentration gradient in the agar.
- broth dilution: the organism is cultured in aliquots of nutrient broth, into which various amounts of a candidate drug have been mixed.
- agar dilution: the organism is cultured on the surface of agar plates, into which nutrient broth and various amounts of a candidate drug have been mixed.

The dilution methods are gold-standards by which MICs can be quantitatively determined. Agar dilution is reported to give somewhat better reproducibility than broth dilution<sup>9</sup>. The disk diffusion method delivers categorical or limited quantitative results, which are sufficient for the majority of clinical management decisions. As will be evident, the disc diffusion test is much less labor-intensive, and thus cheaper than the dilution methods; thus it has reigned in the clinical laboratory, at least until recently. Broth methods have enjoyed a recent resurgence in popularity, incarnated in the form of microdilution methods. These methods are very amenable to automation, thus holding the potential for the best of both worlds: quantitative results cheaply and easily.

### 1.3.2: Standard Protocols

In this section, I will summarize the standard antimicrobial susceptibility testing protocols currently approved for clinical use. The standard protocols were developed and published by the National Committee for Clinical Laboratory Standards (NCCLS), in an attempt to standardize clinical testing methods. Among other

benefits, having standard methods makes it reasonable to correlate susceptibility results to clinical findings, to compare methods to each other, and to modify standards as deemed appropriate by the community. My purpose here is not to present the technical details, but to introduce the methods, as a background for discussing their strengths and shortcomings, and for comparison of GMD-based protocols and results.

### **Broth Macrodilution**

- a series of test tubes is prepared, each containing a 1 ml mixture of nutrient broth and the candidate drug. By the method of serial dilutions or equivalent, the tubes are prepared so that the drug concentrations decrease by factors of two, from the highest desired concentration, *i.e.* the highest concentration achievable or reasonable in the patient.
- To each of the sample tubes, a 1 ml inoculum containing  $\sim 1-10 \times 10^5$  CFUs is added, (final density:  $\sim 0.5-5 \times 10^5$  CFUs/ml), and incubated.
- After incubation, the tubes are scored for visible growth. The MIC is defined as the minimum drug concentration which inhibits visible growth, *i.e.* turbidity, in the tube, with a "very faint haziness or a small button of possible growth generally disregarded"<sup>10</sup>.

### **Broth Microdilution**

- A series of drug dilutions is prepared as above, except that the final volume of broth, drug and inoculum adds up to 0.1 ml. Typically, this is done in a 96-well microtiter tray, taking advantage of their relative cheapness, and the availability of small-volume handling devices developed for serology.
- Each well is inoculated with  $\sim 50,000$  CFUs, (final concentration of  $5 \times 10^5$  CFUs/ml), and incubated.
- the MIC is defined as the minimum concentration which inhibits visible

growth in the wells, where the criterion for growth is "a definite turbidity, a single sedimented button 2 mm or larger, or more than one button"<sup>10</sup>. For some drugs, this cutoff is not very sharply defined.

One factor that contributes greatly to the popularity of this method is the commercial availability of prepared trays, containing either frozen broth/drug mixtures, or lyophilized mixtures that require only rehydration. Clearly, this reduces one source of technical error in performing the test. The latest advance in automation has been devices which opto-electronically 'read' the trays after incubation.

### **Agar Dilution**

- A series of agar plates is prepared, each with various amounts of the candidate drug, usually in the form of two-fold serial dilutions.
- Each plate receives replicate inocula of 1 to 2  $\mu\text{l}$ , on order of 10,000 CFU each, and each to a spot 5 to 8 mm in diameter.
- the MIC is defined as the minimum concentration which inhibits visible growth in the spots, with a "very fine, barely visible haze, or single colony disregarded"<sup>9</sup>.

### **Disc Diffusion Test**

- A standard inoculum is prepared, having a final density of about  $10^8$  CFU/ml. The inoculum is spread, using a Q-tip, over the entire surface of a nutrient agar plate.
- Within 15 minutes, antibiotic disks are applied to the agar plate. These disks, which are ~7 mm in diameter, are impregnated with a standard amount of a candidate drug; this amount is chosen to reflect the attainable serum levels, given clinically useful dosages. When the disks contact the agar, the drug is rehydrated, and diffuses into the agar in a well-characterized fashion.

- After incubation, the plate will be covered with confluent growth of the organism, except in circular zones adjacent to discs containing drug to which the organism is susceptible. These zones of inhibition are measured, to the nearest millimeter with calipers, templates, *etc.*.
- The zone diameters are translated into susceptibility categories, by referring to a standard table; the categories are susceptible (S), resistant (R), moderately susceptible (MS), and either conditionally susceptible (CS) or intermediate (I).

The standardized disc diffusion result tables are derived by correlating, over hundreds of strains, zone diameters with broth-dilution MICs. The categorical limits are then derived from achievable serum drug levels, or urine drug levels for drugs which are used exclusively for urinary tract infections. Typical zone diameters for 'susceptible' results are 12-30 mm; in many cases, the difference between the 'resistant' and 'susceptible' categories is a mere 1 mm, suggesting a number of technical errors which can subvert the method.

Essentially, the disc diffusion test is a race, between the characteristic diffusion times for the drugs through the agar, *vs.* the growth rate of the organism. Thus, the method has a number of predictable limitations:

- It is only applicable to organisms which have fairly consistent, predictable growth rates.
- It is only applicable to organisms for which the methods and results have been carefully standardized.
- Generally speaking, typical drug diffusion rates are such that only rapidly growing organisms, *e.g.* *S. aureus* and *Enterobacteriaceae*, are suitable for the test. The recent demand for disc diffusion tests for fungal infections has resulted in attempted modifications for those organisms, which are universally slow-growing with respect to bacteria.
- Drugs which diffuse poorly in the agar, *e.g.* the polymyxins, give unreliable results.

### **Incubation Time**

In each of the above protocols, for bacterial conditions, incubation is done at 35 °C, for 16-20 hours. It is noted that, in emergent conditions, some tests can deliver preliminary results in shorter times, on order of 3-4 hours. However, one study found general disagreement between early results and overnight results, for microdilution methods<sup>11</sup>. In some cases, the difference was as much as a four-fold increase in the MIC, after 18 hours of incubation *vs.* 3 hours. However, there was much better agreement when a higher inoculum density was used for the 3 hour test, *i.e.*  $10^7$  CFUs/ml, *vs.* the standard  $10^5$  CFUs/ml for the overnight test.

### **Inoculation Density**

In each of these protocols, a standard inoculum is prepared. This involves visual comparison to a turbidity standard, the McFarland 0.5 standard, which is a precisely prepared barium-sulphate precipitate<sup>12</sup>. A bacterial suspension which matches the 0.5 McFarland is approximately  $5-50 \times 10^7$  CFUs/ml, depending on the species<sup>9</sup>. It is rather surprising that a step with order-of-magnitude precision, at best, is acceptable in these standard protocols, especially since all of them are reported to be sensitive to variations in the inoculation density.

### **Preculture**

It is also noted that all of the standard methods require a pre-culture step. Primarily, this is in order to isolate pure strains from polymicrobial specimens. Even without this requirement, it is commonly the case that there are not enough organisms in the specimen to perform the test. For example, in the broth microdilution method, typically 60 wells would be inoculated, each with about 50,000 CFUs, for a total of  $3 \times 10^6$  CFUs. This would be easy to get from a clinically infected urine specimen, which has  $\sim 10^5$  CFU/ml, but impossible for infected blood or cerebral-

spinal fluid, which may have only 1 organism/ml. For rapid methods such as the Vittek (*v.i.*), even more CFUs are needed, as heavier inoculation has been seen to improve the correlation of rapid method results with those of overnight methods.

The combined requirement of isolation plus sufficient numbers is at the heart of the time barrier: in order to go from a single CFU to a colony of  $3 \times 10^6$  CFUs requires 22 cell divisions. In order to obtain a 1 ml,  $\frac{1}{2}$  McFarland standard inoculum would require 26 to 29 divisions. Under the optimum conditions, the most rapidly growing organisms require 0.3 hours per division. Growing on agar, for which the delivery of nutrients is limited both by the medium and by colony geometry<sup>13</sup>, certainly 0.5 hour is more realistic, if not optimistic. Thus, at a minimum, we are up to a required 11 to 15 hours, just to get a sufficiently large inoculum, for the fastest growing organisms. For the large number of pathogens which are not as fast growers, (*e.g.* yeast, for which an optimal doubling time is about 1.5 hours), the pre-culture time is correspondingly longer; *i.e.* 22 to 29 divisions will require 33 to 44 hours for yeast, even under optimal growth conditions.

It is evident from these simple calculations where the bottleneck in the testing process is. It is clear that any modification to the standard protocols which decreased the number of CFUs needed would speed up the testing accordingly; one modification would be to simply reduce the number of drugs and dosages *initially* tested, *i.e.* to verify or disprove the clinicians initial choice.

The gel microdroplet method, introduced later in this chapter, has as its primary strength the potential to break this bottleneck, by performing the strain isolation in a matter of minutes. In cases where the specimen has a large number of organisms in it, *e.g.* urine, the need for pre-culture will be essentially eliminated. In other cases, where a small number of organisms are available, the pre-culture time is expected to be greatly shortened.

### 1.3.3: Susceptibility Testing for Antifungal Agents

Anti-fungal susceptibility testing has only become commonplace in recent years, due primarily to two factors:

- The incidence of systemic fungal infections has been historically low. The recent advent of chemotherapies which suppress the patient's immune response, either intentionally or as a side effect, has been cited as contributing to an increasing rate of fungal infections. Fungal infection is also common in persons with with Acquired Immune Deficiency Syndrome, in some cases with organisms which are almost never pathogenic, *e.g.* brewer's yeast<sup>14</sup>.
- Until the late 1970's, there were few antifungal agents approved for clinical use. Moreover, until the early 1980's, resistance to the most frequently used drug, Amphotericin-B, was not common enough to be clinically significant<sup>15</sup>.

As a result of the relatively new demand for anti-fungal testing, the demand for standard methods of testing has been even more recent, and as yet unsatisfied. Nevertheless, the methods published by the American Society for Microbiology<sup>16</sup> will serve as the *de facto* standard for the purposes of this thesis.

In general, the same methods used for testing anti-bacterial agents are available for testing anti-fungals: *i.e.* broth dilution, agar dilution, and disk diffusion. However, these methods are complicated by such factors as instability and relative lack of solubility of some of the drugs, as well as the sensitivity of the methods to inoculum density, initial state and growth rate of the cells, *etc.* In this thesis, for which the model organism is a yeast, I have chosen to use a broth macro-dilution assay to derive a reference MIC. The detailed protocol appears in Chapter 4.

#### 1.3.4: Automated Methods for Susceptibility Testing

Conceptually, a susceptibility test can be divided into three steps, as indicated in the protocols above. Automation has impacted testing at all three steps:

- setting up the test, *e.g.* dispensing drugs, standardizing inocula, *etc.*
- assessing growth after incubation, *e.g.* reading turbidity, inhibition zone diameters.
- interpreting the results. *i.e.* correlating growth assessments with MICs, serum levels, and other information amenable to a computerized data base.

Until recently, automation did not significantly speed up testing. Certainly, less time was required for setting up the tests, thus increasing laboratory throughput, but obtaining results was still limited by the biology, in particular the need for a pre-culture isolation step. However, the automated methods do eliminate many sources of technical error, such as volume handling, thus they require much less labor and technical skill. Moreover, by reducing the level of inter-laboratory and intra-laboratory variability due to technical error, quality assurance programs can be streamlined and thus be made cheaper.

From the perspective of this thesis, I will focus on (for lack of a better term), highly automated methods, those for which the technician is responsible primarily for delivering a volume of standardized inoculum (*e.g.* at  $\frac{1}{2}$  McFarland turbidity) of the organism to the device, and the device does the rest. This includes delivering a standard amount of the inoculum to each of several testing chambers, delivering a standard amount of drug to each chamber, and assessing growth in each well before and after (maybe during) incubation. The most highly automated methods then process these results using a computerized data base, and generate a report.



I will not attempt an exhaustive list of automated methods proposed or commercially available; such lists are readily available<sup>17</sup>, though rapidly changing. I do wish to make these points, however:

- by definition, all methods of susceptibility testing, automated or not, are based around a growth assay; at the risk of stating the obvious, one has to be able to detect growth of a drug-free control, in order to detect inhibition in the presence of drug.
- As of 1985, all automated methods for susceptibility testing that have been fully clinically evaluated, and approved by the Food and Drug Administration (FDA), used optical density, or related photometric methods, to assess growth<sup>17</sup>. This has the advantages of being intuitive, closely related to the standard methods of detecting growth (*e.g.* broth macro-dilution), and feasible with cheap and reliable devices such as light-emitting diodes (LEDs) and photo-transistors.
- From a technical perspective, the commercially available devices seem to differ mostly in (i) the measurement method (*e.g.* LED *vs.* halogen bulb), (ii) the number of measurements made (*e.g.* before-after *vs.* multiple measurements) and (iii) the interpretation of those measurements, as embodied in the computer algorithms which map a measurement set into an MIC result.
- All of the automated methods require a pre-culture step, and formation of a standard inoculum. Isolation is required since many (if not most) clinical specimens are poly-microbial. A standard inoculum is strongly desired, since it ties the method to a standard method; *i.e.* it is likely that there is a direct relationship between the ease of acceptance and approval of a new, automated method, and its degree of similarity to existing, standard methods.

### The Vitek System

The state-of-the-art in automated testing is represented by the Vitek device (McDonald-Douglas / Vitek Systems, Hazelwood, MO). Again, without going into great detail, I will describe some basic features, since I will refer to the device occasionally throughout the thesis.

The Vitek is based around a 'card' (about the size of a credit card), containing 30 wells of 50  $\mu$ l capacity each. Each well contains a lyophilized nutrient-drug mixture. The technician is responsible for performing the pre-culture step, isolating several colonies, and preparing a standard,  $\frac{1}{2}$  McFarland inoculum. Then the device takes over:

- The inoculum is automatically distributed to each of the wells of the card by a vacuum device.
- The card is put into a carousel, with other inoculated cards, which is put into the incubator/reader module. At pre-determined times, (or at random times, on demand by the operator), the card is moved from the carousel into the reader, as in a jukebox, and each well is read by a LED / photo-transistor pair.
- The optical density measurements are stored, analyzed, displayed and reported by a dedicated computer.
- Cards can be processed individually or in batches, and can be read at rates up to 120 per minute. After the test, the card can be sterilized and disposed.

Aside from practically eliminating the need for a technician, the Vitek is one of the few automated methods marketed as a *rapid* method. Some typical speeds for identification (ID) and susceptibility (MIC) tests are:

---

Test	Test Time (hours)	Test Resolution
Gram negative ID	4-18	~70 species
Gram negative MIC	4-10	11 drugs
Gram positive ID	4-15	> 30 species
Gram positive MIC	6-10	11 drugs
Urinary pathogen ID	13	9 species
Urinary pathogen MIC	4-10	11 drugs
Yeast ID	24	~25 species
Anaerobe ID	4	> 75 species
Neisseria / Haemophilus ID	4	> 25 species

---

Some of these numbers are very impressive; indeed, for some tests, the results *could* be available at the time of initial choice, *if* the initial pre-culture step could be avoided. However, as impressive as the technology is, it does not address that fundamental, rate-limiting step; if the test times listed above were divide by 10 or 100, the test would still be an overnight test, due to this limitation. Conversely, by directly addressing that step, the GMD method may form the basis of a breakthrough in testing.

### 1.3.5: Future Methods for Susceptibility Testing

The classical paradigm of predicting susceptibility by an organism's identity is foiled, for the most part, only by the existence of resistance. The specific resistance mechanism is coded, of course, by specific genes. This forms the basis of a proposed means of susceptibility testing: identify the organism, *and* confirm or disprove the presence of resistance-genes, and choose an antibiotic accordingly.

Within the past decade, the use of a gene-probe to detect genes which confer (one type of) resistance was demonstrated for the first time<sup>18</sup>. The strategy, to hybridize resistance-conferring genes with radio-actively labeled complementary DNA fragments, has the potential to revolutionize clinical testing, among other applications. There has been a consummate flurry of activity in the area; *e.g.* in 1988, 28 papers describing the development of probes or probe methods appeared in the *Journal of Clinical Microbiology*<sup>19</sup>. The recent development of a method for routinely synthesizing DNA fragments with covalently attached fluorescent dyes, such as fluorescein<sup>7</sup>, enlarges the possibilities further, *e.g.* using flow cytometry instead of autoradiography to read the test results.

A recent review of progress to date in the development of resistance gene-probes<sup>8</sup> demonstrated both impressive results and optimism for the future, appropriate for a representative of the commercial sector. Most types of resistance appear to be acquired, *i.e.* imported into a cell from another cell, typically *via* a plasmid; thus most of the probe development has been directed toward these plasmids. However, in a review of the same technology from the perspective of a Microbiology Laboratory Chief, several potential problems are noted<sup>19</sup>. Many of the points raised are aimed more at factors affecting applicability of the technology for routine testing in clinical microbiology laboratories (discussed in Chapter 5), and seem likely to be addressed in the near future. As in the classical testing methods, the key to acceptance will be automation, which is reportedly on the horizon<sup>8</sup>.

Aside from these issues, it seems likely that a large barrier to applicability will be the need to develop and maintain massive libraries of probes. As of 1988, at least 20 distinct, plasmid-mediated  $\beta$ -lactamases had been identified<sup>8</sup>;  $\beta$ -lactamases, enzymes which cleave the  $\beta$ -lactam ring common to all penicillins, are the basis of the most clinically significant types of penicillin-resistance. To date, at least 12 distinct plasmid-encoded enzymes conferring resistance to aminoglycoside antibiotics have been found, and at least 10 for tetracycline resistance. There is at least an acknowledgement that more generic probes for detecting broader classes of *e.g.*

$\beta$ -lactamases would help clinical applicability. Lastly, there is some expectation that evolution will provide new genes for resistance, as well as more complex resistance schemes which may involve multiple genes, thus requiring equal expansions in the library as well as more complex testing schemes.

Other potential or demonstrated problems include:

- There are documented cases where cells carry the genes for resistance to a particular drug, but are nevertheless susceptible to the drug. The key of course, is that the genes must be expressed in order to confer resistance, making plain the difference between genotypic and phenotypic resistance. For example, intrinsic (*i.e.* non-plasmid) genes for  $\beta$ -lactamases are present in the DNA of a variety of pathogens, but seem to require a mutational event in their regulatory mechanism to actually express the gene<sup>8</sup>.
- There are unresolved issues with regard to specificity and sensitivity. For example, according to product literature, a commercially available probe for *N. gonorrhoeae* will non-specifically react with at least 11 species of bacteria, thus requiring preliminary culture and testing to eliminate the possibility of a false positive result. Likewise, some probes can be expected to react positively with mammalian cells commonly found in specimens, as well as normal, non-pathogenic flora, which are known to frequently carry, and sometime transmit resistance-conferring plasmids. On the other hand, recent use of a probe to detect penicillinase-producing *N. gonorrhoeae* directly in urethral exudates of males was reported to be 91% sensitive and 96% specific compared to a standard method performed on isolated colonies<sup>20</sup>; some optimism is clearly justified.

For the sake of comparison, as of 1988, gene probe methods were sensitive enough to detect  $\sim 1-10 \times 10^4$  microorganisms, or target DNA sequences, setting the required

inoculum size somewhat lower than for standard methods. In addition, certain amplification strategies, such as targeting ribosomal RNA, or using the polymerase chain reaction (PCR), may make it possible to use very low inoculum numbers, possibly down to a single cell. If this technology is successfully developed, it could have an enormous impact on testing direct clinical specimens, such as cerebral spinal fluid or blood, where 1 microorganism per ml is considered serious.

### 1.3.6: Summary

Manual MIC determinations by broth or agar macrodilution are really too expensive to consider doing on a routine basis. As is evidenced by the descriptions above, the methods are labor intensive, require moderate levels of technical ability, and are tedious to perform. In addition, since small variances from standard protocols can result in significantly different results, constant Quality Assurance is required; until recently, daily QA procedures were required, contributing to the costs.

The development, by Kirby and Bauer in 1966<sup>21</sup>, of the disc diffusion method permitted more routine testing. As described above, the test can be set up quickly, requires less technical skill, and removes some of the possibilities for technical errors. On the other hand, other sources of error are introduced; for example, one study showed standard disk drug levels to vary between 67% and 120% of their nominal values (S.Brecher, personal communication). The test is also amenable to automation, *e.g.* with devices that dispense a desired set of test disks onto agar plates, in an optimum configuration, *e.g.* Dispense-O-Disc (Difco) or the Sensi-Disc System (BBL), and with opto-electronic methods for determining zone diameters. The discs are also cheap, about 10 cents each. However, the method has its limitations, including applicability only to a subset of potential pathogens, namely those for which standardization is both possible and has been done. As discussed above, disc diffusion test delivers only categorical, or limited quantitative susceptibility results, but this is acceptable, and possibly desired, since it answers the clinician's bottom-line questions about a drug's effectiveness in a given case.

Manual broth microdilution methods have all of the disadvantages of macrodilution methods. However, the combination of semi-automated volume-handling devices, and ready-to-use trays with pre-dispensed nutrients and drugs has made the method very popular. In a 1983 survey of about 1,00 laboratories by the College of American Pathologists, 40% of reporting laboratories used one of the three dilution methods discussed, (although not to the exclusion of the disk test), and of those, about 80% used commercially prepared trays<sup>10</sup>. Many products, such as those from American MicroScan combine miniaturized antimicrobial susceptibility and identification tests in the same tray. In combination with an opto-electronic reader, and a computer which reads and interprets the tray after incubation, the number of highly skilled and expensive lab technicians needed is greatly diminished.

The recent development of gene-probes will likely have a significant impact on clinical testing, especially on direct testing of clinical samples, and detection of genes which confer resistance. It is expected that some if not all of these probes could be adapted to use in GMDs, *e.g.* to signal a cell's identity from a mixed-species specimen, or to signal the unexpressed potential for resistance in a cell species.

As discussed above, all of the current and proposed methods, with the possible exception of gene-probe technology, require a pre-culture step, which is severely rate-limiting. Technically, a GMD-based method has the potential to obviate the pre-culture step. In order to begin an assessment of the method it is now appropriate to introduce it and describe it.

### **Section 1.4: GMD-based Growth Assay**

In this section, I will describe, on a functional level, the GMD-based growth assay which forms the basis of this thesis work. Before proceeding, it is appropriate to define the term "growth", as it is used here; this in turn depends on two other terms which will be used widely: "biomaterial" and "biomass".

### 1.4.1: Growth, and the Measurement Thereof

When a CFU is cultured on a agar plate under suitable conditions, one observes the formation of a colony, which "grows", *i.e.* increases in size, until nutrient exhaustion, toxin accumulation, or some other event causes growth to stop. The increase in colony size reflects the fact that at least some cells in the colony are accumulating intra-cellular material, by taking in nutrients and manufacturing sub-cellular components. I use the term biomaterial to refer to this broad class of compounds used, accumulated, or manufactured by cells: proteins, nucleic acids, fatty acids, carbohydrates, phospholipids, glycoproteins, proteoglycans, *etc.*, which in turn make up the cell membrane, cytoskeleton, ribosomes, chromosomes, enzymatic pathways, and other sub-cellular components. I will refer to the sum of these biomaterials, either within a cell, or in a colony, as the biomass of the cell or colony; 'dry weight' would be an equivalent term. Finally, by growth I mean an increase in total biomass over some period of time, *i.e.* an incubation period, again either within a cell or in a colony.

It is important to note the distinction I am making between growth and division. Colonies increase in size because they are accumulating biological molecules, not because they are dividing. The division is a consequence of the fact that some of the molecules manufactured by the cells serve to partition a large mother cell into two smaller daughter cells. To be sure, division is important for growth; when cells are cultured in suspension, division maintains a favorable surface-area to volume ratio for feeding and excretion, giving rise to maximum growth rates. Division is also important to disease, as it gives rise to disease spreading, either within or between hosts. Indeed, most antibiotic therapies aim not to kill the infecting cells, but to inhibit cell division, but the mechanism of drug action almost invariably is to disrupt the cellular mechanisms of growth as defined here, such as disrupting protein synthesis.



From these definitions, one would infer that to measure growth, in GMDs or otherwise, one needs to measure cellular or colony biomass, and its change with time. However, such an undertaking is not practical in general, and certainly not so for GMD-based methods. Instead, we choose a readily measurable, reliable (hopefully) indicator of biomass. For a macroscopic method, the indicator might be as simple as the dimensions of the colony, although colonies typically have irregular shapes. For the GMD-based growth assay our approach is to measure the amount of an indicator biomaterial present in a microcolony; specifically, to date we have used two such biomaterials: proteins and nucleic acids. These have the desirable property of sufficient generality such that a consistent increase of either leads to the plausible conclusion of growth. The details of measuring the indicator biomaterials, which for this work are done by flow cytometry, will be taken up later in this chapter.

It is important to recognize that, by the definitions above, growth generally occurs before division, so that the GMD method is fundamentally able to measure growth in less than the average division time of the cell. It should also be pointed out that by using a more specific indicator, *e.g.* measuring the amount of a particular cell-surface marker, the growth assay can be transformed into a cell-state, identity, or functionality assay. Further extensions, such as combined growth and functionality assays, should be straightforward, but are beyond the scope of this thesis.

#### 1.4.2: GMD-based Growth Assay: Expected Results

The central idea of the GMD-based growth assay is:

- GMDs are used to isolate and contain individual cells or colony-forming units from a cell suspension
- GMDs contain the progeny of the initial cells within the GMD, producing a microcolony

- The total amount of an indicator biomaterial in each microcolony is measured before and after an incubation period, and growth is inferred from the difference.

For this discussion, the details of GMDs are not important; for now I will use the term as a place holder for a method which can be used to "isolate and contain" cells as described, and which support cell viability and growth, especially by allowing free exchange of nutrients and waste products with a suspension medium. Initially, I will also put aside the question of how the colony-forming units get inside the GMDs.

An idealized GMD-based growth assay is shown schematically in Figure 1.1. This figure illustrates the basic idea of the method, and indicates the form in which experimental data will be processed and presented in later chapters. Indeed, this figure serves as an "expected result", against which real data will be compared.

The left column of Figure 1.1 is a series of drawings, depicting "microscopic" views of a GMD preparation, taken at intervals equal to one average cell division time. As indicated by the labels to the left, time increases in the downward direction. In these drawings, the larger, gray circles represent GMDs and the smaller, light circles represent individual cells. One GMD is seen to contain a two-cell colony-forming unit; the remaining GMDs contain either 0 or 1 cell. As time passes (reading vertically down the column) these cells are seen to divide repeatedly to form microcolonies of two or more cells. A non-growing CFU is seen to remain unchanged in its GMD.

### **Biomass Distributions: Log Histograms**

The remaining panels in Figure 1.1 are histograms depicting the expected statistical distribution of biomass for the GMD "samples" depicted in the drawings. In prac-

tice, these histograms would be derived by measuring the indicator biomaterial in several thousand GMDs, of which the ones shown in the drawings are representative.

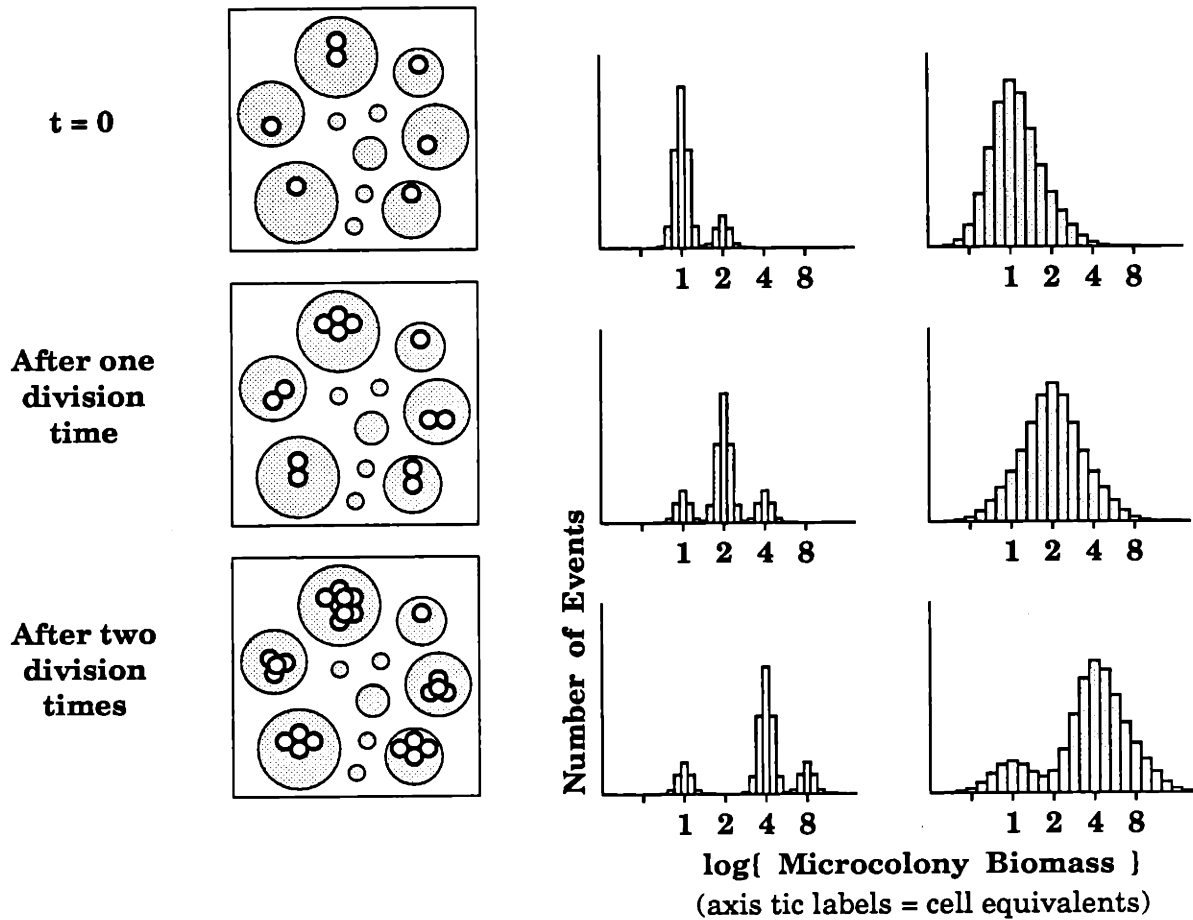


*Figure 1.1: Schematic view of GMD-based growth assay*

The biomass distributions, as well as the data presented in later chapters, are in the form of log histograms, which are derived by:

- collecting a set of biomaterial measurements. Each such measurement represents the amount of indicator biomaterial contained in one GMD, *i.e.* the total amount of indicator biomaterial in all of the cells contained therein.

- computing the logarithm of each measured biomass value
- computing and plotting the frequency-of-occurrence of these log results, either as raw number of events per value range ( bin), or normalized by the total number of GMDs in the sample to give relative frequency.

Log histograms are used strictly for the convenience of human observers; for data analysis, raw biomaterial measurements are just as useful. However, for this application, log histograms give rise to more meaningful visual comparisons. Under a commonly used model for macroscopic colony growth under ideal culture conditions, colony biomass increases exponentially with time<sup>13</sup>. As a mathematical consequence, the statistical distribution of colony biomass, when plotted in the form of a log histogram, remains unchanged as time passes, except for a characteristic shift to the right, at a rate related to the colony growth rate. For each doubling in colony biomass, the distribution shifts by the same amount,  $\log(2)$ ; by normalizing the log axis by the mean single-cell biomass, the axis can be labeled with "cell equivalents".

The histograms shown here were generated by a simple mathematical model. In particular, the model assumes a Gaussian distribution for the amount of indicator biomaterial in one cell, when plotted as a log histogram; this assumption is based on empirical observations of biomaterial measurements; almost any unimodal, approximately symmetric distribution would be appropriate here. Each of the log histograms consists of the sum of three such distributions, corresponding to the three sub-populations present in the GMD sample depicted in the drawings:

- single-cell viable CFUs, and their progeny
- two-cell viable CFUs, and their progeny
- non-viable CFUs

Within each column, the assumed sub-population distributions have identical variances, but differing means. Within each row, the sub-population distributions have identical means, but different variances. The significance of these parameter choices will be discussed momentarily.

The center column depicts the expected statistical distributions of measurements when DNA is used as the indicator biomaterial. The expected variance in these results would be primarily measurement variability, *e.g.* due to staining and instrumentation noise, rather than variability in the indicator itself. The variance is small enough that we can easily distinguish the sub-populations in the histogram, making it easy to see what happens upon incubation. Among the possible indicators, only DNA would be expected to have such a low variability<sup>22</sup>. It should be pointed out that the use of DNA as an indicator would give rise to a different kind of growth assay, namely one which was sensitive to cell division, rather than growth, as defined above. For the purposes of antibiotic susceptibility testing, this would usually be acceptable, though from a technical viewpoint, measuring bacterial DNA requires a good (read expensive) flow cytometer.

- The top panel depicts the expected log histogram obtained from the GMD sample at time "t=0". The distribution is bimodal, reflecting the "microscopic" drawing; the larger peak corresponds to the GMDs which contain one-cell CFUs (5/6 of the occupied GMDS), and the smaller peak corresponds to the GMDs which contain two-cell CFUs (1/6).
- The middle panel depicts the histogram that would be expected after incubating the GMD sample for one average division time. Here, both cells in the initial two-cell CFU have divided, thus forming a four-cell microcolony; the corresponding peak in the histogram has shifted to the right, but is otherwise unchanged, as discussed above. The initial 1-cell CFUs have not all performed the same; under the "microscope", we see that four of them divided to form 2-cell microcolonies, while the remaining one did not divide. Accordingly, the large peak in the t=0 histogram has split into two smaller peaks. One, representing the 1-cell CFUs which have divided, has shifted to the position initially occupied by the 2-cell CFU; the other, representing the non-dividing CFUs, has remained in its initial position.

- The bottom panel depicts the histogram expected after incubating the GMD sample for another average cell division time. Here, all of the growing cells have divided once more, and the corresponding peaks have shifted to the right by another  $\log(2)$ , with no change in variance. The peak representing the non-growing cells still remains in its initial position.

The right column of Figure 1.1 depicts the expected statistical distributions of measurements when a more general indicator biomaterial, such as protein or nucleic acids are measured. The expected variance in these results is dominated by the cell-to-cell variability in the indicator itself; these particular indicators are intimately involved with, and thus depend strongly on the state of the cell, which has considerably more variability than the amount of DNA. Of course, measurement variability, especially due to staining, can still be significant. From a modeling perspective, the histograms shown in the right column are identical to those in the center column, except the variance parameter used to generate the sub-populations is larger. The expected variance is no longer small enough that one can easily distinguish the sub-populations in the histograms, although the changes due to microcolony growth are readily apparent, and good measures of growth.

- The top panel depicts the expected log histogram obtained from the same GMD sample at time "t=0". In contrast to its "DNA-only" counterpart, shown in the center column, the t=0 distribution is not bimodal but only skewed, reflecting the respective fractions of one-cell and two-cell CFUs.
- The center and bottom panels depict the expected histograms after incubating for one and two average cell division times, respectively. As before, the sub-populations of the overall distribution which derive from the growing cells exhibit a characteristic shift to the right. Where there is overlap with the sub-population due to non-growing cells, the shape of the overall distribution changes as time progresses; once the "growing" sub-population has shifted enough that there is no such overlap, the

shape of the distribution remains constant; indeed, it is the same as the  $t=0$  distribution, in accordance with the previous discussion of log histograms.

Using distribution-fitting techniques, one could attempt to disentangle the three sub-populations, or at least enumerate growing *vs* non-growing CFUs. However, as suggested by Figure 1.1, simpler statistical measures, such as the mode of the distribution, can be used to quantify microcolony growth, and this will be the approach taken in later chapters.

### Log Histograms and Exponential Growth

In this section, I will fill in some of the mathematical details of the previous discussion. For a GMD occupied by one or more viable cells, the change in biomass upon incubation is ideally multiplicative, due to the exponential growth characteristic of microorganisms. In particular, if  $M_0$  is the biomass of the initial CFU, and  $M(t)$  is the colony biomass at some later time,  $t$ , then under ideal growth conditions,

$$M(t) = M_0 e^{\mu t} \quad (1.1)$$

$$\ln\{M(t)\} = \ln\{M_0\} + \mu t \quad (1.2)$$

where  $\mu$  is the specific growth rate, and is assumed constant over the incubation time<sup>13</sup>. Thus, over a sample of microcolonies, the statistical distribution of  $M(t)$ , should be identical to the distribution of  $M_0$ , only shifted by the "characteristic shift" term,  $\mu t$ ; this term is always positive, so the shift is always rightward. As noted above, if we incubate for one cell division time,  $\mu t = \ln(2)$ , and the distribution shifts by  $\ln(2) = 0.69$ , but is otherwise unchanged. Conversely, when displayed as a linear histogram, the distribution of  $M(t)$  gets wider and wider as time passes. By considering the  $\exp\{\mu t\}$  term as a multiplicative scaler, and applying the the scaling rule for random variables, it follows that the standard deviation of  $M(t)$  likewise in-

creases exponentially. The incremental computational cost of computing log histograms is well worth the improved ability to visually interpret the results.

It is important to note, however, that the "shifting" behavior of equation 2.2 assumes that  $\mu$  is constant. In reality, one expects that  $\mu$  itself will be randomly distributed in a population, *i.e.* that cells don't all grow at the same rate. In this case, equation 1.2 still holds, but the sum of two random variables implies a *convolution* of their distributions<sup>23</sup>; this assumes that  $M_0$  and  $\mu$ , *i.e.* a cell's initial biomass and its growth rate, are statistically independent, which is not necessarily true. The result of convolution with the distribution of  $\mu$  would be a combined rightward shift and spreading (*i.e.* increasing variance) of the distribution of  $M$  as time progresses. Under the assumption of statistical independence, we can make use of the simple relationship between the means of the pre- and post-incubation distributions, in terms of  $\bar{\mu}$ , the population mean growth rate:

$$\text{Mean}\{\ln(M)\} = \text{Mean}\{\ln(M_0)\} + \bar{\mu} t \quad (1.3)$$

### Life Cycle of Cell Suspensions

Further confounding the simple assumptions behind Equation 1.1 is that for each cell in a sample, the specific growth rate,  $\mu$  is in fact time-varying. With some simplification, upon being mixed into fresh nutrient medium, a cell inoculum will undergo three phases of growth:

- lag phase: Cells respond to an abundance of nutrients by turning on the mechanisms of uptake and synthesis; this would involve turning on certain genes, production of ribosomes, *etc.* The rate of biomass production and accumulation increases, eventually followed by the onset of cell division.
- exponential phase: Biomass production hits its maximum rate, limited by the rate of nutrient delivery, and ultimately, the turnover rates of enzy-



matic pathways, ribosomes, *etc.* As biomass increases, the capacity to produce more biomass increases; ideally, this is expressed by the differential equation:  $dM(t) = \mu M(t)$ , which is integrated to give the exponential equation, 1.1

- **stationary phase:** As growth increases, eventually the gradual exhaustion of nutrients and accumulation of toxic waste products causes the growth rate to fall. In the long term, the growth rate will go to zero, as the biomass production mechanisms are dismantled. Total biomass may actually fall, as cells break down biomass to extract energy. Finally, cells will begin to die, (or in some cases, sporulate), as their environment becomes too hostile to maintain normal cell viability.

This life cycle can be incorporated into the previous treatment by treating the specific growth rate as being time-varying,  $\mu(t)$ ; we will assume that the differential equation  $dM(t) = \mu(t) M(t)$  is still valid, at least for lag and exponential phases. Integration yields a modified equation 1.2:

$$\log\{M(t)\} = \log\{M_0\} + \int_0^t \mu(\alpha) d\alpha \quad (1.4)$$

A common simplification is to treat  $\mu(t)$  as piecewise-constant; in particular, that  $\mu(t)$  is zero during the lag phase, and then constant over the exponential phase, then returns to zero for stationary phase. This leads to the result:

$$\begin{aligned} \log\{M(t)\} &= \log\{M_0\} & t \leq \tau \\ \log\{M(t)\} &= \log\{M_0\} + \mu (t-\tau) & t > \tau \end{aligned} \quad (1.5)$$

where  $\tau$  is called the lag time. The lag time should be considered as a random variable, since for a given cell  $\tau$  depends on the cell state just prior to inoculation. Indeed, in studies of macroscopic colony growth, the lag time is often modeled with a Gaussian distribution centered on its mean value, and with a variance that dominates any variance in cell growth rate during exponential phase<sup>24</sup>. Again, under

the assumption that  $M_0$  and  $\tau$ , the initial biomass and the lag time, are statistically independent, we can predict the behavior of  $\log\{M\}$ . The term  $\mu t$  serves to shift the initial biomass distribution to the right, with no other changes as before; the term  $\mu \tau$  serves to convolve the initial biomass distribution with that of  $\tau$ , thus spreading it out somewhat. It should be noted that once all of the cells have reached exponential phase, no significant further spreading is expected, if the cells all attain the same growth rate,  $\mu$ .

Further development of this concept could lead to some interesting studies regarding the effects of different drugs, and different drug levels, on individual cells in a population. For example:

- a drug which acts on all cells uniformly, *e.g.* decreasing the specific growth rate of all cells, will be manifested as an effect in the characteristic shift *rate* only.
- a drug which affects some cells more than others (*e.g.* a spectrum of resistance), will be manifested by changes in the *spreading* effect of the initial  $\ln\{M_0\}$  distribution, with respect to the drug-free control.

## Section 1.5: Summary

In this chapter, I set out to both motivate and introduce the use of GMD technology for antimicrobial susceptibility testing. The central points are:

- The delivery of the best, and least expensive care for patients with infection is hampered by a delay in obtaining antimicrobial susceptibility results.
- The delay in results is due to the fundamental and related problems of the necessity of isolating pure strains, and the need for sufficient numbers of organisms to perform the susceptibility tests.

- The gel microdroplet based approach can obviate the need for a separate isolation pre-culture, and thus greatly speed up susceptibility testing.

So far, I have only presented GMD technology at a conceptual level. In the next chapter, I will examine some technical issues in detail, in order to demonstrate that the particular methods used in this thesis fulfill the functional specification given here.

---

*Chapter 2***Description of Methods**

---

In the previous chapter, I used the terms ‘GMD’ and ‘flow cytometry’ as place holders for somewhat underspecified technologies, defined mostly by their functionality; in this chapter, I will focus on the details of those technologies. The intent is to provide a suitable background for discussing the applicability of these specific technologies to the overall goals of this thesis, as well as for consideration of the experimental results which follow. Thus, this chapter will focus on issues such as the properties and merits of agarose gels, diffusion in microdroplets, design and function of flow cytometers, and properties and problems related to fluorescent dyes and GMDs.

**Section 2.1: Gel Entrapment and Culture of Cells**

In this section, I will provide a background for discussing the specifics of gel microdroplets, by outlining some of the central issues, and reviewing the experiences of other researchers. In general, this discussion will be framed by the functionality required by the problem at hand. In particular, in reviewing these methods, we will need to focus on the required ability to:

- Isolate and contain individual colony-forming units and their progeny
- Support growth, especially by allowing the delivery of nutrients and removal of wastes from the cells
- For antibiotic testing, permit the unhindered delivery of agents to the cells at known concentrations

### 2.1.1: Existing Technology: Gel Macrodroplets

The technology of gel entrapment and culture of cells has received much attention in the last decade, most commonly in the context of possible bio-reactor design.<sup>25</sup> Generally, the methods discussed are more macroscopic, involving gel slabs, or droplets on the order of 1 mm diameter or more. With respect to bulk method, the use of droplets has the advantages that:

- owing to the smaller typical dimensions, and to their favorable geometry (*v.i.*), gel droplets present a smaller barrier to diffusion, making it easier to supply or extract compounds from the entrapped cells
- by surrounding the droplets with a permeability barrier, *e.g.* a membrane or hydrophilic/hydrophobic interface, the entrapped cells can be easily chemically isolated from each other
- by physically manipulating the droplets, *e.g.* by magnetic forces, one can easily separate interesting cells from a bulk population<sup>26</sup>.

Some of the prominent examples of entrapping cells or other entities in droplets are:

- the use of liquid microdroplets to isolate and study individual molecules *e.g.* of the enzyme  $\beta$ -galactosidase<sup>27,28</sup>
- entrapment and culture of viable animal cells, especially hybridoma cells, in gel droplets, for purposes such as monoclonal antibody production<sup>29-32</sup>
- encapsulation of cells in gel or liquid droplets surrounded by a semi-permeable membrane, as a means of transplanting cells without invoking an immune response<sup>33-35</sup>
- encapsulation and culture of microorganisms in membrane-surrounded gel droplets, for the purpose of detecting and isolating mutants from a parental population<sup>36</sup>

- immobilization of plant cells in gel droplets, for production of high-value compounds<sup>37, 38</sup>
- encapsulation of plant protoplasts in gel droplets. for the purpose of stabilizing the cell during genetic transformations, including by electroporation<sup>39, 40</sup>

### 2.1.2: A New Technology: Gel Microdroplets

The GMD method enlarges the envelope of cell entrapment and culture technology, by moving to a droplet size of 100  $\mu\text{m}$  or less. Doing so involves certain costs, but they are far outweighed by the benefits, which include:

- further reduction of diffusional barrier, almost to the point of diffusional transparency
- rapid changes in concentration of accumulated product, in cases where a permeability barrier exists.
- the ability to make rapid measurements of large numbers of droplets via flow cytometry.
- the ability to sort large numbers of droplets using fluorescence-activated cell sorting

GMDs can be made from a number of materials, and can be inoculated by a number of methods. In later sections, I will discuss some of the commonly used materials and methods, as well as their relative merits from the perspective outlined above. First, however, it is appropriate to consider in some detail the specific advantages afforded to GMDs by their geometry and size.

### 2.1.3: Diffusion in Spherical Geometries

Gel materials are generally considered to be anti-convective, meaning that molecular transport via fluid flow through the gel will not be significant; this is discussed in more detail in a later section. Thus, in the absence of other motive forces, such as electrical fields, the bulk of molecular transport will be via diffusion. Inasmuch as molecular transport will determine the suitability of GMDs for supporting growth, a brief look at diffusion in spherical geometries is appropriate here.

Figure 2.2 depicts two geometries, spherical and rectangular. I have included the rectangular geometry for the purposes of comparison, since:

- it can be used to predict diffusion in macroscopic, slab culture of cells. It was stated previously that droplet culture provides a diffusional advantage over slab culture, and this will afford an opportunity to quantify the effect.
- many readers may be familiar with the rectangular one-dimensional case, since it predominates the droplet culture literature.

In words, the assumptions depicted by the drawings are:

- In each case, the molecule of interest,  $M$ , diffuses freely in the gel. This neglects any interactions of  $M$  with the gel, such as sieving or binding; these will be discussed later.
- In each case, there is only a one-dimensional variation in the concentration of  $M$  inside the gel, in particular, the distance from the gel-bath interface. Thus, for the spherical case, we consider  $c(r,t)$ , where  $r$  is the radial position in the droplet; we assume there are no angular variations. For the rectangular case, we consider  $c(x,t)$ , where  $x$  is the distance from the gel boundary, as shown, and assume no variations in the other dimensions.

- In each case, the gel surface is bathed by a medium in which the concentration of M is constant,  $C_0$ . This requires, in effect that the volume of the bath greatly exceeds the volume of the gel, so that the diffusion of M into the gel does not noticeably change its concentration in the bath.
- Initially, *i.e.* at  $t=0$ , the concentration of M in the gel is zero. As stated, this would only apply to the case where something, such as a drug were added to the bathing solution. However, the results presented here can be applied to the more general case where the concentration in the bathing medium changes, *e.g.* from  $C_0$  to  $C_1$ , by mathematically splitting the problem into steady-state and transient responses. The results shown here describe the transient response, whereas the steady state response is just  $c(\text{inside gel}, t=\infty) = c(\text{bath})$ .

To solve for the diffusional transient response requires solving the diffusion equation:  $D\nabla^2c = \partial c / \partial t$ , subject to the conditions stated above. This procedure, and the mathematical result, are outlined in Appendix 4.

The solution to the diffusional transient response is best appreciated in its graphical form, which is also presented in Figure 2.2. On each set of axes is drawn a family of curves, where each curve represents the concentration of molecule M, as a function of position within the gel, at different times,  $t$ , after the bath concentration of M changes value. More precisely, these profiles are drawn for different values of diffusion time,  $T$ , defined as  $x^2/D$ . The parameter  $T$  is *not* the "characteristic diffusion time", which is geometry-dependent; here, we want to compare the concentration profiles, in terms of the same parameter.



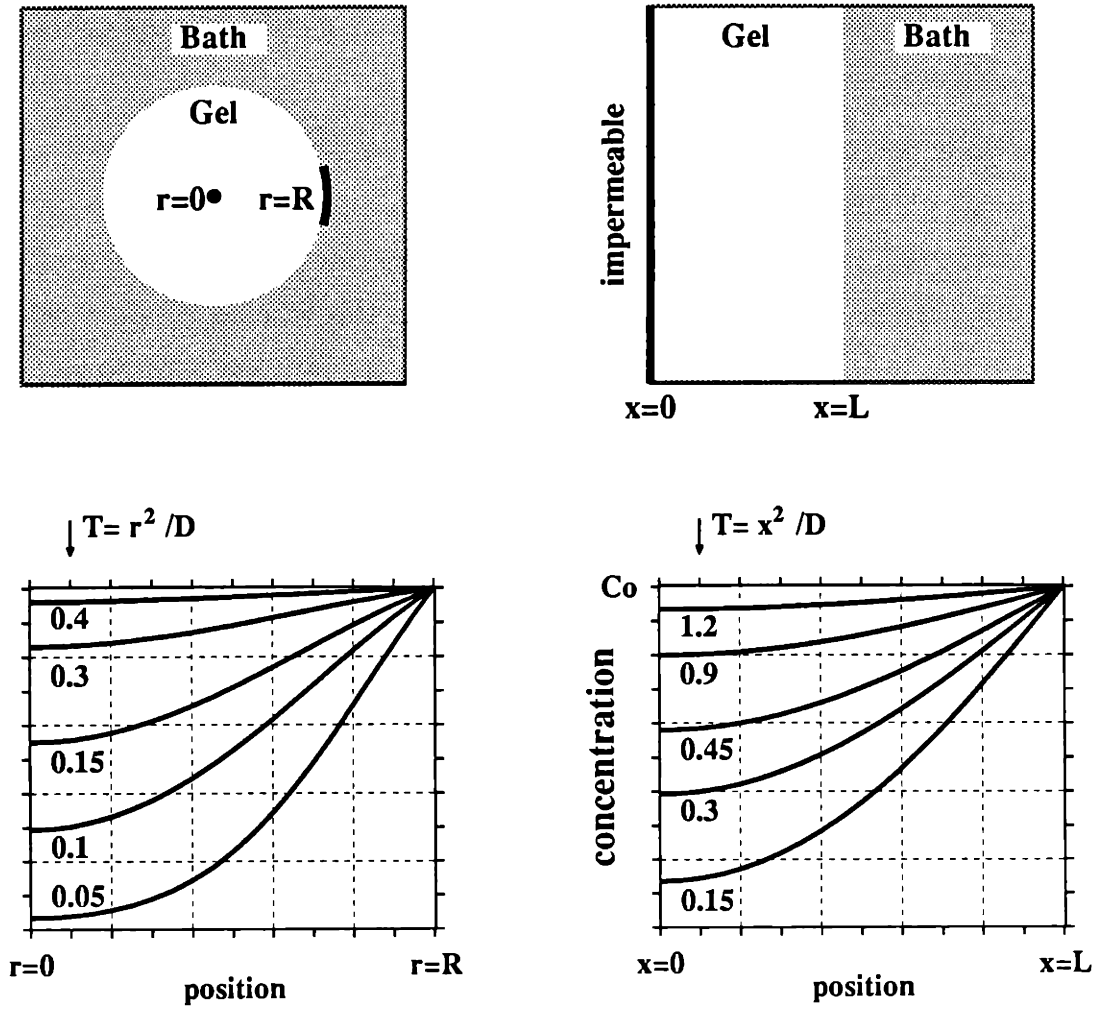


Figure 2.1: Concentration profile evolution in spherical geometry

### **Culture in Droplets: Geometric Advantage**

At  $T=\infty$ , the concentration profile for both cases would be completely flat, with  $c(r,t) = 1$ . The quickness with which the concentration profile approaches the steady state is a good indicator of the capability for diffusional transport. From the two families of curves, we observe that the concentration profile relaxes from its initial state in very similar, though not identical manners, except that for the spherical case, the relaxation happens three times faster; in particular, whereas in the rectangular case, the concentration profile achieves 90% of its final value at about  $T=1.2$ , for the spherical case, this happens at  $T=0.4$ .

Although an accident of the math, it is heuristically reasonable that diffusion in the spherical case should be three times faster, since molecules can diffuse into the gel from all three directions (*i.e.*  $x$ ,  $y$ , and  $z$ ), whereas in the rectangular case, only one dimension is available. Supporting this reasoning, heat-flow analysis for cylindrical geometries<sup>41</sup> indicates a similar family of curves, with the temperature (concentration) profile evolving at roughly twice the rate as for rectangular 1-dimensional geometries.

### **Culture in Microdroplets: Size Advantage**

Earlier, it was asserted that by going to a smaller size, GMDs offered a significant advantage with respect to macrodroplet culture. We are now in a position to quantify that statement. As might be expected, the diffusion time,  $T$ , varies as  $x^2$ , so it is readily apparent that, *e.g.* a 10-fold decrease in droplet size, from 1mm to 100  $\mu\text{m}$ , will speed up diffusion by a factor of 100. To see whether this might be significant, we consider the diffusivities of some actual molecules<sup>42, 43</sup>, summarized in Table 2.1:

Molecule	MW kDalton	$D \times 10^7$ $\text{cm}^2/\text{sec}$	$0.4 \cdot T(80 \mu\text{m})$ sec	$0.4 \cdot T(1\text{mm})$ sec
Glycine	0.075	93	0.69	110
Glucose	0.18	67	0.96	150
Tryptophan	0.20	68	0.94	150
Sucrose	0.34	46	1.4	220
RNase (pancreatic)	14	12	5.3	830
Lysozyme	14	10	6.4	1000
$\alpha$ -Lactalbumin	16	10	6.4	1000
BSA	66	6.1	10	1600
Hemoglobin	68	6.9	9.3	1400
Tropomyosin	93	2.2	29	1.3 hr
$\gamma$ -globulin	160	4.5	14	0.6 hr
Fibrinogen (Human)	330	2.0	32	1.4 hr
Myosin	490	1.1	58	2.5 hr
Bushy Stunt Virus	11,000	1.2	53	2.3 hr
Tobacco Mosaic Virus	40,000	0.44	150	6.3 hr

*Table 2.1: Diffusion times ( $T=r^2/D$ ) in 80  $\mu\text{m}$  GMD vs 1mm droplet*

It is evident from these results that, completely independent from the nature of the gel material, diffusional limitations alone can greatly limit mass transport to cells in large (> 1mm) droplets. This almost certainly is a factor in observations of some researchers that, in large droplets, the growth of immobilized cells (plant cells in alginate) occurs only at the periphery of the droplet<sup>44</sup>. Although some researchers tend to blame the gel, Guiseley, (a principle in the gel industry) correctly notes<sup>43</sup> that "we cannot blame the tortuosity of the gel matrix for diffusional limitations", and notes that based on a mathematical model<sup>45</sup>, a 1 mm maximum droplet size is recommended.

Based on the values in Table 2.1, I would say that 1mm is still large, from a diffusional perspective; the fact that medium-weight molecules such as serum albumin would take half an hour to diffuse to the center of such a droplet may be a problem. Extension of this result to include molecular consumption, *i.e.* by a cell immobilized in the gel would make more explicit the significance of these diffusional limitations.

Of course, the goals of this thesis work strongly differ from the goals of the bulk of the immobilized cell community. I am concerned with minimizing the effect of the gel on cell growth and viability. Most of the immobilized cell community is concerned with maximizing production of certain high-value compounds, at minimum cost, and in a way which can be scaled up to meet demand; altering cell state will often be tolerated, and in some cases is desirable<sup>46</sup>.

#### 2.1.4: Gels and Their Properties

In the previous section, we considered GMDs strictly from a geometric viewpoint, neglecting any effects of the gel material. However, it turns out that the properties of the gel are the major determinant in the success of gel microculture, and thus of GMD-based antibiotic testing. In this section, I will outline the critical properties of the gels, with emphasis on gels used for cell immobilization and culture, and with required functionality in mind.

- Gelation / dissolution conditions: the physical conditions (temperature, pH, *etc.*) to maintain the gelable material in the sol state, to gel it, and to maintain it in the gel state, should not affect cell viability.
- Molecular sieving: in the gel state, all gels of interest here are composed of a net of linear polymeric fibers, which acts as a molecular sieve. Most small molecules will freely diffuse in the space between the fibers, but the transport of larger molecules may be hindered or prevented by their interaction with the gel fibers. The "effective pores" in the gel are distri-

buted in size, around an average which decreases monotonically with the concentration of gel material.

- Convection suppression: owing to the small effective pore size in typical gels, there is considerable resistance to convective fluid flow. The dependence on pore size makes this effect more prominent as gel concentration increases.
- Charge: the monomeric units which make up gels of interest frequently carried charged groups at physiologic pH's. Charge may affect cell growth either directly, or indirectly by affecting molecular transport within the gel. For example, calcium-mediated interaction between anionic sites on proteins and gels may greatly hinder protein transport<sup>43</sup>.
- Gel Strength and Mechanical Stability: The ability of a gel to "isolate and contain" cells and their progeny depends first on how strongly its polymeric fibers bind to each other, or to intermediary agents, and in the long term on the resistance of those bonds to changes resulting from cell metabolism or growth. On the other hand, a gel that is too strong may physically prevent a gel from enlarging, or may alter growth in a more subtle manner. For this application, we want "just enough" gel strength to hold the microcolony together, and allow manipulation and measurement, but no more.
- Syneresis: during gelation, most gel materials tend to contract, and expel water; this increases the effective gel concentration in the droplet, which in turn decreases pore size, *etc.*. In addition, the consequent squeezing of the cell by a mesh of fibers may negatively affect growth of immobilized cells.

### 2.1.5: Review of Gels for Cell Immobilization

In this section, I will summarize and compare the gel materials commonly used for cell immobilization. It is no secret that, for GMD methods, we use derivatized agarose gels; this is in contrast to the majority of the community, who seem to prefer alginate or carrageenan. My purpose here is to compare these materials, at an introductory level, and to extol the relative virtues of agarose. A detailed review of

physical properties of alginate, carrageenan, and to a lesser extent, agarose, has been prepared by Guiseley<sup>43</sup>.

Agarose is a linear polymer of the disaccharide:  $\beta$ -D-galactose - anhydro- $\alpha$ -L-galactose, more simply termed agarobiose, and which is shown in Figure 2.2. Historically, the term agarose was used to refer to the gelable fraction of the polysaccharide mixture called agar agar, which was found to be comprised of the most electrically neutral of these polysaccharides.

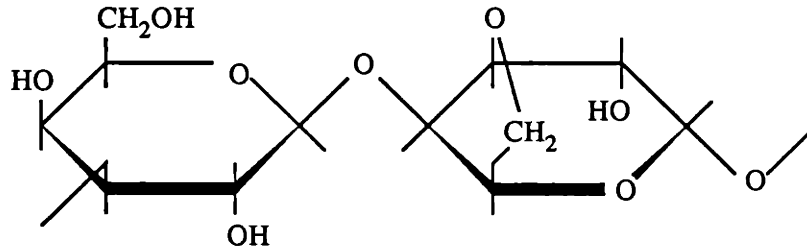


*Figure 2.2: The Agarobiose Dimer*

In solution, the agarose polymer exists as a random coil; upon gelation, the polymers combine to form double helices, which in turn combine in bundles; the gel is comprised of a dense network of these bundles<sup>47</sup>. The bundle network forms an irregular mesh, with inter-bundle "pores" containing water. The size and density of these pores are one determinant of the ability of molecules to pass freely through the gel. The density of the fiber-bundles, and thus the pore size, depend on the gel concentration.

Two important and naturally occurring modifications of agarobiose are the presence of ester sulfate, as shown in Figure 2.3, and pyruvate ketal; these groups confer fixed negative charge on the agarose molecule. The most neutral agarose has essentially no pyruvate, and very low amounts of sulfate: 0.10% (w/w) or approximately 1 sulfate-ester per 310 agarobiose dimers.

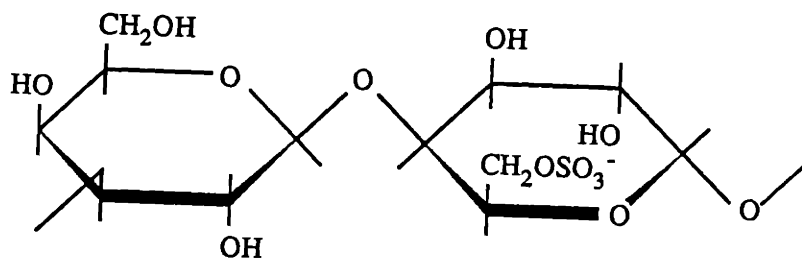


*Figure 2.3: Agarobiose with sulfate ester*

The melting and gelation temperatures of native agarose can be lowered by synthetic substitutions of the four hydroxyl (-OH) groups of agarobiose, with an increasing effect as a greater fraction of the available hydroxyl groups are substituted<sup>48</sup>. In practice, these groups are replaced by hydroxyethyl groups to produce low melting point (LMP) and ultra-low melting point (ULMP) agarose<sup>49</sup>.

The derivatization of native agarose to produce LMP and ULMP affects other physical properties, presumably by preventing the helices from packing as tightly in the formation of the fiber-bundle network<sup>50</sup>. For instance, the gel strength is markedly reduced. Likewise, average size of the inter-bundle "pores" is decreased, consistent with the increased "sieving" property of these gels. To make this more concrete, some of the properties of 2½ % gels are presented in Table 2.2<sup>51-54</sup>; looking slightly ahead, 2½ % ULMP agarose was used for the experiments in this thesis.

	melting temp °C	gelation temp °C	gel strength g/cm <sup>2</sup>	pore size nm ± sd (4% gel)	protein cutoff kDalton	nucleic acid cutoff base prs
native	95	37	-2000	106 ± 52	> LMP	> LMP
LMP	65	32	-500	42 ± 52	> ULMP	< 40
ULMP	55	20	-75	22 ± 18	~ 200	< LMP

Table 2.2: Properties of 2½ % agarose gels

The other gel materials commonly used for immobilization and culture of cells are :

- alginate: a linear polymer of the derivatized monosaccharides:  $\beta$ -D-mannuronic acid and  $\alpha$ -L-guluronic acid; the major structural polysaccharide of marine brown algae, present in all brown seaweeds<sup>55</sup>. Probably the most commonly used material used for cell immobilization. Gelled by the addition of bivalent cations, typically calcium chloride at 50 to 300 mM; gelling time 0.25 to 12 hours.
- $\kappa$ -carrageenan: linear polysaccharide, with backbone of alternating  $\alpha$ -D-galactose and  $\beta$ -D-galactose, variously modified with ester sulfate; at least 20% of the dimers are sulfonated. Precipitated, by the addition of potassium ions (hence  $\kappa$ ), from carrageenan, a polysaccharide mixture derived from various red seaweeds. Gelled by cooling in the presence of cations, typically 300mM KCl. Typical gel time 1 hour<sup>56</sup>.
- agar: mixture of polysaccharides derived from certain marine red algae. Informally considered as having two fractions: *agaropectin*, consisting of the more highly charged, ungelable polysaccharides, and *agarose*, the gelable fraction, consisting of the more neutral polysaccharides. Gelled by cooling; the agarose fraction gels, and the agaropectin is trapped in the gel matrix.



- gelatin: linear poly-amino acid *i.e.* protein. Gelled by cooling; for use at physiologic temperatures cross-linking is required, *e.g.* with glutaraldehyde at 1.5 to 2.0% Cross-linking agents are usually toxic to cells; glutaraldehyde is normally used as a cell fixative.
- mixtures: *e.g.* agarose/gelatin or alginate/gelatin are reported<sup>57</sup>; typically gelatin is used to increase droplet firmness.

Although it does not influence this thesis work, the choice of gel materials (*i.e.* the popularity of alginate) in large-scale industrial settings may be related to the prices (Sigma, St. Louis, MO) shown in Table 2.3. For antibiotic testing, one would use less than 1 gram of agarose per specimen.

---

alginate (sodium salt)	62
$\kappa$ -carrageenan (high-purity)	145
gelatin (cell-culture tested)	40
agar (purified, plant cell-culture tested)	110
agarose (native)	> 500
agarose (low, ultra-low melting temperature)	> 2200

---

*Table 2.3: Gel prices, dollars per kilogram.*

### Comparison of Gels : Strength and Stability

In general, any of the gel materials listed could fulfill our requirement to "isolate and contain" cells and their progeny. Certainly, the strength requirements for GMDs in suspension are considerably less than for droplets packed into a bioreactor column. Indeed, it is certain that "too much" gel strength will slow cell growth, although in some cases it would be hard to separate the effects of gel strength *per se*, from the effects of the conditions required to provide that strength; *e.g.* a high gel concentration increases not only strength, but the molecular sieve effect as well. As

an example of the effect, Nilsson *et al* demonstrated increasingly slowed growth for mouse hybridoma cells cultured in LMP agarose droplets (100-300  $\mu\text{m}$ ), as the agarose concentration increased from 1% to 3%<sup>58</sup>.

However, some specific details pertaining to gel mechanics and strength are worth mentioning:

- Agarose exhibits thermal hysteresis; at an intermediate range of temperatures, agarose can be either sol or gel, depending on its recent history. For LMP and ULMP derivatives, the intermediate range includes 37°C, which is critical to cell culture work. Agarose depends on hydrogen bonding between helical polymers for its strength. Thus, anything which interferes with hydrogen-bonds will weaken the gel, and can cause it to revert to the sol phase; this includes some "chaotropic" ions such as KI,<sup>59,60</sup> urea, some detergents, *etc*<sup>61</sup>. In addition, the hydroxyethylation of native agarose to form the LMP and ULMP derivatives also weakens the gel, presumably by reducing the ability of fibers to get within hydrogen-bond range<sup>43,50</sup>. As a final plus, although it has not yet been demonstrated to be deleterious to cells, synergetic squeezing of cells during agarose gelation can be eliminated by charge-balancing the agarose<sup>62</sup>, or by adding galactomannan<sup>63</sup>.
- Alginate depends on calcium ions for its strength; unfortunately, many common medium components contain things which chelate calcium ions, *e.g.* phosphate, ATP, or citrate. Usually, this implies a need to provide calcium in excess; the danger is that calcium is known to mediate many important cellular processes, and bathing cells in abnormally high extracellular levels may induce unexpected results. One work-around is the use of other cations, although only barium has been found to give both good gel strength and cell viability<sup>64</sup>.
- $\kappa$ -carrageenan is less sensitive to chelating agents, and thus is a popular alternative to alginate. The gel strength of 2%  $\kappa$ -carrageenan is roughly

the same as for a 2% LMP agarose gel, though it varies strongly with potassium (and weakly with calcium) concentrations<sup>43</sup>. When calcium ions are added,  $\kappa$ -carrageenan gels become hard and synerese, which may inhibit cell growth. Like agarose,  $\kappa$ -carrageenan exhibits thermal hysteresis. The specific gelation and melting temperatures again depend on the potassium (and to a lesser extent, calcium) ion concentrations. The lowest practical gelling/melting temperatures appears to be 35°C and 50°C, respectively; the low potassium level needed to drive the gelation point down this far would result in a fairly low gel strength - approximating that of ULMP agarose.

- agar has a reputation for forming relatively weak gels, which is reasonable, since the large agaropectin fraction is non-gelable, and interferes with the gelation of the agarose fraction.

Strictly from a strength perspective, none of these gels have a particular advantage in the GMD application; however, the relatively benign gelation *conditions* confer an advantage to the low-temperature agarose derivatives.

### **Comparison of Gels: Viability and Molecular Transport**

From a cell culture perspective, there are some interesting comparisons between the gel materials. In some cases, there are well-known affects of the gel on cell growth; in others, an effect on molecular transport may be known or suspected, which could affect cell growth indirectly.

I will begin by discussing of some of properties of agarose, especially as relates to molecular transport, and which can be summarized as follows:

- little is known with certainty
- there are reasons to suspect that agarose may alter molecular transport in some cases, but

- the success of various experiments, including the ones presented in this thesis, indicate that cells are viable and grow normally in agarose

As mentioned previously, agar is a mixture of agarose and anionic polysaccharides called agaropectin. It has been recognized that the agaropectin fraction has an adverse effect on many cells, in particular, inhibiting growth<sup>65</sup>. Indeed, well-known discrepancies in the minimum inhibitory concentration (MIC) of antibiotics tested in nutrient broth, with respect to test results on agar, have been traced to these anionic substituents of agar.<sup>66</sup> On the other hand, Ho and Ko found agarose to be ideal for testing antifungal agents<sup>67</sup>. Had there been any doubt about which gel to use for the GMD method, this report would have removed it. It also raises the question of whether the highly anionic nature of alginate and carrageenan has similar effects on cell growth and viability.

There is little diffusion information available for these gels, *e.g.* diffusivities of compounds in agarose gels *vs* water. Native agarose has a reputation for being very porous, and is nearly electrically neutral. One expects that suitably small molecules should diffuse very freely through the inter-fiber water. On the other hand, path lengths might be increased by pore tortuosity, and since diffusion times goes as the square of diffusion distance, a significant effect on apparent diffusivity might appear. Moreover, the LMP derivatives have smaller pores (see Table 2.3), so to the extent to which diffusion is impeded by the molecular sieve effect, transport may be significantly affected in LMP, and especially ULMP derivatives.

Agarose it is a favorite anti-convective support for electrophoresis of large particles such as DNA fragments, large proteins, cellular fragments, and even viruses. For a given agarose concentration, there is an optimal range of molecular "sizes" which can be separated; this range reflects the distribution of effective pore sizes about its mean, at that gel concentration. As molecules increase in size from zero, they find fewer, longer pore-paths of suitably large size, thus taking longer to move through

the gel. In the presence of an electric field, molecules which are "too small" move at essentially the same speed, unimpeded by the gel, whereas molecules that are "too large" cannot fit through any pores, and thus do not move appreciably from the gel origin. Electrophoresis specifications provide interesting, conflicting information. For example, for a 2½ % LMP gel, the "optimal range" for separation of DNA fragments is about 40 to 450 base pairs,<sup>52</sup> a MW range of 26kD to 290kD. On the other hand, a 5% ULMP gel can be used for electrophoresis of "some native proteins" in the range 50kD to 2000kD;<sup>53</sup> a 5% ULMP gel is much more sieving than a 2½ % LMP gel, yet its useful MW separation range is higher. Presumably, some of this is explained by a difference in conformation; native proteins are usually compact and globular, whereas DNA fragments are typically linear and are thus have higher hydrodynamic drag<sup>42</sup>. A complete description of the interaction of DNA and agarose gel is an area of ongoing research<sup>68</sup>. Nevertheless, these findings may be summarized in a warning, that deceptively small molecules, *i.e.* 26 kD, may interact in a significant manner with 2½ % ULMP agarose gels.

It should be pointed out that, for the experiments presented in this thesis, the molecules which need to be delivered to the microcolonies are very small; the nutrients (glucose, oligopeptide fragments, and vitamins), fluorescent dyes (propidium iodide, fluorescein isothiocyanate), and antifungal agent (Amphotericin-B) are all less than 5 kD. Thus, we would not expect molecular sieving to be a factor here. On the other hand, in 2% κ-carrageenan gel, a marked decrease in diffusivity for glucose (MW 180) has been reported (*v.i.*); so other factors, such as gel charge, may have significance.

In another application, sulfonated agarose beads are used for ion-exchange chromatography for the separation of amino-acids and peptides; molecules with net positive charge displace ions and stick to the negative sulfate groups. We must then expect the same behavior from negatively charged molecules in GMDs, including nutrient oligopeptides, amino acids, *etc.*, as well as dyes such as propidium, which have net positive charge at the pH (6.5-7.0) of these experiments. It should be noted that the

LMP and ULMP agaroses have a low sulfate content (0.1% w/w), or about one sulfate per 310 agarobiose dimers. Consequently, in the presence of an excess of medium, one would expect these sites to be quickly saturated, with no large overall effect on the bulk concentration. The extent to which such bound molecules could "clog up" the pore network, or otherwise hinder the transport of other molecules is not known, and may merit further study.

In structure, there are many similarities between agarose and  $\kappa$ -carrageenan; in the gel state they are both thought to exist in double-helical form<sup>47,69</sup>, they both have a backbone of variously substituted poly-galactose, with the same linkages, *etc.*, so perhaps some additional caution is warranted in the use of agarose. For instance, the concept that the hydration of  $\kappa$ -carrageenan may impede diffusion (*v.i.*) may be applicable to agarose as well.

Alginate gels are reported to provide good viability. Unfortunately, as reviewed by Hulst<sup>70</sup>, "the way to express cell viability is open for discussion", as least as of 1984. Again, the issue is that for the bioreactor community, the measures of interest are macroscopic and commercial; *e.g.* respiration, enzyme activity, *etc.* Once immobilized, and assuming sufficient nutrition, long-term viability is commonly better than that of cells in free suspension; in one case, alginate-entrapped plant cells have been kept biologically active for 6 months<sup>71</sup>.

In a review of diffusion studies<sup>43</sup>, it is reported that the molecules glucose (MW 180), tryptophan (204), and  $\alpha$ -Lactalbumin (15kD) exhibit the same diffusivity in algin gels (up to 4% w/v). However, in 2% gels, there was no measurable inward diffusion of bovine serum albumin (BSA; 69kD), and  $\gamma$ -globulin (155kD) was seen only to diffuse *out* of gels, but not in. Possibly, this is due to an alteration of the gel structure when the large molecules are present at the time of gelation. Another type of transport problem was reported by Felix and Mosbach: a loss of activity of two key enzymes due to the sequestering of positively charged NADP<sup>+</sup> cofactors by the

alginate gel. One of the difficulties in applying or comparing these results (and indeed in using alginate) is that there is a wide batch-to-batch variability in the material composition, *e.g.* mannuronic:glucuronic acid ratio; inasmuch as diffusion rates seem to also vary batch-to-batch, at least one investigator recommends testing each batch for diffusion problems before further use<sup>72</sup>.

κ-carrageenan is also reported to give good viability, but the caveats applied to alginate, *i.e.* regarding how viability is assessed, apply here as well. From a diffusion perspective, there is reason to worry. Although there seems to be little data available for carrageenan, in the same summary of diffusional studies<sup>43</sup>, there is consistent evidence that even for molecules as small as glucose (MW 180), the apparent diffusivity may be decreased by 25% in a 2% carrageenan gel. In another study, there was no measurable diffusion of BSA in 3% carrageenan. One suggested explanation is that water molecules, strongly associated with the carrageenan fibers, greatly reduces the inter-fiber space available for diffusion<sup>73</sup>.

### 2.1.6: Immobilization Methods

Historically, there have been a few methods by which cells have been immobilized in gel droplets:

- dispersion : by mixing the hydrophilic cell/sol suspension into an hydrophobic phase in excess, an emulsion of liquid droplets is formed; soy, paraffin, silicone and mineral oils are popular hydrophobes. The droplets are gelled by cooling the suspension, and then recovered to an aqueous nutrient medium, *e.g.* by centrifugation. The gelation must be temperature dependent, requiring either agarose<sup>29</sup> or carrageenan<sup>37</sup>.
- extrusion: cell/sol suspension is dripped through a needle into a gelation medium; *e.g.* alginate into CaCl. Gelation of the surface begins immediately, and proceeds inward to the center of the droplet. Typical droplet size: 2-4 mm<sup>37</sup>.

- extrusion + air stream: same as extrusion, except that drops are blown off the end of the needle by a puff of air<sup>37</sup>. Reduces droplet size to 0.2-1 mm range.
- vibrating nozzle: same as extrusion, except that needle is fitted with a nozzle, and vibrated rapidly (co-axially) to break up the stream. The drop size is controlled by the jet diameter, vibration frequency, and jet velocity<sup>74</sup>. (This principle is also used in flow cytometer sorters and ink-jet printers)
- molding: the sol is poured into molds and cooled. Clearly, this is limited to materials which at least partially solidify upon cooling, such as carrageenan<sup>37</sup> or agarose-gelatin<sup>57</sup>.

### Comparison of Methods

Dispersion methods have the major drawback that droplets thus formed are not a uniform size. In applications where uniformity is required, size fractionation can be done, but this can greatly diminish the yield, *i.e.* the number of initial cells which end up in usable droplets. This limits the usefulness of the method to those cases where cells are cheap and plentiful. The use of emulsifiers to favorably influence the droplet size distribution has been reported (G. Williams, personal communication), but caution against the detrimental effects of such compounds on viability is warranted.

The other drawback to dispersion is the need to recover the droplets from the continuous phase after gelation. It is particularly important to remove all the oil from the droplet suspension in applications such as drug testing; many drugs will partition into both hydrophilic and hydrophobic phases, thus making it harder to deliver a known concentration to the cells. In addition, for large-scale operations, a method to remove all the droplets from the oil phase is highly desirable, so that the oil can be recycled; otherwise, a rather large waste-disposal problem is apparent.



Extrusion clearly has the benefit of simplicity. To some, the chief drawback is the low throughput, typically 100-500 cc/hour, or about 20-100,000 drops/hour. This output can be increased by using multiple needles, at the expense of droplet uniformity<sup>75</sup>. From the perspective of this thesis, the major drawback is the droplet size; as detailed in the previous section, diffusional limitations would only support cell growth on the periphery of droplets in this size class.

Vibrating orifice methods greatly increase output, reportedly by two orders of magnitude<sup>74,76</sup>. Along with flexibility in droplet size, this method seems very powerful. Unfortunately, viability problems have been reported by some practitioners of this method. In particular, although plant cells seem to retain viability<sup>74</sup> problems have been reported for microorganisms<sup>77</sup>. This is consistent with informal reports of viability problems in the context of cytometric sorting of some mammalian cells, *e.g.* stem cells (J.Bender, personal communication). This raises the possibility that some cells cannot tolerate going through a vibrating orifice device; certainly, in doing so, they would be exposed to considerable shear stress, which might cause membrane disruption. Plant cells may benefit from their cell walls, which could serve to stabilize their membranes, although microorganisms would be expected to have the same advantage.

In the context of GMD production, the vibrating orifice method suffers from the physics of droplet formation: the droplet size is about twice the nozzle orifice. Thus, to get droplets less than 100  $\mu\text{m}$ , one must extrude through a 50  $\mu\text{m}$  nozzle. This is quite difficult to do without clogging; especially for agarose for which any localized cooling can cause the whole apparatus to clog. Nevertheless, a group in Israel has reported success in using such a device with agarose<sup>77</sup>; interestingly, the agarose reportedly starts out at 0.6% (w/v), with low enough viscosity to flow freely, but due to the small particle size, evaporation increases the concentration to the 2% vicinity while the particle is in midflight, thus increasing the gel strength. The effect of the rapid change in the cell's environment, particularly in external osmolarity, that must

accompany such a rapid evaporation is not yet known, though one would presume that the cells are substantially stressed.

### 2.1.7: Gel Microdroplets: Summary and Protocol Overview

For the purposes of this thesis, the overriding consideration has to be that the material and method used for cell immobilization should be as benign and invisible as possible to the cell. With the goal of culturing cells and measuring growth in the presence of different drug levels, it is unacceptable to use a process which may change a cell's viability, ability to metabolize normally, etc. For this reason, the choice of agarose, and specifically the ultra-low melting point agarose, was clear. Given the size requirements, the use of a dispersion method is also clear; in addition to being milder to the cells, it is much cheaper than any vibrating orifice apparatus which could make suitably small droplets.

The full details of the GMD protocol are presented in Appendix I. Here, I present a functional summary:

- GMDs are composed of 2.6% (w/w) ultra-low melting point (ULMP) agarose, *e.g.* Sigma type IX, or FMC SeaPrep. At this concentration, the agarose melts at about 50°C, and gels at 15-20°C. The critical temperatures for culture of bacteria and yeast, *i.e.* 27 and 37°C, are within the intermediate range for thermal hysteresis.
- GMDs are prepared by dispersing molten agarose, at 37°C, into an excess of mineral oil, also at 37°C, to form an emulsion. The emulsion is transiently cooled at 5°C, causing the molten agarose to gel, and is then reverted to 37°C; due to the thermal hysteresis property, the GMDs remain in the gel state, and can be transferred out of the oil phase into an aqueous nutrient medium such as YPD.
- GMDs are inoculated by mixing a cell suspension aliquot into the molten agarose, at 37°C, prior to the dispersion into mineral oil. Cells are

sequestered into individual liquid microdroplets by the dispersion step, and immobilized in the droplet upon gelation.

- GMDs prepared by the dispersion method have a wide variance in size, from 5  $\mu\text{m}$  to 500  $\mu\text{m}$ . Prior to flow cytometry, GMDs of a narrower size range (20-44  $\mu\text{m}$ ) are recovered from the preparation, by sieving.

It is admittedly possible that the combination of shear stress involved in the dispersion, and the transient cooling required for gelation, may affect the cells. As will be seen, there was no indication of such an effect in my experimental results, nor in previous work with mouse hybridoma cells<sup>78</sup>. On the other hand, some experimental results with the bacteria *E.coli* have exhibited a significant lag phase after immobilization in GMDs; this may be an indicator of cell stress (G. Harrison, personal communication).

With these three cell types, there has also been good (> 95%) short-term viability. However, it should be stressed that all three sets of experiments were terminated after no more than 4 cell divisions; thus long-term viability was not assessed. In other experiments, Chinese Hamster Ovary cells have been cultured in GMDs out to at least 7 divisions (G. Williams, personal communication). Thus, there is some reason to believe that cells which survive the immobilization process have good long-term viability.

In general, antibiotic testing should require only a few division times, although in the case of some slow growing organisms, *e.g.* *M. tuberculosis*, this would imply viability for a few days. In addition, it remains to be demonstrated that short-term inhibition of growth serves as an accurate predictor of clinical effectiveness for antibiotics.

## Section 2.2: Flow Cytometry

In this section, I will discuss the other technology which is central to the method of this thesis: flow cytometry. In simplest terms, the function of a flow cytometer is to measure cells. Relative to other methods of measuring cells, such as light microscopy, a flow cytometer offers some distinct and critical advantages:

- It is quantitative. Under a microscope, one can tell that a stained cell is red, or that one stained cell is more red than another. The flow cytometer will quantify the redness, with high resolution. The system used for this work can distinguish at least 1,000 levels of red intensity.
- It is fast. Flow cytometers are usually designed to measure up to 10,000 cells per second. For a variety of reasons, an event rate of only a few hundred GMDs per second were used in this work, but this still allows measurement of 10,000 GMDs in less than 2 minutes, much faster than microscopy. Moreover, there is no fundamental reason which would prohibit GMD rates of several thousand per second.
- Both functional and structural measurements can be made using specialized fluorescent stains. Functional dyes can be used to signal cell pH, membrane potential, etc. Structural dyes can signal total cell protein or nucleic acids; in combination with monoclonal antibodies or cDNA, can signal the presence or absence of very specific entities.
- Multiple parameters are easily measured. This permits measurement of several structural and functional signals simultaneously. By using optics to look in different wavelength bands, and electronics and software which perform de-correlation or de-convolution, measurements from several (5) overlapping spectra can be used. These would be subtle changes in hue to the microscopist.
- Sorting of interesting cells from a population is feasible. For each cell, the optical measurements are compared with appropriate thresholds, and

used to activate a cell sorter somewhere downstream from where the measurements are made.

The advantages of flow cytometry are apparent, but the cost is high. This functionality requires some delicate and somewhat sophisticated fluidics, optics, and electronics. Along with requiring a technically sophisticated operator, this pushes the price of most instruments above \$150,000. Somewhat less expensive flow cytometers are available,<sup>79</sup> as is less expensive technology, such as video microscopy. Frequently, but not always<sup>22</sup>, the usual tradeoff for lower cost is fewer capabilities, and in some cases, lower resolution measurements.

Inasmuch as cost and ease-of-use greatly affect the acceptability of any new clinical technology, I will discuss the interaction of GMD technology with the performance required of the instrumentation. In particular, it is the case that the use of GMDs should make it possible to use lower-resolution, and thus cheaper, equipment for many applications.

### 2.2.1: Principles of Flow Cytometry

There are several flow cytometer designs available from the various manufacturers, again mostly trading off cost and complexity for performance. A nice overview of the competing designs and their relative merits is given by Shapiro<sup>22</sup>. In this section, I will present an overview of the principles which are common to flow cytometers, and present some details of the Ortho flow cytometer used for this thesis, with these goals in mind:

- Present enough detail to make following discussions, especially of data, comprehensible
- Define terminology used later on
- Lay the groundwork for discussions of the interaction of flow cytometer technology with GMD methods.

### The Flow Cell

The heart of the flow cytometer is the flow cell. Its job is to: (i) cause the cells in sample to line up, single file, so they can be individually measured, and (ii) present the cells to the optical subsystem (*v.i.*) for measurement. The major components of the flow cell are show here in Figure 2.4:

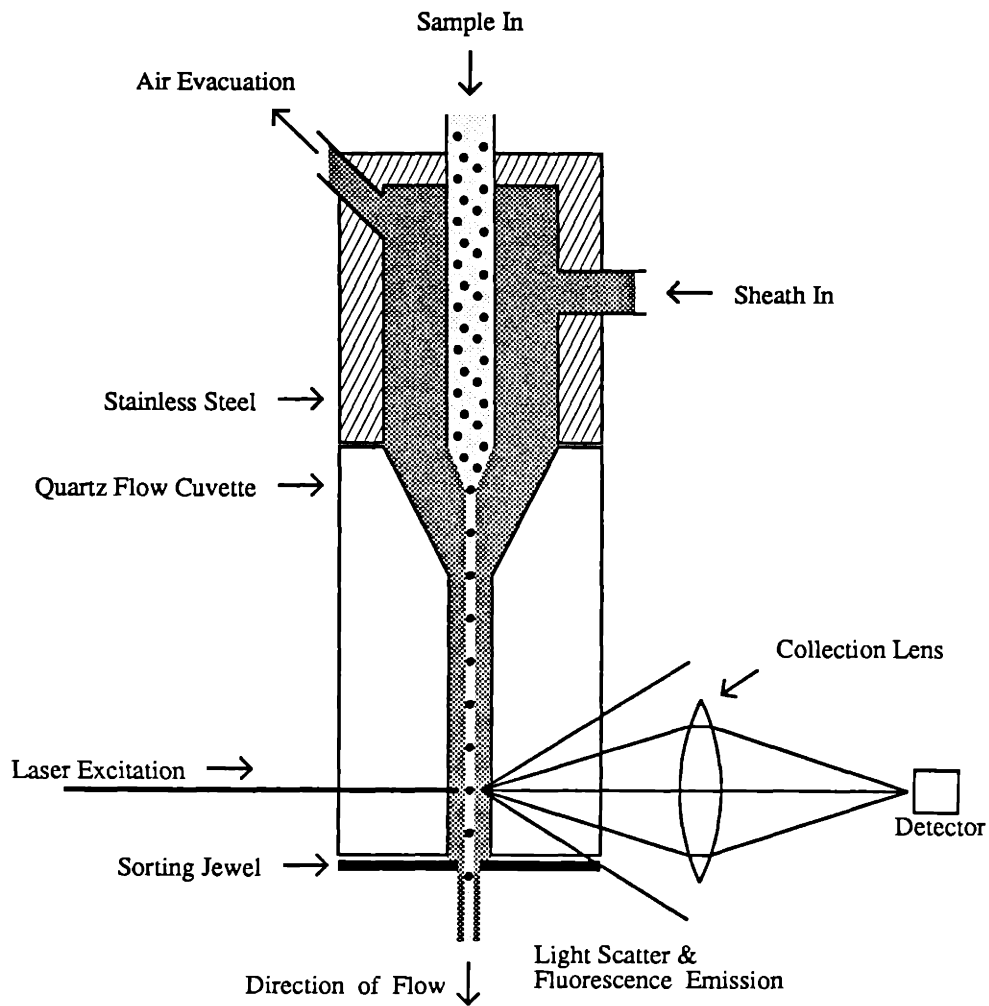


Figure 2.4: Ortho flow cell (schematic representation)

## Hydrodynamic Focusing

The flow cell exploits the principle of hydrodynamic focusing to accomplish its mission. The flow cell is constructed so that as the sample flows through the flow cell, it is surrounded at all times by a sheath fluid. Typically, an isotonic electrolyte such as buffered saline is used; an electrolyte is required for electrostatic sorting, *v.i.*. For the experiments presented in this thesis, the sheath is de-ionized water. The flow cell geometry is such that the sheath flow is laminar in the distal part of the cell, at typical flow rates. The sample is injected into the core of this laminar flow field; the differential between the sample and sheath pressures is adjusted so that the sample occupies only a very small part of the flow field, ideally, just the central streamlines. In practice, the optimal sample pressure is incrementally greater than that required to prevent retrograde flow of the sheath up the sample inlet. This has the desired effects:

- The cells in the sample suspension enter the sheath flow one at a time, allowing individual measurements to be made.
- The position of the sample in the sheath is quite stable, and predictable, *i.e.* to the extent to which the flow is stable.

When optimally adjusted, the sample stream is about 10  $\mu\text{m}$  in diameter; though the diameter can be increased to 50  $\mu\text{m}$  or more by increasing the sheath-sample pressure differential.

It has been reported that the stream diameter increases in the vicinity of an object contained in the stream, *e.g.* a cell<sup>80</sup>. As one would expect, the effect gets stronger as the object diameter approaches that of the sample stream. For a 7  $\mu\text{m}$  erythrocyte in a 10  $\mu\text{m}$  sample stream, the effect is very apparent; as the sample stream is increased to 50  $\mu\text{m}$ , the effect becomes undetectable. Although further study would be needed to be definitive, it is almost certain that GMDs, which for my work are all at least 20  $\mu\text{m}$  in diameter, also deform the sample stream. In my work, the sample stream also carries a red fluorescent dye (*v.i.*); thus, sample stream perturbations

may be transduced into red fluorescence pulses, and contribute to the apparent red fluorescence of unoccupied GMDs. This will be discussed more fully in the next section.

### Sample Illumination

Optical measurements are made by illuminating the sample with a monochromatic source, and measuring scattered light and fluorescent emission, as shown. In cases where relatively high power and signal-to-noise are required, the illumination is invariably a laser. When lower performance is tolerable, a mercury-arc lamp and barrier filters may be used; as usual, the trade-off is a significant cost advantage. On the other hand, the proliferation of small Helium-Neon (HeNe) lasers makes them attractive as cheap, quiet sources; their disadvantage is a relatively limited number of dyes which are excited by their emission (635 nm), and problems related to detection of the long-red to near-infrared emission of those dyes. For the work presented in this thesis, the sample illumination is an Argon-ion laser operation at 488 nm (blue-green) and typically 35 milliWatts.

The sample stream and illumination cross paths in a region called the interrogation volume. Lasers used in cytometry operate in  $TEM_{00}$  mode, implying a Gaussian intensity profile. The beam is further shaped by a crossed-cylinder lens (barrel lens), so that the dimension of the beam at the interrogation volume is 5  $\mu\text{m}$  high and 125  $\mu\text{m}$  wide, measured at the plus-and-minus one standard deviation points of the beam. As discussed later, this is important in making measurements on GMDs, since the vertical height is smaller than many cells of interest, and certainly smaller than most microcolonies of interest.

The non-uniform intensity profile also introduces an important source of measurement variability; cells or microcolonies which traverse the flow cell at differing radial positions will be illuminated with differing intensities. Gray found that, for a disc 7  $\mu\text{m}$  in diameter and 2  $\mu\text{m}$  in thickness, a variation on the order of 2% could be ex-



pected in the measured fluorescence (area mode), as the disc was moved from the illumination center to the edge of a 10  $\mu\text{m}$  sample stream<sup>80</sup>. These dimensions are comparable to those of a moderate size yeast microcolony, so the results provide at least a rough estimate of the errors we might expect; as will be seen in Chapter 3, this variability is minor in comparison to the biological variability in stainable material seen in a sample of yeast cells.

### Flow Cuvette

In the Ortho system, measurements are made in a flat-faced quartz cuvette. This optical configuration is one of the best available, in that it minimizes problems due to interfacial refraction and reflection, and especially variations in same arising from vibrations in the system (either intended or unintended). For comparison, some other commercial systems use a "stream-in-air" configuration, in which the combined sheath and sample are squirted into air, where they intersect the illumination. The benefit of course is eliminating an expensive component; the Ortho flow cuvette costs about \$1,500 to replace. The tradeoff is decreased measurement performance. The surface of the sheath is cylindrical at the point of intersection, and is considerably less uniform than that of quartz cuvette, so there is a variable, generally cylindrical lensing effect, degrading the optical measurements. However, the noise introduced here is often small with respect to the signals being measured, for example measuring DNA in mammalian cells; in these cases, very good measurements can be obtained with this configuration. It is likely that GMD-based methods, by providing a means of increasing the intensity of the signal to be measured, will make it reasonable to use a fluidic-optical system which is more noisy, but much less costly, than that in the Ortho system.

As cells or other objects pass through the interrogation volume, light is scattered by the objects. In addition, the object may absorb some of the incident light energy, and re-emit a fraction of it as fluorescent emission. Light is scattered and re-emitted in all directions; a fraction of the scattered and re-emitted light is collected by one or

more collection lenses, which, through the optical subsystem, delivers the collected light to the opto-electronic subsystem.

### Sorting

As mentioned earlier, many flow cytometers are able to sort interesting cells from the sample, on the basis of the measurements made in the flow cell. In many, including the Ortho, this is accomplished in the following manner.

- break up the sheath/sample stream into uniform droplets
- determine the time delay between the presence of an interesting cell in the interrogation volume and its appearance in a droplet
- deflect the droplets containing interesting cells away from the bulk of the sheath/sample flow by charging the interesting droplets as they are formed, and passing all of the droplets through an electric field to effect the deflection.

Breaking up the stream into uniform droplets is accomplished by passing the sheath/sample stream through a round orifice, the sorting jewel, vertically vibrating the entire flow cell at an appropriate rate. The size of the droplets formed depends on the size of the orifice and the vibration rate, as well as the viscosity of the fluid, and the size of the cell (if any) in the droplet being formed<sup>81</sup>. Other things being equal, larger droplets require larger orifices and slower vibrations. In addition, the sorting of large cells is limited by the physics of droplet formation. One rule of thumb<sup>82</sup> is that the largest cell which can be reliably sorted is 1/3 the orifice diameter. Historically, the largest available jewel has been 100  $\mu\text{m}$ , thus limiting sorting to GMDs less than 35  $\mu\text{m}$ . Lately, as investigators have wanted to sort larger entities, such as pancreatic islet cells, manufacturers have offered 200  $\mu\text{m}$  orifices<sup>83</sup>, and a 400  $\mu\text{m}$  orifice is soon to be offered by Becton-Dickinson (S. Conner, personal communication).

The sorting mechanism for the Ortho system was removed for this thesis work, primarily to reduce a problem of clogging which appears for larger ( $> 50 \mu\text{m}$ ) GMDs. For this thesis, sorting was done on the Becton-Dickinson FACStar cytometer/sorter in the MIT Center for Cancer Research, which uses different optics than the Ortho, but the same sorting principle.

### **Physical Dimensions for the System Used**

- flow chamber:  $250 \mu\text{m} \times 250 \mu\text{m}$  square
- sample stream diameter:  $10 \mu\text{m}$  estimated
- GMD diameters:  $20 \mu\text{m}$  to  $44 \mu\text{m}$
- interrogation volume:  $5\text{-}10 \mu\text{m}$  vertical  $\times$   $125\text{-}150 \mu\text{m}$  horizontal
- sample flow rate:  $\sim 1$  meter/sec

### **2.2.2: Optical Subsystem**

As described above, light scattered or emitted by cells passing through the interrogation volume is collected by collecting lenses and delivered to an optical subsystem for measurement. The Ortho optical subsystem is depicted in Figure 2.5. Again, I will describe this subsystem to the level of detail needed to discuss its impact on GMD measurements.

The optical subsystem is set up on an optical bench. It is comprised of a forward (narrow-angle) and right-angle subsystems. Each in turn consists of :

- collection lens: a high numerical-aperture microscope lens
- dichroic mirrors: reflect light whose wavelength is above some threshold, and passes the rest through (or vice versa)
- barrier filters: pass light whose wavelength is within a specified passband
- blocker bar: removes the light component which is co-axial with the laser

from the forward subsystem. This is required to remove the laser from the forward optical signal, since it is much bigger than any of the optical signals we are trying to measure, and if left in, would damage the sensitive PMTs downstream. The axial component can be measured with a photodiode to derive the "axial light loss", or shadow, that results when a cell passes through the interrogation volume.

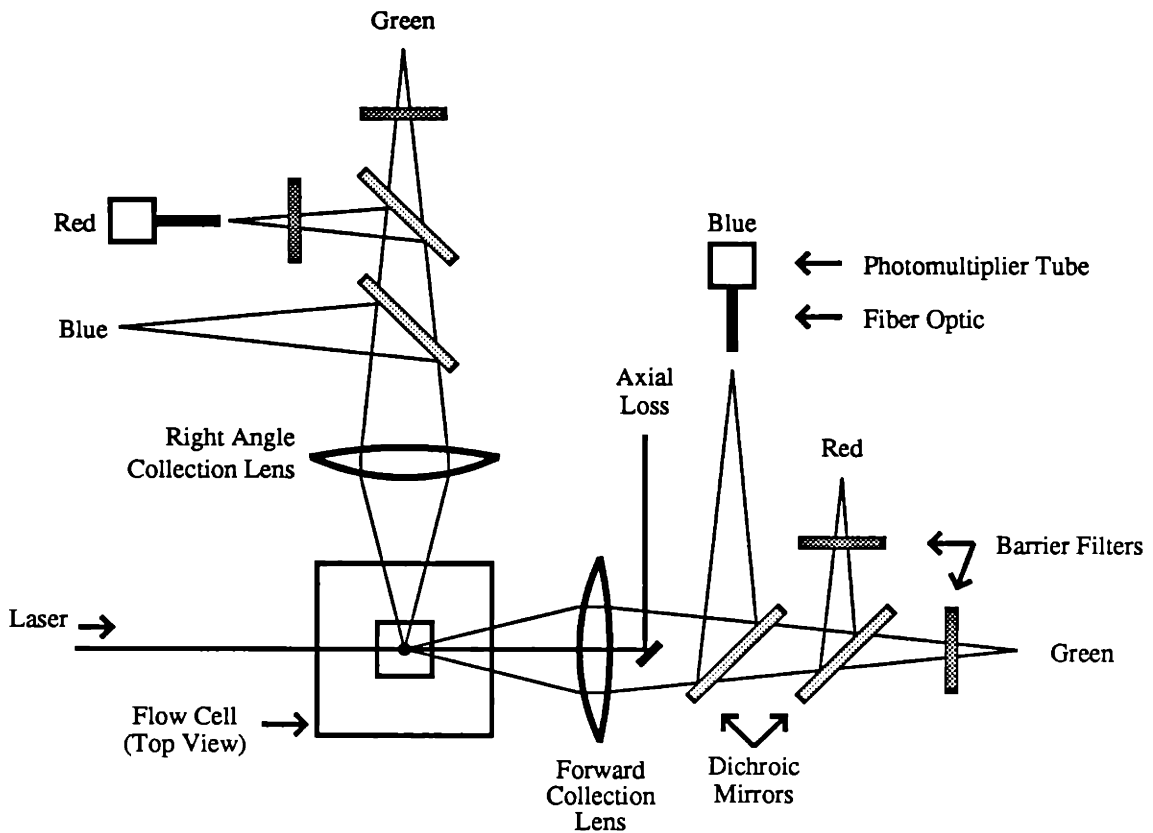


Figure 2.5: Optical Subsystem of Ortho Cytofluorograph

The effect of the optics is to split the light collected by the collection lens into three color bands, which are loosely described as "red", "green", and "blue". For the Ortho system, these bands are:

- Red: wavelengths longer than 630 nm. (longpass)
- Green: wavelengths in the band 515 to 530 nm. (bandpass, tuned to fluorescein emission)
- Blue: wavelengths < 490 nm. (shortpass)

The wavelength cutoffs of these bands are not very sharp; for instance the red barrier filter goes from 1% to 98% transmission over the range of about 610 to 680 nm; 630 nm is its 50% transmission point. However, the passbands are sufficiently separated that there is very little overlap between them. Unfortunately, the emission spectra of popular dyes, such as FITC, are sufficiently broad as to show up in both the red and green channels. However, this cross-channel emission can be corrected for computationally, so much so that using multiple dyes and lasers, four-color analysis can be done in a straightforward manner.

A disadvantage of the configuration shown is that the dichroic mirrors do not fully transmit (or reflect) even in their transmission (reflection) band; rather some fraction, as much as 20% can be absorbed and lost. This is especially bothersome for the Red and Green channels, since emitted light must experience two dichroic mirrors before getting to the barrier filters. An alternate, improved configuration, not available on the commercial machines, has been proposed by Steinkamp<sup>84</sup>. The ability to measure very small biological signals, such as bacterial DNA, with standard commercial cytometer equipment has been demonstrated<sup>85,86</sup>. Others have found it necessary, when measuring such weak signals, to remove all the dichroic filters, and use only a barrier filter<sup>87</sup>. This clearly reduces the usefulness of the cytometer. On the other hand, by containing the progeny of initial cells, GMDs effect a kind of biological amplification, that should make it possible to make such measurements without modifying the cytometer in this manner.

The Ortho system has four PMTs, of which two or three are used for the experiments presented here. One selects the optical parameters to be measured by connecting the PMTs to the bench-mounted apparatus with fiber optic light guides.

### 2.2.3: Electrical Subsystem

The electrical subsystem is comprised of the photomultiplier tubes (PMTs) and their pre-amplifiers. The job of the PMTs is to transduce the photon flux coming in to an electrical current. Each PMT current is input to a pre-amplifier, which converts it to a voltage, bandpass filters it, and amplifies it for further processing.

The pre-amplifiers also perform a baseline correction operation. The baseline correction circuit measures and averages the baseline voltage (ignoring pulses which occur when a cell goes through the interrogation volume), and subtracts it from the instantaneous voltage to produce a zero baseline. Baseline correction is required because there is almost always a DC current produced by the PMTs, even in the absence of anything "interesting" in the interrogation volume. Sources of this signal include low-level light leakage, and PMT leakage and dark current. However, for many experimental protocols, including the ones presented in this thesis, the major source is fluorescence of one or more dyes present in the sample stream. Indeed, some dyes, such as the propidium iodide used in my protocols, *require* the presence of unbound dye in sample solution, because the dye binds in an equilibrium fashion to its binding sites, rather than covalently. As discussed above, it is likely that the presence of a GMD in the sample stream perturbs the stream, notably increasing its diameter; such an event would cause a transient increase in fluorescence, which would be transduced into a voltage pulse above the baseline. This effect may be a contributor to the apparent red fluorescence of empty GMDs, discussed in the next section.

Thus, the output of the pre-amplifier is, for each object passing through the interrogation volume, a voltage pulse, whose amplitude (from 0 to 10 Volts) signals the instantaneous light intensity, above baseline, collected by the corresponding section of

the optical subsystem. Strictly speaking, the instantaneous signal is smoothed somewhat by the bandpass characteristics of the pre-amplifier, with a high-frequency cutoff in the vicinity of 1 MHz. The output of the electrical subsystem is a set of (up to 5) pulses for each such object, which characterize some physical or biological aspect of the object. These pulses are input to the Data Acquisition System (described in Appendix 2), and from thence into data analysis programs.

## Section 2.4: Flow Cytometry and GMDs

As described in Chapter 1, the function of flow cytometry in the context of GMD-based methods is to provide a measure of the microcolony biomass within occupied GMDs, by measuring the amount of a fluorescently labeled indicator biomaterial within each one. In practice, this is a straightforward extension of flow cytometry of cells, and is depicted in Figure 2.6.

In the schematic shown, all of the GMDs (grey circles) are occupied with up to 4 cells (small, white circles); to the right of each GMD is a sketch of the expected PMT pre-amp output, as the GMD passes through the interrogation volume. As shown here, when the height of the laser beam at the interrogation volume is less than the size of a microcolony, the effect is to "slit-scan" the microcolony as it passes by.

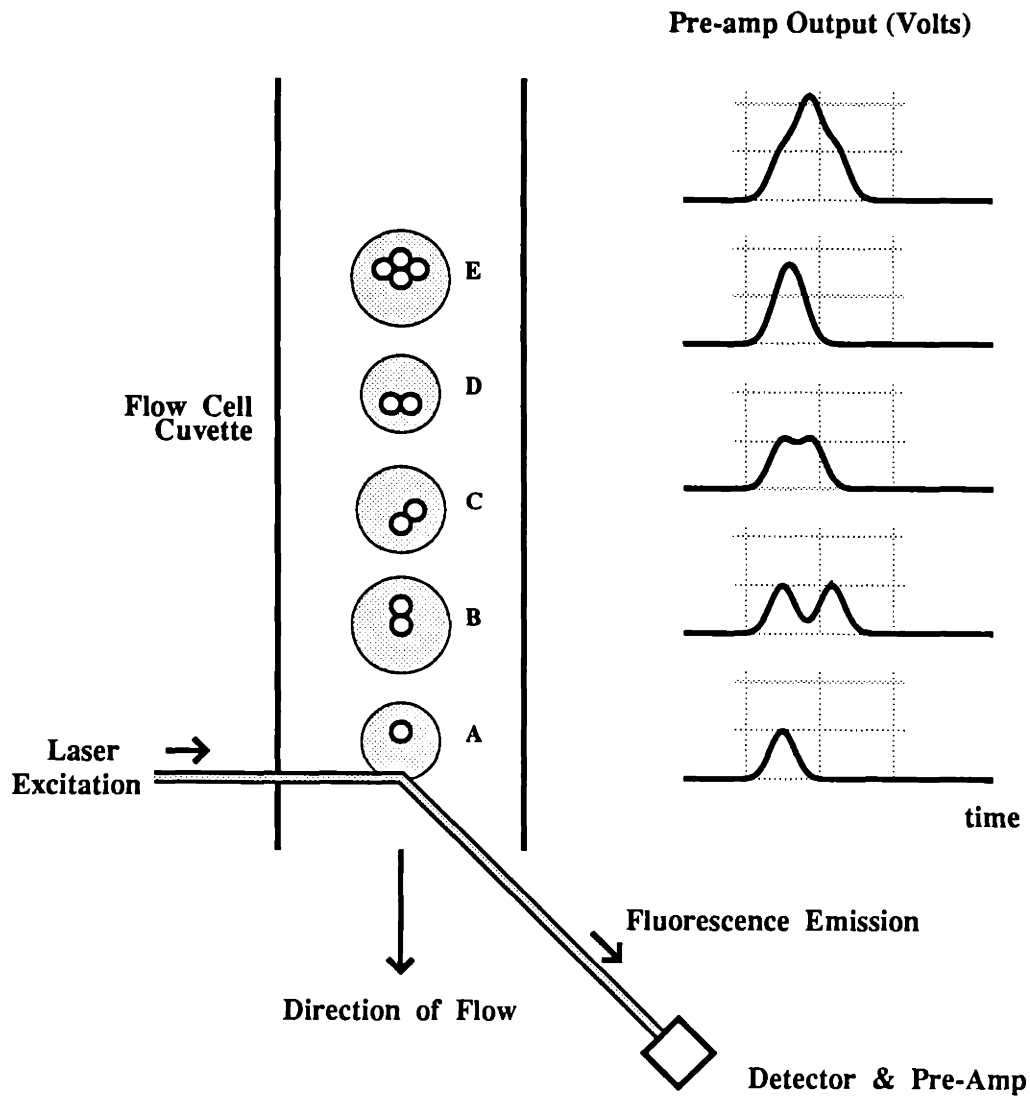


Figure 2.6: Flow cytometry of a GMD sample

The voltage sketches indicate a point which bears emphasizing: the best measure of *total* biomass indicator in a microcolony is the *area* (i.e. time-integral) of the voltage pulse which appears at the pre-amp output when a GMD passes the laser beam. This is because:

- in general, the microcolony will be bigger than the height of the laser beam (5-10  $\mu\text{m}$ ) at the interrogation volume, though this will not generally be true for small bacterial microcolonies.



- microcolonies are expected to be asymmetric, causing the pre-amp output to depend on the orientation of the microcolony as it traverses the interrogation volume. The tendency of flow cell hydrodynamics to orient non-spherical objects along the flow-cell axis<sup>81</sup> will likely be reduced by the spherical, convection-resistant GMD. The pulse area for symmetric, uniformly sized and stained objects can often be inferred from pulse height, for instance; however, as made clear by the waveforms of Figure 2.6, pulse height is not a good predictor of pulse area, nor of total biomass.

As it turns out, total cellular biomaterial is one of the most common parameters of interest, and the cells being studied (usually mammalian) are also larger than the laser waist. Thus pulse area is a very commonly used flow cytometry "mode", and there is nothing unusual about GMD cytometry in this regard.

#### 2.4.1: Triggering on GMDs

The process of measuring pulse areas in general, as well as the particular implementation used for this thesis, are discussed in Appendix I. Here, I wish to summarize and to make a point regarding GMDs: immobilizing microorganisms in GMDs makes it easier to make flow cytometric measurements of them, and relaxes some of the performance requirements for the cytometer.

For a variety of reasons, pulse area measurements are made "in real time", as the sample is run through the cytometer, as opposed to storing the waveforms and making the measurements at a later time. As detailed in Appendix I, this requires first detecting the pulse, and in particular the beginning and end of the pulse, in order to turn the measurement circuits on and off. For bacteria, typical pulse widths are only 1-2 $\mu$ sec, so this requires some moderately fast circuitry. Additionally, the optical signals arising from bacteria are relatively small, requiring a good (expensive) optical subsystem to derive a reliable trigger signal.

On the other hand, GMDs are relatively big, somewhat bigger in fact than the mammalian cells which cytometers more commonly measure. Cytometric measurement of GMD-immobilized microorganisms is made easier by triggering on the optical signals, such as light scatter, arising from the GMD. In essence, the scatter associated with the GMD gives "advance warning" to the cytometric circuits that a biomaterial pulse may be imminent, and enables the measurement circuits to be turned on in time to make a good measurement. The light scatter due to GMDs is a fairly strong signal, and can be fortified by adding scattering centers to the gel;<sup>88</sup> thus, obtaining a reliable trigger signal from GMDs does not require the same high optical performance required for triggering on free microorganisms.

The penalty for making pulse-area measurements triggered on GMD scatter is that if the GMD is even weakly fluorescent, the integral of that fluorescence over the volume of the GMD can result in a substantial signal; this is considered in the next section. For some applications, it will be a good idea to collect a measure of GMD size, *e.g.* width of the scatter signal, in order to attempt compensation of the biomass signal for fluorescence of the GMD; as will be evident in the next section, this compensation may be non-trivial.

#### 2.4.2: GMD Flow Cytometry and Fluorescent Stains

The final component of the GMD-based growth assay is the choice and application of fluorescent labels for the indicator biomaterial. There are several reasonable choices from the perspective of the biology, and I will discuss two specific examples momentarily. First, however, it is important to consider the interaction of dyes in general with GMDs and flow cytometry.

It is useful for this discussion to divide the universe of dyes into two parts:

- equilibrium dyes: associate with the indicator biomaterial, *M*, according to the equilibrium reaction:  $D + M \rightleftharpoons DM$ . At all times, some fraction of the "free" dye (*i.e.* unassociated), *D*, will be present, as quantified by the

dissociation constant for the reaction. Usually, the dye-indicator complex has different fluorescence properties than the free dye, so the amount of bound dye can be quantified.

- covalent dyes: attach themselves "permanently" to the indicator biomaterial, M, via a chemical reaction of the form:  $D + M \rightarrow DM$ . In theory, any excess unreacted dye can be washed away after the reaction is complete, thus removing a potential source of error.

As indicated previously, the goal of measuring the total biomass in an occupied GMD can be confounded by non-specific staining of the GMD itself; *i.e.* any dye which is associated with the gel material generates a signal which is added to the signal due to dye "specifically" bound to the indicator biomaterial. Due to the integration operation required to measure total biomass, even low levels of non-specific labeling can be significant, especially when the integration is triggered on the GMD scatter signal.

In particular, experience in our laboratory has indicated a significant effect when attempting to measure very low level biomass signals, such as yeast DNA, or bacterial protein or nucleic acids. GMDs do provide a work-around for this problem; by allowing growth to occur, these biomass signals increase, and quickly become large with respect to the integrated GMD fluorescence signal. This is not the most desirable approach, since we are interested in early growth; instead, further development is warranted, and may include:

- identification of dyes which do not contribute a non-specific stain signal. As explained below, these would require a covalent dye.
- developing a good measure of GMD size, and correcting the biomass signal by subtracting the estimated component due to background staining.

The mechanism of non-specific staining would of course depend on the particular dye, but might include:

- covalent attachment to the gel material, or an impurity thereof
- electrical attraction to charged groups on the gel; *e.g.* the anionic sulfate esters sprinkled throughout agarose
- other forces such as hydrogen bonding, *etc.*

Even in the absence of any of these interactions, equilibrium dyes will always produce a non-specific stain signal, due to a diffusional limitation which merits explanation. Figure 2.7 schematically depicts the passage of GMDs through a flow cytometer flow cell (a more complete view of the flow-cell assembly appears in Figure 2.4). As shown, the sample consists of empty GMDs, suspended in a dye solution. After the sample is injected into the sheath, the free dye will begin to diffuse out of the GMD into the sheath fluid. As discussed in Section 2.1, the gel is highly anti-convective. There may be some "washing out" of the dye near lateral surfaces of the GMD, where the effective pore length, and hence the hydrodynamic resistance, of the gel is lowest; however, convective transport of the dye is not expected to be significant overall.

Using the analysis of section 2.1 as a guide, we can predict that diffusion will not be sufficient to remove the free dye from the GMD before the GMD arrives at the interrogation volume; a more definitive prediction would require solution (probably numerical) of the diffusion equation subject to the boundary and initial conditions implied by Figure 2.7.

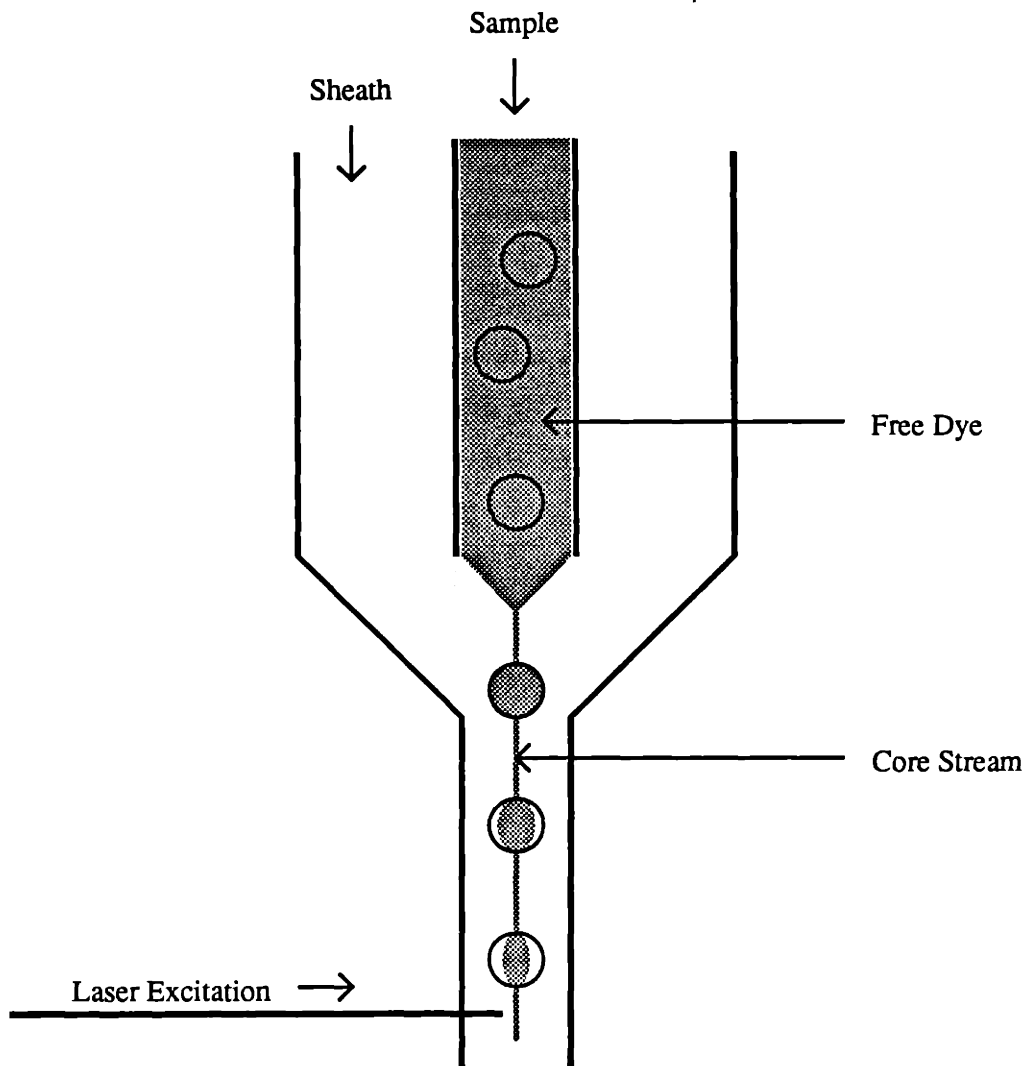


*Figure 2.7: Diffusion of Free Dye Out of GMDs*

We start by dividing the initial concentration profile of the dye in the GMD into two parts: the dye inside within the cylinder defined by the core stream radius, and the remainder. The solution to the diffusion equation would then be the superposition of the responses to each of these two initial conditions.

- Despite the fact that the dye inside the cylinder will diffuse radially with time, the net fluorescence measured will be the same as for the core stream between GMDs, and will be "nulled out" by the baseline correction

circuit of the PMT pre-amps; thus, this portion of the initial condition will not contribute to the free-dye signal we are considering here.

- Starting at  $t=0$ , the concentration profile of the dye outside the cylinder will relax, with some fraction going into the sheath, and some diffusing inward, toward the center of the GMD, where for this portion of the initial condition, the initial concentration is zero. Thus, we expect a lower *net* flux out of the GMD than in the uniform, spherically symmetric case of Section 2.1
- From Table 2.1, we estimate a diffusivity for small dye (MW 500) to be  $D \sim 40 \times 10^{-7} \text{ cm}^2/\text{sec}$ . For a  $20 \text{ }\mu\text{m}$  GMD, the smallest size used in these experiments, and this value of  $D$ , we obtain a diffusion time of  $T=250 \text{ msec}$ .
- After entering the sheath fluid, each GMD travels a distance of less than 10 mm before arriving at the interrogation volume; at typical flow rates of 1-10 meter/sec, the time delay is on the order of 1-10 msec, or  $< 0.04 T$ .
- Finally, from Figure 2.1, we see that at  $0.04T$ , there is significant diffusion relaxation of the concentration profile for the outermost half of the sphere, *i.e.*  $r \in (R/2, R)$ , but that a significant amount of dye does remain, and will contribute to the "free-dye" error signal under consideration.
- For larger GMDs, the free-dye signal gets bigger (for a  $40 \text{ }\mu\text{m}$  GMD,  $T=1 \text{ sec}$ ; for an  $80 \text{ }\mu\text{m}$  GMD,  $T=4 \text{ sec}$ ).

We conclude from this argument that diffusional limitations alone can result in a free-dye signal when equilibrium dyes are used. When other factors are included, *e.g.* tortuosity of the gel (longer diffusion paths), attractive interactions between the dye and gel (lower effective  $D$ ), the dye concentration in the GMD relaxes even more slowly, and the free-dye signal gets even bigger.

### 2.4.3: Fluorescent Labels for Nucleic Acids: Propidium Iodide

In the experiments presented in this thesis, I have chosen to use double-stranded RNA and DNA as the indicator biomaterial for microcolony biomass, and the fluorescent dye propidium iodide (PI) to stain it with. Propidium is a small (MW 668) molecule which intercalates into double-stranded nucleic acids (DSNA). Unbound in solution, it is excited by green-blue wavelengths, and emits weakly in the red. Upon binding to DSNA, the fluorescence increases 10-fold, and there is a slight shift in the emission spectrum ( $\lambda_{\text{max}} = 630\text{nm}$ ); this is thought to be related to the hydrophobic environment internal to DSNA. There are several considerations to use of this dye, including:

- Propidium is an equilibrium dye, and thus must be present in the flow cytometry sample, implying a free-dye signal as discussed above. In practice, the free dye signal has been tolerable for use with yeast total DSNA, as well as for mammalian cells, either DSNA or DNA only<sup>78</sup>. However, the free-dye signal has foiled attempts at measuring yeast DNA-only, and bacterial total-DSNA.
- Propidium is charged (2+), and does not normally cross the cell membrane; thus in order to stain DSNA, the membrane is permeabilized by exposure to 50% methanol for 10 minutes. This step also kills the cells, stopping growth, and mildly fixes the cell, though not as drastically as a cross-linking agent *e.g.* glutaraldehyde. It is likely that the GMD performs many of the functions of a fixative, *i.e.* preventing the cell from falling apart, and keeping large cellular components from diffusing away.
- Like all equilibrium dyes, in order to make good quantitative measurements, PI must be present in excess in order to ensure saturation of the binding sites; *i.e.* only in the saturation condition is it reasonable to assume that the total bound dye is proportional to the total available binding sites. The saturation requisite clearly competes with the need to minimize the free-dye signal. The minimum amount of dye needed

depends on the amount of stainable material present, *i.e.*  $\mu\text{g}$  of DSNA. Fortunately, I was able to identify a dye concentration ( $0.5\mu\text{M}$ ) for which the DSNA in a typical sample was saturated, and for which the free-dye signal was tolerable.

- For the most accurate measurements of DSNA after long incubation times, *i.e.* when the amount of stainable material has increased many-fold, it might be necessary to increase the PI concentration to maintain saturation. Once out of saturation, further increases in stainable material would result in an increasingly smaller increments of bound dye, and an underestimate of biomass increase. For the experiments presented in this thesis, there was no evidence of a desaturation problem.
- The binding rate of PI to DSNA depends on the PI concentration, as well as diffusion through the GMD and cell membrane. Experiments have shown that 5 minutes is sufficient to achieve equilibrium in free yeast cells (*S. cerevisiae*), under conditions similar to the protocols of this thesis<sup>89</sup>; I typically used 15 minutes. After several division times, the rate of diffusion through the outermost cells of the microcolony to the inner cells must also be considered. In the case of large microcolonies of mammalian cells, in 44-88  $\mu\text{m}$  GMDs, 45 minutes stain time was required<sup>78</sup>.
- For yeast in exponential phase, approximately 90% of the DSNA signal is due to RNA. As an indicator of biomass and growth, RNA is reasonable, since RNA is a requisite for protein synthesis. As an indicator, RNA is tricky, though; any artifact which affects the RNA signal can be misinterpreted as changes in growth. For instance, RNases (enzymes which cleave RNA) are common contaminants of glassware and media; RNase is also present in cells, and in many arenas, special steps are required to ensure its inactivation<sup>90</sup>. Based on the discussion of DNA electrophoresis (section 2.1), it is reasonable to guess that the diffusion of RNA fragments longer than 40 base pairs would be retarded by the gel matrix. Nevertheless, RNase has been shown to be effective in deleting the RNA-propidium signal in mammalian cells<sup>78</sup>, and must be strictly avoided here.



- Preliminary experiments showed that the DSNA-propidium signal for methanol-fixed free *C. utilis* cells was sensitive to the ionic strength of the suspending medium, and that it degraded with time. This is due in part to the fact that ionic strength affects the tightness of DSNA winding, which in turn affects propidium intercalation. I found that a 10mM phosphate buffer was a good compromise in terms of signal strength and stability.

In summary, propidium iodide has the advantage of being simple, cheap, and quick. However, caution must be employed in its use; in order to reasonably compare the biomaterial signal from any set of samples, the dye conditions must be the same; *i.e.* dye concentration, suspending medium, fixation, stain time, *etc.*

Ethidium homodimer, is related to propidium iodide, and has a much higher affinity for DSNA than propidium;<sup>91</sup> in theory, this would permit lower levels of free dye in the sample, and possibly reduce the free-dye signal. Preliminary experiments have not shown any significant improvement however, perhaps indicating an interaction between the dye and the gel, or a higher fluorescence of the unbound dye. I believe further investigation is warranted.

Ethidium monoazide is also related to propidium, and is unique among that family in being a covalent dye. In particular, it covalently binds to nucleic acids at the binding sites for ethidium<sup>92</sup>. The dye is light-activated, *i.e.* a photolysis step (~ 10 minutes) precedes formation of the covalent bond. Considering the implied ability to wash out the unreacted dye, the free-dye signal should be greatly reduced; I consider further investigation more strongly warranted than for the homodimer. On the other hand, there is the risk that the dye will bind to the gel, at least in small amounts; this has proven to be a significant problem for the covalent dye FITC, as described below.

#### 2.4.4: Fluorescent Stain for Proteins: FITC

As mentioned, the DSNA-propidium signal is not large enough in bacteria for use in the GMD-method. More precisely, the signal is not large enough with respect to the free-dye signal discussed above; thus for bacteria, we have used a covalent dye.

Fluorescein Isothiocyanate (FITC): is another small (MW 389) dye molecule, used to covalently attach the highly fluorescent fluorescein molecule to proteins. The isothiocyanate reacts with amines, to form a covalent bond; in particular, with the  $\epsilon$ -amino group of lysine (a prevalent amino acid constituent of cellular proteins), and the free amino terminus of amino acids and polypeptides. In collaboration with Dr. Harrison of our laboratory, I have successfully used this dye to measure growth of bacteria (*E. Coli*) immobilized in GMDS<sup>93</sup>, although considerable data processing was required. Based on those experiments, the following observations are made.

- FITC apparently stains the agarose gel, albeit weakly, and possibly non-covalently. The size of the gel-stain signal increases with the stain time, and decreases gradually if the GMDs are left to stand in water. In the particular protocol, we stained 40 minutes with FITC, and "de-stained" the gel at least overnight, and sometimes for several days. The asymmetry of these times clearly indicates that more than diffusional limitation is involved.
- FITC is pH-sensitive; both the excitation and emission spectra change substantially (8-10 fold) over the range pH 5-9. Thus, any experimental artifact which causes a pH difference between samples may be incorrectly interpreted as a difference in growth. Since protons diffuse very rapidly in water, and based on the previous discussion of outward diffusion from GMDs once they enter the sheath fluid, it may be required to buffer the sheath fluid to avoid the pH artifact. Preliminary experiments did not strongly support this requirement, however.

- The FITC-protein signal seemed quite stable over time, once destaining was completed. One might expect that many proteins would diffuse out of the cell once the membrane was permeabilized, although methanol is mildly denaturing. Indeed, small labeled proteins probably *do* diffuse out of the cell during destaining. These labeled, denatured proteins would diffuse through the gel more slowly than the free dye (see table 2.1), and may even stick to the gel's sulfate groups (section 2.1). Preliminary experiments with cell-free GMD preparations exhibited the same large stained-gel signal, and the same long destaining requirement; it does not appear that the contribution of labeled proteins is significant by comparison.

In summary, FITC provided a strong signal for cellular protein, and allowed us to measure growth of the bacterial microcolonies, after a division or two. However, a staining protocol which calls for destaining overnight cannot be considered as the basis for a "rapid" method of antimicrobial susceptibility testing.

## Section 2.5: Summary

In this chapter, I have presented some technology-specific aspects of the GMD-based growth assay described in Chapter 1. This has revealed both attributes and possible limitations of the particular implementation of the GMD method used in this thesis.

In summary:

- The size of GMDs should allow very rapid diffusional exchange of molecules with the bathing medium.
- Agarose should provide a very inert support matrix for growth, and immobilization conditions are not expected to stress the cells.
- Molecular sieving by the ultra-low melting point agarose may come into play for molecules as small as 26 kD; this should not be apparent in the experiments presented here, since all molecules of interest are below 5 kD.

- Electrical interaction between the gel and certain molecules, *e.g.* binding to sulfate groups, may noticeably affect transport of charged molecules, notably oligopeptides.
- Flow cytometry should provide good measures of microcolony biomaterial content, with little or no modification of standard cytometric protocols.
- Due to their size, GMDs should make it easier to make good measurements of microorganisms by providing a large, robust signal to trigger from.
- A unresolved issue, and one which currently prevents this method from working well in the presence of weak biomass fluorescence signals, is the relatively large signal arising from the retention of free dye in the gel, or non-specific staining of the gel. However, there are numerous candidate dyes which should be evaluated soon, and hundreds of candidates to consider<sup>94</sup>.

---

*Chapter 3***Growth Experiments**

---

As described in Chapter 1, the basis of conventional antimicrobial susceptibility tests is a growth assay; the cells under study are cultured in the presence of increasing amounts of antibiotic, and the amount of growth under each condition is measured and compared to growth in a drug-free control. Thus, the development of a GMD-based susceptibility test must be preceded by the demonstration of a GMD-based growth assay. In this chapter, I will demonstrate such an assay, and compare its performance with a quantitative reference method: optical density.

**Optical Density as Reference Method**

Optical density was chosen as a reference method for these experiments, because:

- OD measures biomass (*v.i.*); since the GMD method is also based on measurements of biomass, comparison to OD is logical. In particular, the two methods should both be sensitive to growth, as defined in section 1.2, without cell division.
- OD inherently measures a large number of cells, thereby theoretically reducing the sampling error ( $\sim N^{-1/2}$ ) in the measurement. A typical optical density measurement interrogates a sample of  $10^6$  to  $10^8$  cells, for which the sampling error is low, less than 0.1%. Of course, there are noise sources unique to the OD method, such as false scatter from air

bubbles, stray particulates, *etc.*, that must be minimized through careful technique.

- OD is a relatively rapid measurement.
- Finally, as of 1985, *all* of the automated methods for antimicrobial testing which had been fully evaluated and FDA approved were based on optical density or related photometric measurements<sup>17</sup>. In particular, OD is the basis for many state-of-the-art rapid susceptibility testing methods, currently in clinical use, such as the Vitek system (McDonald-Douglas Vitek Systems, Hazelwood, MO), and the AutoSCAN-4 (American Scientific Products div. of American Hospital Supply Corporation). From a long-term perspective, it makes sense to compare the GMD method to the basis of existing clinical technology, looking for relative merits of each method.

### Physical Basis for Optical Density Measurements

Measurements of optical density are made by passing light of a narrow band of wavelengths through the sample, and measuring the amount of light which emerges. In the instrument used here, the photodetector is coaxial ( $0^\circ$ ) with the incident light, so the measurement is of transmitted light. The incident light is scattered by particles, such as cells, suspended in the sample; thus as the amount of suspended material increases, scattering increases, and the transmitted light decreases. The conventional wisdom is that absorbance of incident light by cellular material is negligible at the wavelengths used (500-600 nm), so that optical density is predominantly a measure of turbidity. In practice, absorption by the suspension medium can be significant, as can fluorescent re-emission; these need to be carefully controlled for by the use of blanks.

Analytic expressions for the amount of light scatter, which require solutions of Maxwell's equations, are available for limited, ideal cases<sup>95</sup>. In each case, the solutions depend on the viewing angle and distance, the particle size, and the relative

refractive index *i.e.* the refractive index of the particle material, with respect to the refractive index of the suspending medium. Lorenz (1890), Mie (1908) and Debye (1909) independently provided solutions for scattering by spheres. Lord Rayleigh (1871) described a theory applicable only for particles much smaller than the wavelength of the incident light. Under certain conditions, scatter from particles larger than the incident wavelength can be described by Rayleigh-Debye theory, wherein each small volume element of the particle is modeled by Rayleigh scattering; the light scattered by the each of the elements is combined (with interference), and the net intensity field is viewed at an observation point far from the particle.

Typical OD measurements use an incident wavelength of 500-600 nm, whereas the typical bacterial cells are 500 x 2000 nm in dimension; of course, yeast (> 3000 nm) and mammalian cells (> 7000 nm) are even larger. Thus Rayleigh-Debye scattering is used as the basis for photometric analysis of cell growth<sup>96</sup>. Unfortunately, the assumptions behind the commonly cited results ignore (out of necessity for mathematical tractability) many aspects of physical reality, especially the distribution, within a cell suspension, of cell sizes, shapes, masses, volumes, and refractive indices, as well as non-uniform refractive indices, *i.e.* granularity, within the cells themselves.

Nevertheless, the approach taken to the Rayleigh-Debye model, *i.e.* considering a large particle as the sum of many small scattering particles is the basis of the result that total light scatter increases with biomass. For the case of bacteria and yeast, subject to numerous assumptions, the mathematical solutions assert an explicit relationship<sup>96</sup>:

$$OD \propto (\text{cell dry mass})^2 \times (\text{cell density}) \times f(n, n_0, \lambda)$$

where  $n$  and  $n_0$  are the refractive indices of the cells and media, and  $\lambda$  is the illumination wavelength. This relationship has led to the widespread use of optical density measurements to estimate biomass. However, as pointed out by Koch<sup>97</sup>, the interrelationship of the physical parameters results in an inverse-square law, which states that the optical density is proportional to inverse of the cell radius squared.

In a sample of cells with different sizes, the optical density is proportional to the inverse of the total surface area of the cells in the sample. Thus, turbidity is not a true measure of biomass, as it is sensitive, for example, to cell shrinkage or swelling due to changes in osmotic pressures. The inverse-square law applies best to particles in the size range of about 0.5 to 2  $\mu\text{m}$ , notably bacteria. For larger particles such as yeast, the dependence on cell size is more complicated, if not intractable. However, the general result still holds, *i.e.* the sensitivity of optical density to physical changes other than biomass accumulation, and can be expected to appear in experimental results.

Finally, it should be noted that optical density measurements inherently represent bulk averages. In many important cases, including exponential growth phase, the *population average* cell size and dry mass can be assumed constant; under that assumption, optical density is then a reasonable measure of cell density, or total sample biomass.

### Section 3.1: Macroscopic Growth Measurement: Optical Density

The goal of this first experiment is to demonstrate the macroscopic growth assay, based on tracking optical density of a cell suspension with time. In exponential growth phase, the cell concentration,  $\rho$ , should increase exponentially with time. Since  $\text{OD} \propto \rho$  under this condition, (as discussed above), a plot of  $\log(\text{OD})$  *vs.* time should reveal a straight-line portion, whose slope is the average cell division time.

#### Protocol 3.1

Part numbers and media compositions appear in Appendix 3.

- *C. utilis* (ATCC #9226) was grown up on YM-agar plates. Several colonies were transferred to buffered YNBD broth, and incubated overnight with rotational agitation, at 26°C. In the morning, I diluted 7.5 ml of the cell suspension with 7.5 ml fresh YNB, and incubated with rota-



tional agitation for 2 hours at 26°C; this was in order to get the cell suspension in nearly exponential phase for the experiment.

- I empirically determined the dilution necessary to achieve the desired initial optical density for this experiment: 160  $\mu$ l of cell suspension in 5 ml of buffered YNBD produced an  $OD_{530}$  of 0.025. Haemocytometer counts reveal that this corresponds to an initial cell density of  $5.2 \times 10^6$  cells/ml.
- 1.6 ml of cell suspension was mixed into 50 ml buffered YNBD in 50 ml polypropylene cell culture tube. 5 ml was transferred into a glass test tube for optical density reading. The remaining 45 ml was incubated with rotation, at 26°C.
- The  $OD_{530}$  of t=0 sample was measured, and glass tube rinsed with DIW.
- At periodic intervals, another 5 ml aliquot was transferred from 50 ml culture tube to glass test tube,  $OD_{530}$  measured, and glass tube rinsed.

## Results

Logarithms of the raw  $OD_{530}$  data were computed, and plotted *vs.* time, as shown in Figure 3.8. A minimum-square-error line was fit to the linear segment of the curve (t=75 to 430 min). From the slope of this line, a doubling time was determined:  $\log(2)/\text{slope} = 97$  minutes. These results are discussed in conjunction with the results of the GMD-based growth assay, the next experiment.

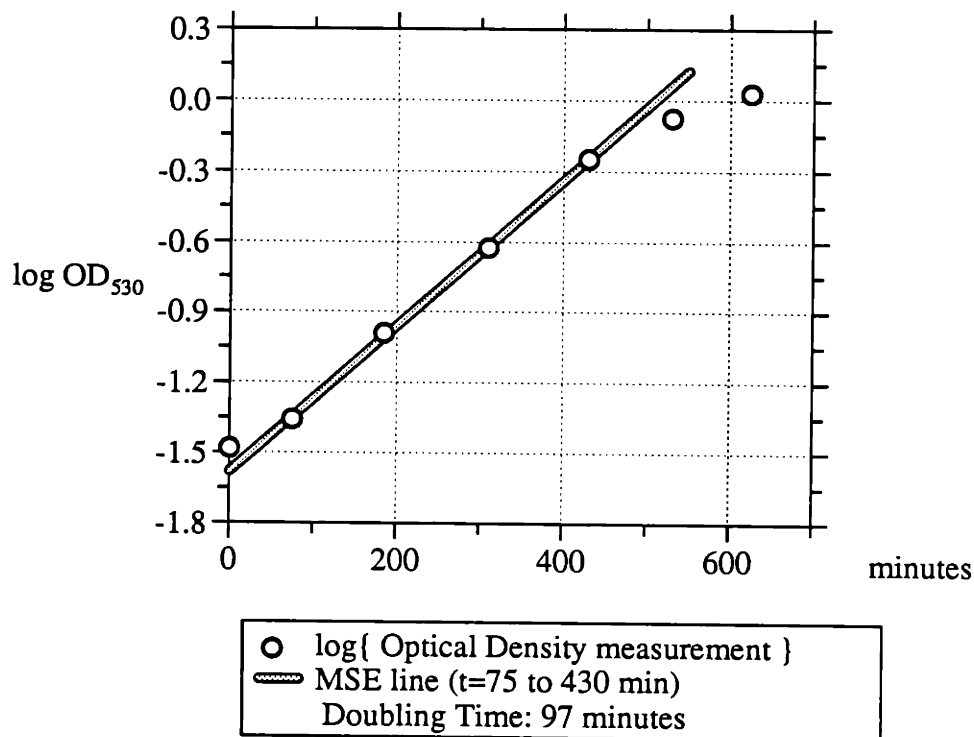


Figure 3.1: Growth of *C. utilis*, by optical density measurements

### Section 3.2: Measurement of Growth by GMD-based Growth Assay

The goal of this next experiment is to demonstrate the microscopic GMD-based growth assay, based on tracking microcolony biomass in a cell population, with time. In exponential growth phase, microcolony *biomass* should increase exponentially with time, as discussed in section 1.2. By the GMD method, the integrated fluorescence of an indicator biomaterial is used to measure biomass (chapter 2). Thus, a plot of the mean log{indicator fluorescence} vs. time should reveal a straight-line portion, whose slope is the average biomass doubling time.

**Protocol 3.2**

The details of the GMD preparation, fixation, sieving, *etc.*, are fully presented in Appendix 1. Here, I summarize, and fill in details particular to this experiment.

- *C. utilis* (ATCC #9226) was grown up on YPD-agar plates. A colony was transferred to YPD broth, and incubated overnight, with rotation, at 26°C.
- *C. utilis* cells were immobilized in GMDs (2½ % ULMP), using the protocol of Appendix 1. The cell inoculum was 100 µl, at a concentration of  $1.2 \times 10^8$  cells/ml, as measured by haemocytometer count of a 1:50 diluted sample. The final concentration in agarose was  $2 \times 10^7$  cells/ml; at this cell density, Poisson statistics predicts that 30% of 36 µm GMDs will be occupied by one CFU, 9% will be multiply occupied, and 61% will be empty. This was qualitatively confirmed by microscopy.
- The GMDs were prepared in nine aliquots, each ultimately being a suspension in 5 ml of YPD (*i.e.* after transfer of the GMDs from oil to aqueous suspension, as detailed in Appendix 1). The first aliquot was immediately fixed by adding 5 ml of methanol, for a final concentration of 50% (v:v). The remaining aliquots were incubated in 15 ml polypropylene tubes, with rotation, at 26°C.
- Aliquots were taken every 30 minutes, and methanol-fixed as above.
- After all aliquots had been fixed, each was washed and sieved: GMDs between 20 µm and 44 µm diameter were extracted from the suspension by sieving, then washed with DIW, then washed and resuspended in 1.5 ml of 10mM phosphate buffer, pH7. The samples were stored in 1.5 ml polypropylene microcentrifuge tubes, and left overnight in the refrigerator.
- In the morning, a 14.8 µM propidium iodide working solution was prepared by adding 15 µl PI at 1000 µM to 1.0 ml DIW. The samples

were stained by adding 51  $\mu\text{l}$  of the working solution to each 1.5 ml sample; the final concentration was 0.5  $\mu\text{M}$ . Samples were allowed to stain for at least 15 minutes, so the dye could equilibrate.

- Samples were analyzed with the flow cytometer, with excitation at 488 nm, 35 mWatts, with light-mode (*i.e.* constant light-intensity) power regulation. For each of 32,000 GMDs, 90° red fluorescence (RF,  $\lambda > 630\text{nm}$ ) was measured, integrated, and stored using the DAS (Appendix 2), triggered on 90° blue scatter. The PMT gains were: 90° red: 1.9 and 90° blue: 1.65. The gain of the blue scatter channel determines the rate of false triggering by debris in the sample, *etc.* Typical event rates were about 100/sec, and a gain of 1.65 produced a reasonable ( < 10/sec ) noise rate.
- On our data analysis system, the  $\log_{10}$  of the raw fluorescence data was computed, and input to a statistics program which produced these histograms, and computed the mean  $\log\{\text{RF}\}$  of each.

## Results

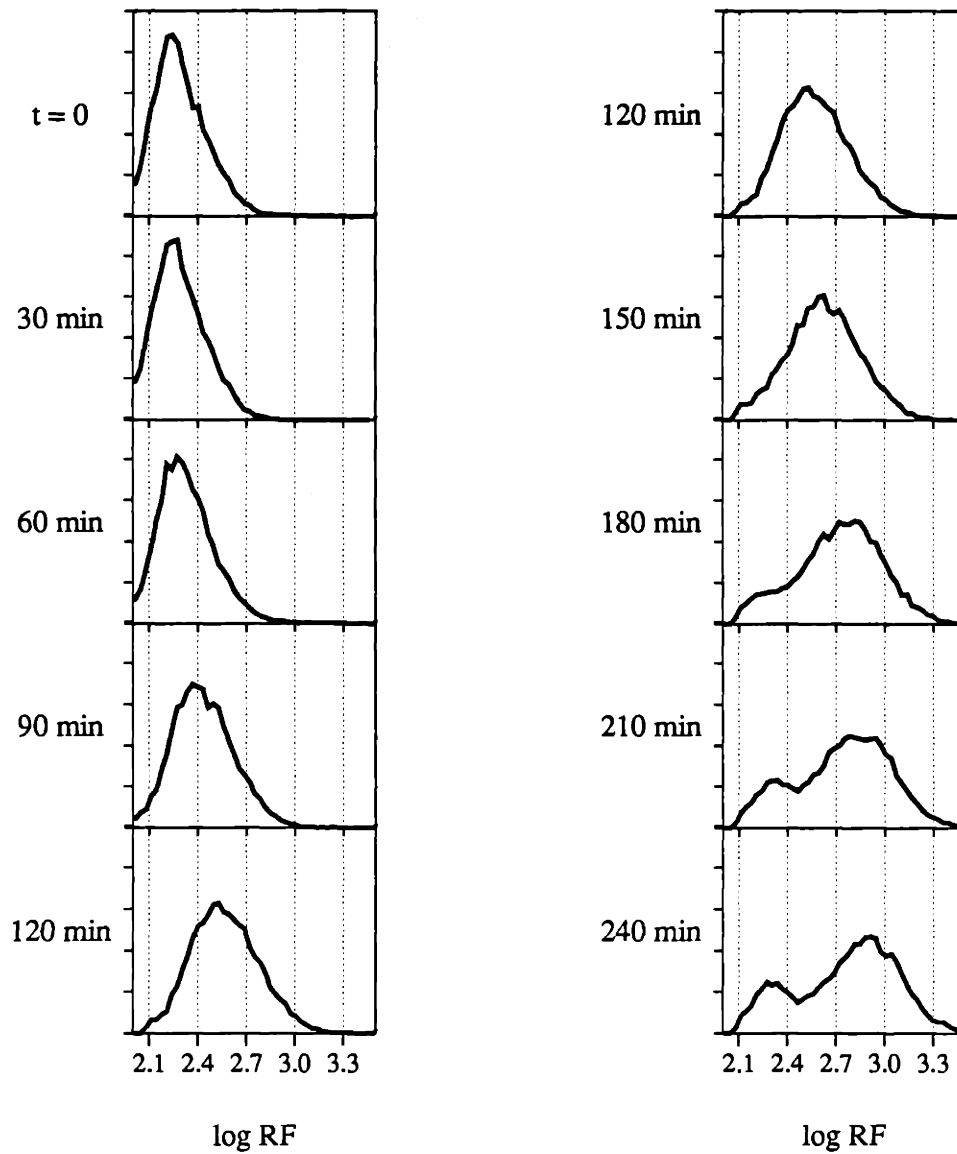


Figure 3.2: Growth of *C. utilis* in GMDs, by flow cytometry

The histograms shown in Figure 3.2 demonstrate the initial distribution of PI-stained biomass, and the increase in same, as incubation time increases. Some important features, discussed below, are:

- The GMDs themselves have a significant RF signal due to integration of the low-level non-specific labeling of the gel. However, the RF distribution due to GMDs is not shown in this data; it is offscale to the left of the data shown.
- At  $t=0$ , we see the initial distribution of PI-stained biomass. The  $t=0$ , 30, and 60 min distributions look nearly identical, and the  $t=90$  sample is the first to exhibit a clear shift in the RF distribution. Continued growth, reflected by continued shift in the RF distribution, is seen in the remaining samples.
- Starting at time  $t=180$ , we see the appearance of a second peak, in the same location as the initial peak of  $t=0$ . This peak increases with increased incubation time.

The mean  $\log(\text{RF})$  value from each GMD sample was plotted *vs.* the corresponding incubation time, to generate a growth curve, shown in Figure 3.3. The samples from  $t=60$  to 180 minutes were fit with a minimum-square-error (MSE) line. From the slope of the line, a biomass doubling time was computed for the CFUs in GMDs:  $\log(2)/\text{slope} = 85$  minutes. In addition, for the  $t= 210$  and 240 minute samples, a curve-fitting procedure was used to estimate a mean  $\log(\text{RF})$  for the right-most RF sub-populations, and plotted on the same graph (filled circles). The left-most sub-populations are presumed to *not* represent growing microcolonies (see below); the curve-fitting method is illustrated in Figure 3.4.

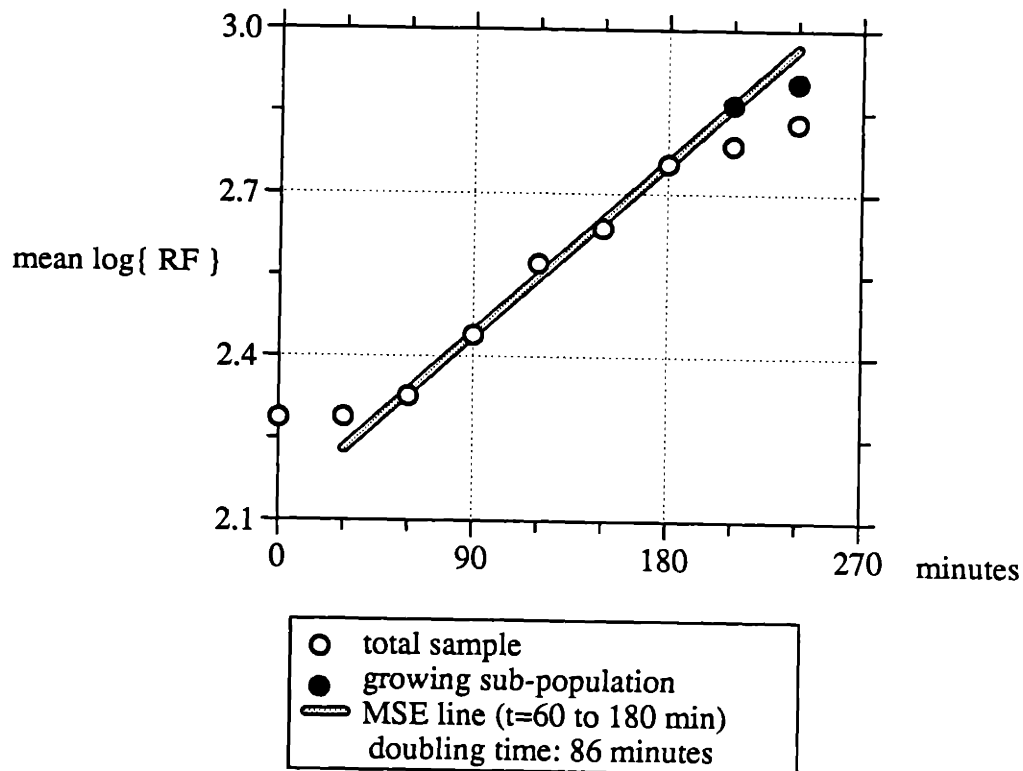


Figure 3.3: Growth of *C. utilis* in GMDs: mean  $\log\{RF\}$  vs. time

## Section 3.3: Discussion

### 3.3.1: Comparison of Growth Assay Results

These results demonstrate the ability to observe and measure the growth of *C. utilis* microcolonies in GMDs, and show good agreement, both qualitative and quantitative, between the results thus obtained and those of the gold-standard, optical density. The following points should be considered:

- In both methods, we were able to observe a short initial lag phase, followed by an exponential growth phase. MSE fits to the growth curves gave a cell number doubling time of 97 minutes (optical density method)

and a microcolony biomass doubling time of 85 minutes (GMD method). The nominal division time for this microorganism is 90 minutes.

- A likely contributing factor to the difference in doubling times is that different media were used for the two experiments. For the OD experiment, I used buffered YNBD (Yeast Nitrogen Base plus dextrose), a standard medium for yeast; YNBD is the medium used for standardized clinical broth dilution testing of antifungal agents<sup>16</sup>. For the GMD experiment, I used YPD, a much richer medium for yeast. YPD has about 4 times as much dextrose and nitrogen source as YNBD and thus would be expected to support higher growth rates than YNBD. The choice to use YPD was made for practical reasons: it was found to result in higher GMD yields, due to an apparent surfactant property of one of its constituents. In the future, for the purpose of conforming to community standards, an additional step of transferring GMDs from YPD to YNBD after manufacture should be added; of course, one would have to demonstrate that the transfer step did not stress the cells.
- In each case, there was an *apparent* slowing from exponential growth late in the experiment. While this may be genuine slowing, due to *e.g.* nutrient exhaustion, milieu changes, *etc.*, it may also be an artifact of the methods. In particular, it is well known that optical density is linear with cell concentration only over a limited range<sup>96,98</sup>. To extend the linear range requires calibration of OD to known cell concentrations, and conversion of OD data to concentration data; this was not deemed necessary for this experiment. On the other hand, GMD microcolony biomass is limited at the top-end by GMD break-out, discussed below.
- By mathematically extracting the right-most sub-population of the log RF distribution at  $t=210$  and  $240$ , and plotting the mean  $\log\{RF\}$  for those sub-populations, the linear range of the GMD-based growth curve was extended. This indicates continued exponential growth of immobilized microcolonies, at least through  $t=210$  minutes. The deviation at  $t=240$  may reflect a slowing of growth, or may reflect hitting a hard limit on microcolony size for these GMDs; based on the log RF plots of Figure 3.2, as well as microscopy, at  $t=240$ , many



microcolonies are 16-20 cells, and physically cannot get bigger without breaking out of the smaller GMDs. Certainly, for this exploratory type of experiment, this sub-population analysis is useful; for other applications, it may only be necessary to know whether there was *any* growth at later times, which could have been correctly answered by simpler methods, such as the uncorrected mean-logs, or with the mode of the distribution.

- In the GMD data, the lag phase of 60 minutes was intentionally induced by using an inoculum from early-stationary phase; in other experiments, cells were taken in exponential phase, and no significant lag was seen; this supports the conclusion that these cells tolerate the GMD protocol without feeling stressed.
- The log RF histograms of Figure 3.3 are qualitatively consistent with the expected results of the GMD-based growth assay, as presented in Chapter 1. Under the microscope, at  $t=0$ , the initial immobilized CFUs were noted to consist predominantly of 1 or 2 cells, with a few 3-cell and 4-cell CFUs seen. The corresponding log RF distribution is seen to be skewed, and is consistent with the model of Section 1.2, *i.e.* the sum of nearly symmetric but fairly broad distributions, each corresponding to 1- or 2- (and a few 3- or 4-) cell CFUs. One might attempt to apply distribution-fitting methods to estimate the fraction of 1, 2, 3 and 4-cell CFUs, but there is no good reason to do so here. Also, to my knowledge, a justifiable model for biomass distribution is lacking; the Gaussian assumption of section 1.2 was based on empirical observation, although certainly the Gaussian distribution is widely used for analysis of DNA-content measurements<sup>99</sup>.

### 3.3.2: Microcolony Break-out

The log RF histograms for  $t=180$  minutes onward exhibit an sub-population emerging to the left of the "growing microcolony sub-population". The fact that this sub-population appears in the same location as the initial  $t=0$  distribution leads to the

tentative conclusion that these are 1-2 cell CFUs, and at least two possible interpretations:

- This is the non-growing sub-population of the initial inoculum, which was included in the model of Section 1.2, or
- these are CFUs that escaped from their GMDs and are suspended freely in the sample.

The evidence strongly favors the second interpretation:

- Microscopy of these samples reveals free yeast cells mixed with the GMDs, whereas the observed fraction of non-growing, immobilized CFUs is very small.
- The cytometric histograms indicate that the sub-population increases with incubation time. A non-growing sub-population would be expected to remain the same, and perhaps decrease as some long lag-time cells start growing. Conversely, a break-out sub-population would be expected to increase with incubation time, as average microcolony size increases and more GMDs fracture.
- The yeast cells have a significant size ( $\sim 4 \mu\text{m}$ ), especially with respect to the smallest GMDs ( $20 \mu\text{m}$ ). In addition, the ultra-low melting point agarose has a very low strength. Thus, as the microcolonies grow, it is *expected* that they will weaken or fracture some of the GMDs.
- One expects, and microscopy confirms that in some cases, the initial CFU is located near the edge of the GMD; as the CFU divides, the progeny may escape from the GMD, without actually breaking the GMD.

Thus, there is consistent evidence for break-out. The only puzzle is that the sieving step, which follows incubation and fixation, should remove everything smaller than  $20 \mu\text{m}$ , including free yeast cells. However, after the sieving step, the GMDs are exposed to further stresses, such as pipetting, mixing (especially in the staining step),

and traversing the fluidics of the cytometer; it is plausible, but not yet proven, that this breaks GMDs which have been fractured, or breaks off progeny at the GMD surface, reintroducing free cells into the cytometer sample. Certainly, stress-reduction in the protocol is possible and warranted. In particular, for staining after sieving, the GMDs should be gently suspended in a dye-buffer mixture, rather than the current method of mixing the dye into the GMD suspension.

It should be noted that yeast are larger than the smallest GMDs that result from the GMD dispersion protocol of Appendix 1; thus after dispersion and gelation, and transfer to aqueous phase, there are free yeast remaining in the sample. These should be removed from the sample by the sieving step, and microscopy confirms that, with adequate washing, they are removed.

For the purposes of antibiotic susceptibility testing, break-out may or may not be a problem. The central issue here is whether the inhibition of growth can be demonstrated before the bulk of the microcolonies break out of their GMDs; as we will soon see, for the model system of this thesis, the answer is 'yes'. We could, if necessary, decrease the degree of break-out by going to a higher gel concentration, thus obtaining a higher gel strength, or using the LMP agarose, which forms stronger gels than ULMP. I would however advise caution; stronger gels may impede microcolony growth. Also, based on the discussions of section 2.1, the molecular sieving effect of agarose increases with gel concentration. Of the two options, I would prefer switching to LMP agarose, since at the same concentration, it is both stronger and less sieving than ULMP agarose.

### **Specific Labeling of GMDs**

In cases where it is critical to distinguish free cells from cells immobilized in GMDs, it would be possible to label the GMD gel material; this would provide an unequivocal trigger signal for cytometry, so that free cells in the sample could be ignored. Two possible methods are to (i) covalently bind a fluorescent dye to the agarose, or

(ii) co-entrap small (0.1  $\mu\text{m}$ ) fluorescent beads in the GMD; both methods have been demonstrated in our laboratory (G. Williams, G. Harrison, personal communication). Initial experience showed that activation of the agarose for dye attachment, *e.g.* by cyanogen bromide, altered the physical properties of the gel, possibly in an undesired manner, by promoting cross-linking of the agarose. On the other hand, commercially prepared beads were found to contain preservatives, *i.e.* antimicrobial agents such as sodium azide, which required dialysis for removal.

It was also observed, as expected, that the emission from the GMD label crossed over into the red fluorescence channel; *e.g.* the fluorescein emission spectrum extends well into the orange-red wavelengths. Presumably this could be computationally corrected; however, this presumes that the red fluorescence which comprises the signal, *i.e.* PI-stained nucleic acids, is large compared to the fluorescence of the gel. In effect, labeling the gel only worsens the problems of non-specific labeling of the gel discussed in Chapter 2. It is possible, though not demonstrated, that the non-specific labeling itself can be used as a gel-label in the manner proposed. However, for these experiments, if not in general, I concluded that the loss of signal-to-noise ratio due to labeling the gel would not be worth the gain of being able to distinguish free cells from GMD-entrapped cells. In future experiments where fluorescent cell-identity signals are to be collected, *i.e.* for polymicrobial specimens, labeling the gel would reduce the number of color channels available, and would likely decrease the signal-to-noise ratio in the same manner.

### 3.3.3: Cell Viability in GMDs

As discussed in Section 2.1, for the purpose of antimicrobial susceptibility testing, it is critical to determine the extent to which cell viability is compromised by GMD immobilization and culture. The results of this experiment, which of course only apply to *C. utilis*, are very promising. Consideration of the later time samples suggests a good cloning efficiency. In order to derive a worst-case estimate of cloning efficiency, I manually split the  $t=240$  distribution into two sub-populations, as shown in Figure

3.4. Counting the events in each sub-population demonstrates that 20% of all RF measurements were in the left-most of the two. In the worst case, all these events would represent non-growing cells, and an estimate of 80% cloning efficiency would be warranted. However, microscopy indicates that a significant majority of these events are due to free cells in the cytometry sample; thus a cloning efficiency in excess of 90% is more realistic. Indeed, microscopy indicates a cloning efficiency in excess of 95%, although careful quantitation, *i.e.* counting large numbers of GMDs by microscopy, was not done for this experiment. A more quantitative evaluation is included as part of the growth inhibition experiment, presented in the next sections of this chapter.

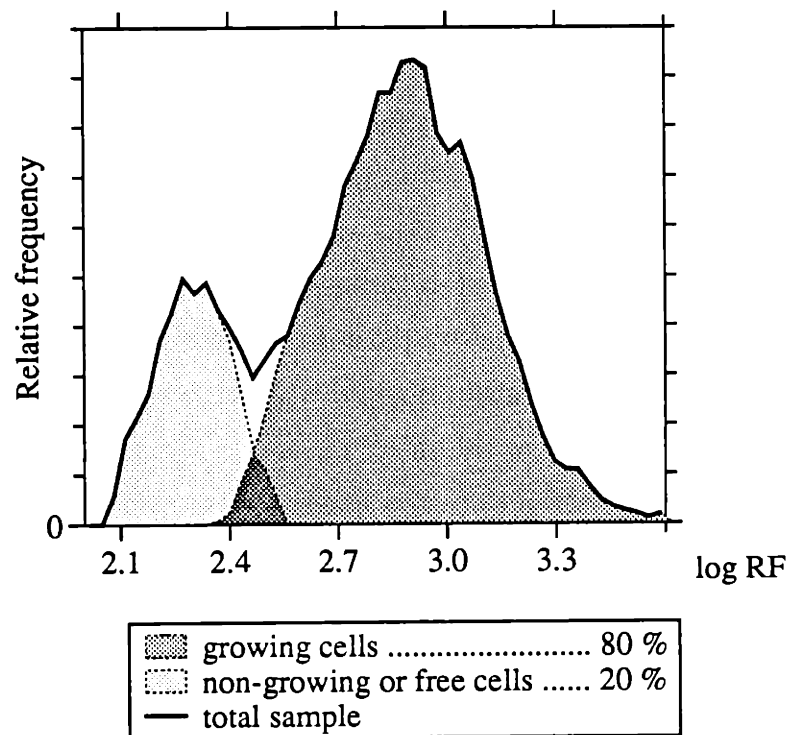


*Figure 3.4: Sub-population estimation by curve-fitting*

Finally, the growth rate of the viable CFUs is very good, equal to the nominal growth rate, and consistent with the results for free-cells in suspension, given the

difference in media. These findings support a tentative conclusion that cell viability is not compromised by this protocol.

For extending this work, however, this conclusion needs more support. An experiment is needed to quantitatively show the changes in viability, if any, resulting from GMD culture with respect to culture in free suspension. For example, using a vital stain, such as carboxy-fluorescein diacetate (CFDA)<sup>94</sup>, in conjunction with PI (without intentional cell permeabilization) it should be possible to track the viable and non-viable fractions of a cell population with time. Stringently quantifying viability in GMDs, for comparison, will require modifications of the protocols used for this thesis.

- The first confounding factor is free cells in the samples, due to cell break-out, inadequate washing, *etc.* Using only a single color, *i.e.* red fluorescence (RF), it is essentially impossible to distinguish free, viable cells from cells which have not grown. Further, my experience was that even the combination of RF and light scatter was not sufficient to make the distinction; the integrated scatter from free yeast CFUs was significant and comparable to small GMDs. One possible protocol modification would be to use a viability stain such as carboxy-fluorescein diacetate, (CFDA), and eliminate the cell fixation step. A simpler approach would be to mark the gel in some fashion, either with a fluorescent label or scattering centers (to increase the scatter signal from GMDs), so that by using two optical measurements, one could distinguish free cells from GMD-entrapped cells.
- The other serious problem with using the current protocol to test viability is that we depend on a relatively large RNA component to develop a large enough propidium signal (RF) to see above the non-specific binding of the gel (section 2.3). Cells which have been dead for some time, undernourished, or cell spores, cannot be expected to have this large RNA com-

ponent. Thus, in the experiment presented, a population of dead, DNA-only cells would be obscured by the gel fluorescence, and unavailable for further analysis. This comment is also relevant for bacterial protein staining with FITC (section 2.3); cells which have not been recently well-fed, happy and growing could not be expected to have enough protein to develop a biomaterial stain large enough to overcome the non-specific staining of the gel.

### **Section 3.4: Measurement of Growth Inhibition by Optical Density**

Although the growth of microcolonies can be observed under the microscope, another experiment is useful to support the conclusion that this method is actually measuring growth, as opposed to some unexpected artifact. In this section, I will present such an experiment, one which shows that in the presence of inhibitory levels of Amphotericin-B, growth inhibition is observed in similar fashion by the conventional optical density method, as well as by the GMD-based method. This naturally leads into the MIC experiments of the next chapter.

#### **Protocol 3.3**

The data used here is a subset of the data taken for a larger experiment, a conventional serial drug dilution MIC assay. The full experimental protocol is presented in the next chapter, along with the full data set. In this section, I have extracted a small subset for comparison to the GMD assay results presented in the next section, and here summarize the salient protocol features:

- *C. utilis* (ATCC #9226) was grown up on YM-agar plates. Several colonies were transferred to YNBD broth, and incubated overnight, with rotation, at 26°C.
- A serial drug dilution procedure was used to prepare a set of 50 ml polystyrene tubes, each containing 50 ml of YNBD, with Amphotericin-B drug concentrations ranging from 0.031 µg/ml to 2.0 µg/ml.

- Each tube was inoculated with 800  $\mu\text{l}$  from the yeast suspension; this was pre-determined to yield an initial  $\text{OD}_{530}$  of about 0.025.
- For OD measurements, 5 ml from each sample was transferred to a glass test tube, suitable for the spectrophotometer. The same tube was used for all readings, and rinsed with DIW between samples.
- $\text{OD}_{530}$  measurements were made on all of the samples at  $t=0$ , then the remaining 45 ml cell suspensions were incubated, with rotation at  $26^{\circ}\text{C}$ .
- At periodic intervals, additional  $\text{OD}_{530}$  measurements were made on all of the samples.

### Results:

Logarithms of the raw  $\text{OD}_{530}$  data were computed, and plotted *vs.* time, for the drug concentrations 0.06  $\mu\text{g}/\text{ml}$  and 1  $\mu\text{g}/\text{ml}$ , and for the three earliest sample times; the result is shown in Figure 3.5. Notable points include:

- The data has been normalized to correct for slight differences in initial  $\text{OD}_{530}$  to facilitate visual comparisons. Ideally, these differences would arise solely from differences in inoculum concentration; in reality there is a moderately substantial noise component due to such things as variation in orientation of the glass test tube, *etc.* Nevertheless, this does not detract from the interpretation of the data.
- The sample tubes were also inspected visually for turbidity, which is the basis for the classic MIC assay. The samples with zero and 0.06  $\mu\text{g}/\text{ml}$  Amphotericin-B were seen to turn cloudy after sufficient incubation, whereas the 1  $\mu\text{g}/\text{ml}$  sample remained clear; this is interpreted to mean that 1  $\mu\text{g}/\text{ml}$  is inhibitory.
- The  $\text{OD}_{530}$  measurements confirm and quantify the visual inspection. In the control and 0.06  $\mu\text{g}/\text{ml}$  samples, an increase in turbidity is seen, at



least over these early times. There is somewhat less overall growth in the 0.06  $\mu\text{g/ml}$  sample. The 1.0  $\mu\text{g/ml}$  sample, on the other hand, shows an increased turbidity over the first sample interval, 105 minutes, but no further increase.

- The net increase in log OD is about 0.15. We cannot conclude, however, whether this represents an increase in biomass, cell number, or just a coincidental change in physical properties, due to the action of the drug (*v.i.*), that causes the scatter signal to increase.

These results are discussed further, in conjunction with the results of the GMD-based growth inhibition assay, the next experiment.

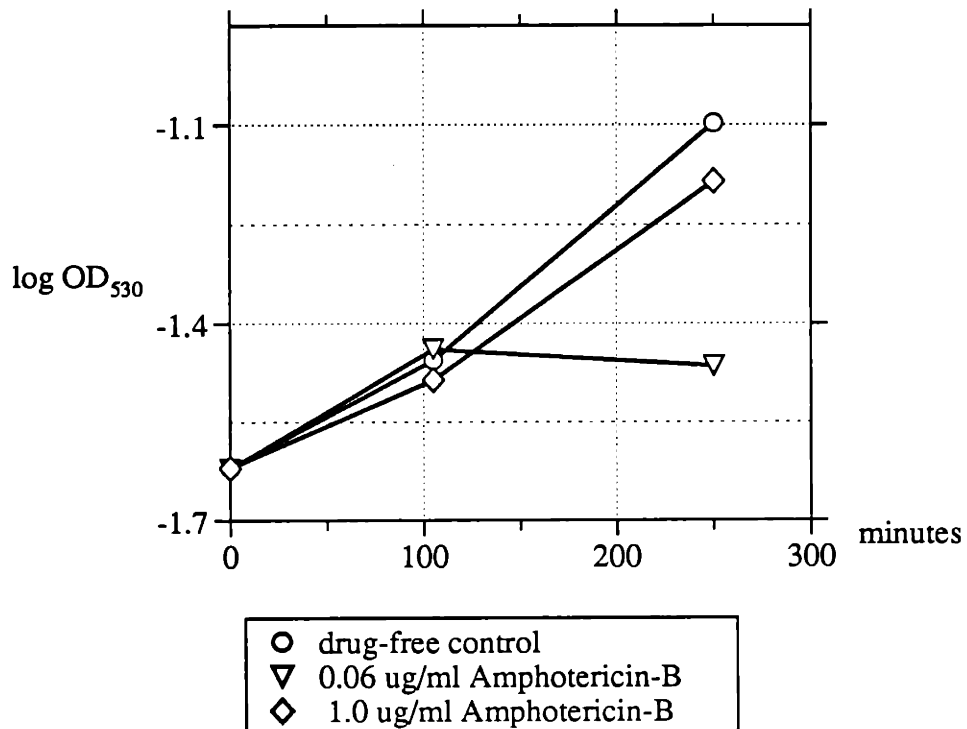


Figure 3.5: Growth Inhibition of *C. utilis* by Amphotericin-B: Optical density

## Section 3.5: Measurement of Growth Inhibition by GMD Assay

### Protocol 3.4

This protocol is identical to protocol 3.2, except that some of the GMD aliquots are incubated in the presence of Amphotericin-B. Here, I outline the protocol, with full description of differences; unless noted otherwise, the details of GMD formation, handling, and flow cytometry are identical to protocol 3.2.

- *C. utilis* (ATCC #9226) was grown up on YPD-agar plates, transferred to YPD broth, and incubated overnight, with rotation, at 26°C.
- *C. utilis* cells were immobilized in GMDs (2½ % ULMP), at a final concentration of  $2 \times 10^7$  cells/ml.
- The GMDs were prepared in ten aliquots, each being a suspension in 5 ml of YPD. 200 µl of 20 µg/ml Amphotericin-B working solution (see protocol 4.1) was added to four aliquots (final concentration of 0.77 µg/ml), and 10 µl of Amphotericin-B working solution was added to three other aliquots, (final concentration of 0.04 µg/ml); the final three aliquots were drug-free controls. Amphotericin-B must only be added *after* the GMDs are transferred from the oil phase to the aqueous nutrient broth, (see Appendix 1), otherwise the drug will partition significantly into the oil phase.
- Seven aliquots (two each of 0, 0.04 µg/ml, and three at 0.8 µg/ml) were incubated with rotation, at 26°C.
- A drug-free aliquot was immediately sieved (20-44 µm), fixed in 50% (v:v) methanol for 5 minutes, washed, and resuspended in 1.5 ml phosphate buffer. Two drug-added aliquots (one each of 0.04 and 0.8 µg/ml) were allowed to sit, without incubation, for 10-15 minutes, to allow equilibration of the drug with the cells. Then, they were each sieved, fixed, washed, and resuspended in the same manner.

- The second set of three aliquots (0, 0.04, and 0.8  $\mu\text{g/ml}$ ) were sequentially sieved, methanol-fixed, washed and resuspended after incubation for 2 hours. The final three aliquots were sieved and fixed, *etc.*, at  $t=3.5$  hours. The samples were stored in 1.5 ml polypropylene microcentrifuge tubes, and left overnight in the refrigerator.
- In the morning, the samples were stained by adding 51  $\mu\text{l}$  of a 14.8  $\mu\text{M}$  propidium iodide working solution (see protocol 3.2) to each 1.5 ml sample; the final concentration was 0.5  $\mu\text{M}$ . Samples were allowed to stain for at least 15 minutes, so the dye could equilibrate.
- Samples were analyzed with the flow cytometer, with excitation at 488 nm, 45 mWatts, with light-mode power regulation. For each of 32,000 GMDs, 90° red fluorescence (RF,  $\lambda > 630\text{nm}$ ) was measured, integrated, and stored using the DAS (Appendix 2), triggered on 90° blue scatter. The PMT gains were: 90° red: 2.0 and 90° blue: 1.65. Histograms of  $\log_{10}\text{RF}$  were computed off-line on our data analysis system, and are shown below.
- After approximately 6 hours of incubation, a small portion of the final 1  $\mu\text{g/ml}$  aliquot was mixed with PI (final concentration about 50  $\mu\text{M}$ ), and examined by fluorescence microscopy. The sample was neither sieved, nor fixed; the goal was to assess cell viability by PI exclusion (*v.i.*).

## Results

As in the growth experiments, the flow cytometer measurements are summarized in the form of log histograms of red fluorescence, shown in Figure 3.6; in this case, the histograms are overlaid to facilitate visual comparisons, and grouped by drug concentration. In order to help quantify growth at the different drug levels, the mean  $\log(\text{RF})$  was computed for each aliquot, and plotted *vs.* the sample incubation time; the result is shown in Figure 3.7.

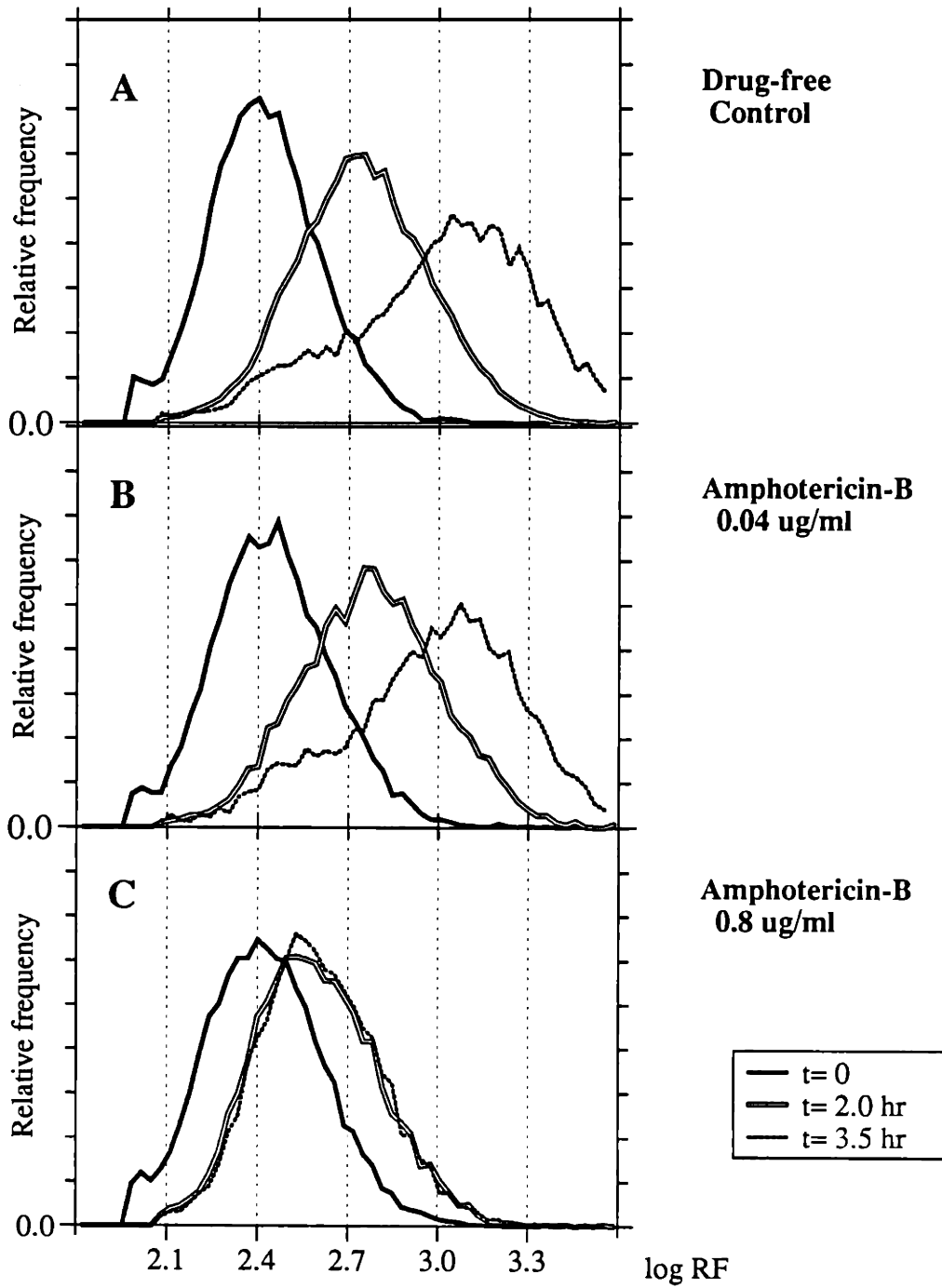
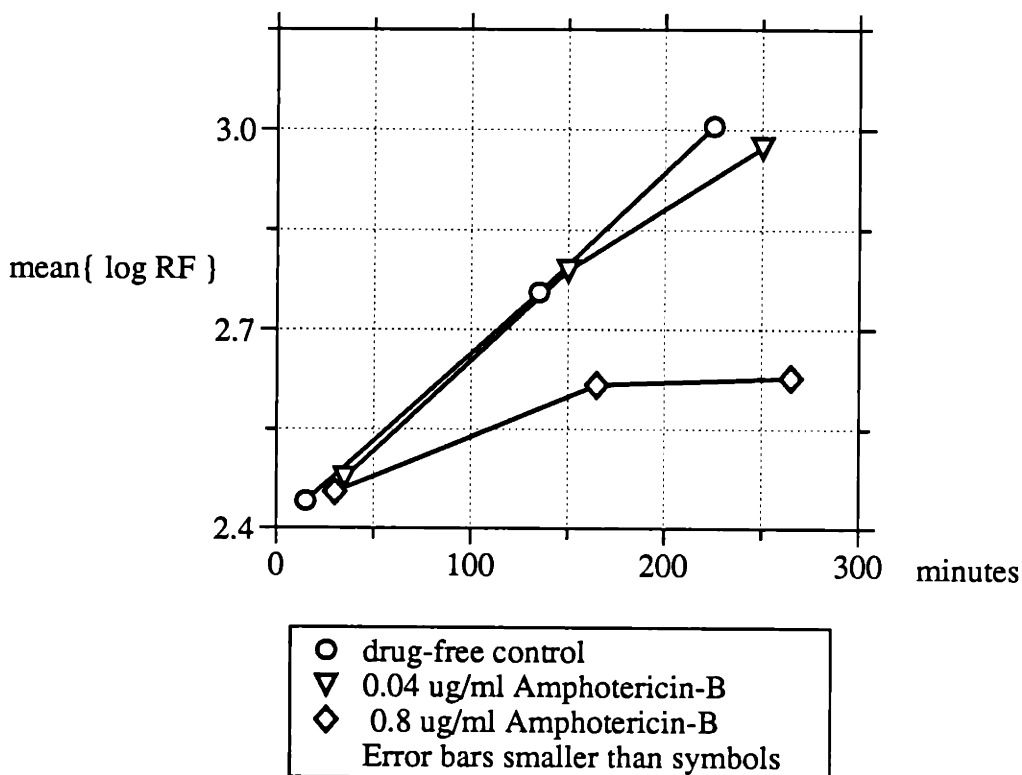


Figure 3.6: Growth inhibition of *C. utilis* by Amphotericin-B : GMD assay

A point of explanation is in order here. In this protocol, at each nominal time point, *i.e.* 0, 2 and 3.5 hours, the samples were sieved and fixed sequentially. This is in contrast to other experiments where samples were fixed simultaneously by adding methanol directly to the GMD suspension before sieving. The sieving, fixation, *etc.* takes at least 15 minutes. Thus, the actual incubation time for each sample can differ from the nominal values used in Figure 3.7, by 30 minutes or more. While this time-spread does not materially affect the qualitative results of visual comparison, there is a measurable amount of growth in 15 minutes; thus the true incubation times were used to plot the mean log RF in Figure 3.7.

As in the growth assay, the histograms shown in Figure 3.6-A demonstrate the initial distribution of PI-stained biomass, and the increase in same, as incubation time increases. The histograms in Figure 3.6-B and -C show a different behavior as the GMDs are incubated in the presence of increasing amounts of Amphotericin-B. Some important features, discussed below, are:

- At  $t=0$ , the drug-free control (A) shows the initial distribution of PI-stained biomass. The  $t= 2$  hour and 3.5 hour distributions exhibit qualitatively the same characteristic shift in  $\log\{\text{RF}\}$  as was seen in the growth experiment.
- The series of log histograms for the aliquots with 0.04  $\mu\text{g}/\text{ml}$  Amphotericin-B (B) added is qualitatively the same as that for the drug-free control. This serves to demonstrate that there are no unexpected artifacts related to the drug itself, *e.g.* drug-dye interactions, at least not at this low concentration, and no artifacts related to the drug-addition protocol.
- At  $t=0$ , the sample with 0.8  $\mu\text{g}/\text{ml}$  Amphotericin-B (C) shows the same initial distribution of PI-stained biomass as the drug-free control. The  $t= 2$  hour distribution exhibits a clear shifts in the RF distribution, though less than in the control. There is no apparent RF shift between 2 and 3.5 hours.



*Figure 3.7: C. utilis in GMDs, plus Amphotericin-B: mean log(RF) vs. time*

The log plots of Figure 3.7 reinforce the conclusions of visual comparison of the distributions, and reveal some less apparent features.

- The drug-free control exhibits nearly exponential growth over the course of the experiment, with a doubling time on the order of 100 minutes.
- The aliquots with 0.8  $\mu\text{g/ml}$  Amphotericin-B exhibits much less net growth over the first 2 hours, and then essentially no growth over the second 90 minutes. The change in mean log RF, about 0.15, corresponds to ~40% increase in biomass, well short of a doubling; this agrees well with the optical density data in Figure 3.5. Based on the OD results, I expect the bulk of the increase in mean log RF actually occurs in the first 90 minutes or so. Due to the sequential fixation protocol, discussed

above, the '2 hour' data point at this drug level was actually taken at 2.5 hours. A repeated experiment with a few samples taken before 90 minutes would be useful for comparison.

- The aliquots with 0.04 µg/ml Amphotericin-B seem to grow as fast as the control for the first 120 minutes, and then to slow down for the second 90 minutes. This was not apparent by visual comparison of the distributions, but is consistent with optical density data presented in Figure 3.5. From the early-time data, it is reasonable to conclude that no significant drug-dye interaction is taking place, at least at this drug level.

### Cell Viability Revisited

Cells with intact membranes exclude most molecules, and especially charged ones such as propidium<sup>94</sup>; thus the lack of PI uptake by cells is used as an indicator of cell viability. To address the issue of the GMD protocol *vs.* cell viability, I added some PI to an unfixed, unsieved aliquot of GMDs, which had been incubating for 6 hours, as well as to an aliquot of the free-cell *C. utilis* suspension that was used to inoculate the GMDs. For each sample, a small fraction of the cells was seen to take up the dye and emit red fluorescence; haemocytometer counts of a few hundred cells indicated very high, and statistically indistinguishable viabilities, of more than 99%. This supports my earlier claims that GMD preparation does not reduce cell viability, but with a *caveat*. The high viability of the inoculum, as well as the good growth of the control indicates that the cells in the inoculum were quite healthy; cells which were less healthy, or had been stationary for a while, might not have been more susceptible to protocol stress.

This result was somewhat surprising, since the GMDs had been incubating in the presence of 0.8 µg/ml Amphotericin-B (this was a spare sample from the experiment). The mechanism of action of Amphotericin-B is to insert into the cell membrane and introduce transmembrane pores<sup>100</sup>; thus, it would have seemed reason-

is no significant transport lag-time for the Amphotericin-B molecule. Further experiments with both assay methods, but using more early-time samples, would be useful to strengthen this claim. However, great experimental care would be needed to control for other confounding variables that might affect the drug-effect time delay, such as cell state.

- When pure strains (*i.e.* single-species) are used for inocula, the GMD method is *not* inherently faster than the optical density method. It is well known that changes in cell mass precede changes in cell number<sup>98</sup>. Both the optical density and GMD-based assays are sensitive to increases in biomass, and therefore both should be able to detect growth in less than an average cell division time. The results of these experiments confirm that prediction, and show that turbidity-based assays are just as fast as GMD-based assays at detecting growth, and the inhibition of growth in the presence of drug, and *vice versa*. In practice, of course, both methods require that the sample contains enough cells to produce a measurable signal. With respect to other current methods, the GMD method has the potential to work from a sample of many fewer cells; this will be discussed further in Chapters 4 and 5. This is critical to obtaining rapid results, since the culture step needed to amplify a clinical isolate to the required cell number can be severely rate-limiting. Finally, as we will see in the next chapter, the OD method may give misleading results in the vicinity of the MIC, requiring a longer incubation time to make an accurate MIC determination.
- A plausible interpretation of the initial growth period is that the pore formation due to Amphotericin-B is tolerated for a short time by the cell, and that synthesis of biomaterial (and possibly division) continues. Eventually, however, synthesis stops, possibly as the cell exhausts its capability to maintain its internal milieu. The results of the viability test (above) indicates that the action of the drug at this level is not too drastic however, as the membrane still excludes molecules as small as propidium. An alternate explanation for the apparent delay in drug action is the time constant for insertion of the molecules into the membrane, and for the aggregation of molecules which is required for pore for-



able if *all* of these cells took up PI through these pores. Considering the small size of PI (670 Dalton, ~ 2 nm largest dimension), we can infer that either the pores are very small, or that there are a relatively few of them. In addition, the structure of Amphotericin-B is such that the pores it forms have hydrophobic interiors; this would further retard the diffusion of propidium, which is charged, through the pores.

### Section 3.6: Discussion and Comparison of Assays

These results demonstrate the ability to observe and measure growth inhibition of *C. utilis* microcolonies in GMDs, in the presence of inhibitory levels of the antifungal agent, Amphotericin-B. The results are consistent with those obtained by turbidimetric measurements. The following points should be considered:

- The classic gold-standard, visual evaluation of turbidity, shows that Amphotericin-B inhibits growth at 0.8  $\mu\text{g/ml}$ . Both the OD and GMD assays confirm a long-term growth inhibition, but only after a brief initial period of growth. Specifically, by either measure, *i.e.* turbidity or fluorescence-labeled biomaterial, there is a definite increase in the biomass signal associated with the sample. This underscores the point that in some cases, the ability to provide a rapid determination of antibiotic susceptibility is rate-limited by the biology, in particular by the mechanism of action of the drug (*v.i.*). In this case, the drug appears to have acted before a doubling in biomass, and both methods detected the result of that action.
- In the absence of the OD experiment for comparison, a possible explanation for the initial growth phase in GMDs would be a molecular transport limitation; *i.e.* that the Amphotericin-B molecules were not immediately reaching the cells, due to some interaction with the gel material. However, the fact that the duration of the initial growth phase is about the same for the two methods, within the admittedly coarse time-resolution of the early-time measurements, argues for the opposite conclusion: there

mation.

### Section 3.7: Summary

In this chapter, I presented experimental evidence that the GMD-based growth assay does in fact work, for the yeast *C. utilis*. Of particular interest:

- The GMD cytometry-derived biomass measurements do exhibit an 'exponential growth' phase, which we would expect of microorganisms.
- The biomass doubling time of the microorganism, derived from the GMD assay, is in very good agreement with the cell-number doubling time, derived from conventional broth suspension and turbidity measurements. The GMD-derived doubling time was in fact somewhat faster, which might be expected since a richer growth medium was used for the GMD method. Additional experiments using the same media are warranted, and straightforward.
- In the presence of Amphotericin-B, at a concentration which inhibits growth as measured by a conventional optical density method, the GMD results also demonstrate inhibition of growth. Both methods are in agreement that for this combination of drug and organism, there is a short growth phase (*i.e.* increased biomass) before inhibition takes effect; the duration of the initial growth phase was the same for the two methods.
- The combination of appropriate doubling time, and appropriate drug response time supports the conclusion that, for the nutrients and drug used here, there is no significant molecular transport limitation.

These results lay the groundwork for the experiments of the next chapter, which aim to derive and compare minimum inhibitory concentrations for Amphotericin-B and *C. utilis*, using both conventional and GMD-based assays.



---

*Chapter 4***Susceptibility Experiments**

---

In this chapter, I will present results of susceptibility determination experiments, for the *C. utilis*, Amphotericin-B system, using three methods:

- the gold-standard method of broth macrodilution, *i.e.* serial dilution of Amphotericin-B in nutrient broth, inoculation and overnight incubation, and visual scoring of the tubes for turbidity. The result will be used as a reference MIC for comparison of other methods.
- optical density measurements, taken at periodic intervals on the macrodilution samples as the gold-standard assay is run.
- the GMD growth assay, run in nutrient medium containing serial dilution levels of drug.

From a clinical perspective, the results of interest are the minimum inhibitory concentrations (MICs) determined by each method, and how they compare with the reference MIC, and with each other. We will also want to compare the relative speed of the methods, and also examine issues related to automation.

**Section 4.1: Macroscopic MIC determination: Turbidity**

The goal of this first experiment is two-fold: (i) to establish a reference MIC for this organism/drug combination by the broth macrodilution method, and (ii) to obtain quantitative optical density measurements as the assay runs, for comparison to the results of the GMD assay.

**Protocol 4.1**

This protocol is based on the the standard method for antifungal testing by broth dilution, as published by the American Society for microbiology<sup>16</sup>. There are some notable differences, however, which are identified and discussed later in this section.

- A stock solution of Amphotericin-B (4000 µg/ml) was prepared, by dissolving 11.4 mg into 2.28 ml of DMSO, then diluting with de-ionized water (DIW). The distributor (Sigma) asserts that the Amphotericin-B powder is approximately 80% active (by HPLC), thus the stock is 4000 µg/ml rather than 5000 µg/ml. This was stored in a glass vial, wrapped in foil, in the refrigerator, as the drug is both light sensitive and thermally unstable.
- A working solution of Amphotericin-B (20 µg/ml) was prepared by mixing 125 µl of the stock into 25 ml buffered YNBD, in a 50 ml polypropylene tube.
- *C. utilis* (ATCC #9226) was grown up on YM-agar plates. Several colonies were transferred to buffered YNBD broth, and incubated overnight, with rotation, at 26°C.
- The serial drug dilutions were carried out in 50 ml polypropylene tubes. First, 10 ml of the Amphotericin-B working solution was diluted with 40 ml of YNBD medium, to produce 50 ml at 4.0 µg/ml. Of this, 25 ml was transferred into a second tube, and diluted with 25 ml of fresh YNBD, to produce 50 ml at 2.0 µg/ml. This dilution step was repeated 5 times into 5 more tubes. Finally, 25 ml of fresh YNBD was added to all tubes to produce 50 ml in each at 2.0 µg/ml through 0.031 µg/ml.
- Each tube was inoculated with 800 µl from the yeast suspension; this was pre-determined to yield an initial OD of 0.025. From each tube, 5 ml was transferred into a glass test tube for a t=0 optical density reading; the

same tube was used for all readings, and rinsed with DIW between samples.

- The remaining 45 ml cell suspensions were incubated with rotation, at 26°C. At periodic intervals, another 5 ml aliquot was transferred to glass test tube, OD<sub>530</sub> measured, and glass tube rinsed.

## Results

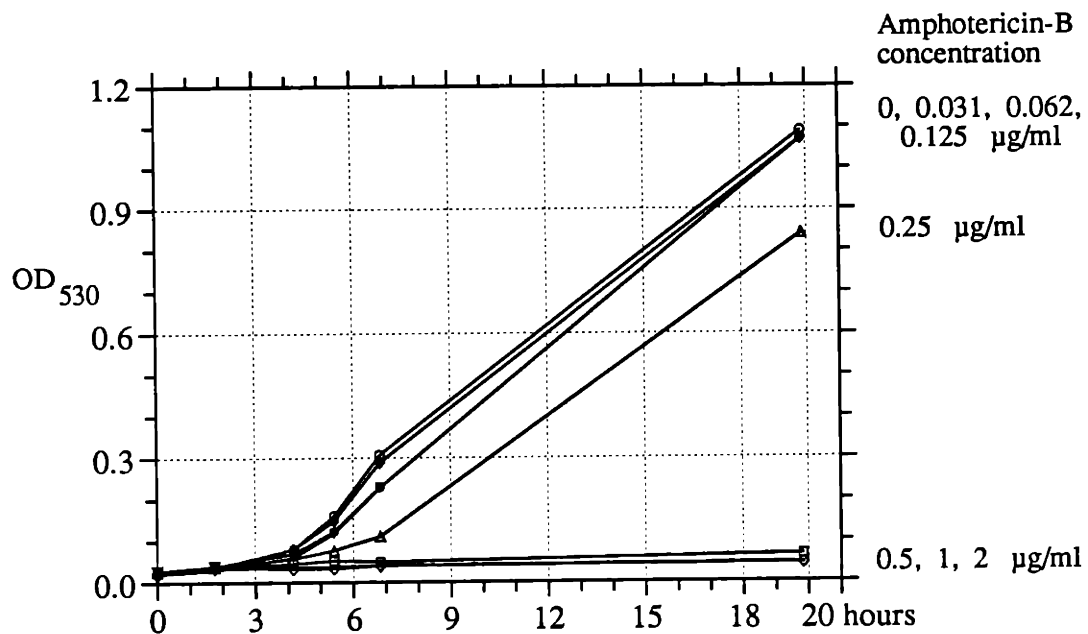
After the final OD<sub>530</sub> reading, at  $t = 20$  hours, the tubes were visually scored for turbidity. No turbidity was seen in those tubes for which the Amphotericin-B concentration was 0.5  $\mu\text{g/ml}$  or greater. For the remaining tubes, turbidity was evident, although there was less turbidity in the tube containing 0.25  $\mu\text{g/ml}$  than in the tubes with less drug. Therefore, invoking standard methods, we have the conclusion that the reference MIC = 0.5  $\mu\text{g/ml}$  It is reassuring that the published MIC range for Amphotericin-B and *Candida* species other than *C.albicans* is 0.2 to 1.56  $\mu\text{g/ml}$ .<sup>16</sup>

Next, the raw OD<sub>530</sub> data was plotted *vs.* time, as shown in Figure 4.8. These plots serve to quantify the visual scoring. I will present a closer look at this data, especially at the earlier times,  $t < 7$  hours, in conjunction with analysis of the GMD results. For now, the key observations are:

- For the control, and lowest drug concentrations, typical growth is seen over the first 7 hours. Had more optical density readings been taken overnight, we would expect a smoother sigmoid growth curve as the cells entered and sustained exponential growth, and then slowed.
- For the intermediate drug levels, 0.0625 to 0.25  $\mu\text{g/ml}$ , there is less net growth over the first 7 hours. However, the 0.062 and 0.125  $\mu\text{g/ml}$  samples were able to catch up to the control overnight, as the control sample slowed down. The 0.25  $\mu\text{g/ml}$  sample was not able to catch up overnight (thus it was visibly less turbid in the morning), but exhibits about the same growth *rate*, *i.e.* slope of the OD *vs.* time line, and would be expect-

ed to catch up to the control if incubated another several hours.

- For drug levels 0.5  $\mu\text{g/ml}$  and greater, there is *almost* no change in OD. As we saw in Chapter 3, there is an increase in OD between  $t=0$  and second time point, for all of the samples; this will be seen more clearly, and discussed, momentarily. In addition, there is a slight increase in OD for the 0.5  $\mu\text{g/ml}$  sample during the overnight incubation. Thus, it is possible that for some of these high drug levels, continued incubation would eventually give rise to turbid growth. However, the standard method calls for the tubes to be scored at a standard incubation time; although there is some ambiguity as to when that time should be (*v.i.*), there is no interpretation that would support waiting long enough for that to occur. Thus, the conclusion for drug levels at 0.5  $\mu\text{g/ml}$  and higher is: no growth.



By Visual Inspection:  
 Tubes turbid < 0.5  $\mu\text{g/ml}$   
 Tubes clear  $\geq$  0.5  $\mu\text{g/ml}$

Figure 4.1: Susceptibility assay: optical density vs. visual scoring

### Protocol Variances

As stated above, there are some notable differences in the protocol used with respect to the standard method. Here, I identify these variances, and consider their possible effects on the results:

- The inoculum used here has a higher cell density than the recommended standard, in particular, about 20 times greater. As discussed below, the effective cell concentration for the GMD assay was also much higher than the standard inoculum density. It is well known that MIC results can be quite sensitive to the initial inoculation density; therefore to make comparisons of the two methods reasonable, I decided to use a higher initial inoculation density for the optical density experiments. Secondly, this was done as practical matter; the recommended inoculum has such a low cell density that no significant OD readings could be taken for about 6½ hours after inoculation. Instead, I chose to start at a cell density which gives approximately the lowest, reasonably measurable OD for our spectrophotometry apparatus.
- The standard protocol calls for inoculation at 30 °C, but I used 26 °C. Fungi normally like to grow in the range of 24-27 °C; incubation at 30 °C is recommended in order to promote conversion of dimorphic fungi in the mold state to the yeast state. In actuality, fungal conversion is optimal at 37 °C, but that temperature promotes inactivation of polyene antifungals such as Amphotericin-B; hence, 30 °C is a recommended compromise. In this work, dimorphism was not observed in the cell samples. Since the cells prefer temperatures of 24-26 °C, and the issue of drug stability was present, I opted for incubation at 26 °C. In general clinical application, incubation at 30 °C might be required. From the perspective of the GMD materials and protocol, this does not present a problem; in our laboratory we routinely work at 37 °C for bacterial and mammalian cell culture.



- The standard protocol is somewhat confusing regarding the incubation time required. The instruction is that the tubes should be "read as soon as the growth control becomes positive, *i.e.* at 24 to 48 hours." Since I used a 20-fold higher cell density in the inoculum, effectively eliminating the need for  $-4$  divisions, I elected to read the tubes somewhat early, *i.e.* 20 hours *vs.* 24 hours. However, in the samples run here, turbid growth was visible in the control less than 5 hours after inoculation, so there is a little conflict in the instructions. Had the tubes been read as soon as the control went positive, the 0.25  $\mu\text{g/ml}$  sample would have been read as negative for growth, and thus the MIC would be 0.25  $\mu\text{g/ml}$ . In consideration of the long-term behavior of the 0.25  $\mu\text{g/ml}$  sample, *i.e.* the delayed growth but eventual turbidity and normal growth rate, I felt that the 20 hour reading provided a more accurate interpretation of the MIC.

## Section 4.2: GMD-based MIC determination

### Protocol 4.2

This protocol is identical to protocol 3.2, except that the GMD aliquots are incubated in the presence of serial dilution concentrations of Amphotericin-B. As detailed below, the dilution steps were a factor of  $\sqrt{2}$ , which were effected not by serial dilution, but by adding the appropriate amount of drug working solution to the GMD samples. Here, I outline the protocol used. Unless noted otherwise, the details of GMD manufacture, handling, and flow cytometry are identical to protocol 3.2.

- *C. utilis* (ATCC #9226) was grown up on YPD-agar plates, transferred to YPD broth, and incubated overnight, with rotation, at 26°C.
- *C. utilis* cells were immobilized in GMDs (2½ % ULMP), at a final concentration of  $2 \times 10^7$  cells/ml.
- Twelve tubes of GMDs were prepared. After transfer of the GMDs from oil suspension to YPD, the GMDs were pooled, and split into twelve ali-

quots of 5 ml, less the volume of drug to be added (*v.i.*) To ten of the aliquots, a volume of 20  $\mu\text{g/ml}$  Amphotericin-B working solution (see protocol 4.1) was added. The volumes added, and the corresponding drug levels were:

552	320	226	160	113	80	56	40	28	14	$\mu\text{l}$
2.20	1.28	0.90	0.64	0.45	0.32	0.22	0.16	0.11	0.056	$\mu\text{g/ml}$

- A drug-free aliquot was immediately fixed by adding 10 ml of 75% (*v.v*) methanol for a final concentration of 50%. The eleven remaining aliquots were incubated with rotation, at 26°C.
- After incubation for 4 hours, the remaining aliquots were all methanol-fixed in the same manner, and stored in 50% methanol overnight in the refrigerator. In the morning, the aliquots were each sieved (20-44  $\mu\text{m}$ ), washed, and resuspended in 1.5 ml phosphate buffer. and stored in 1.5 ml polypropylene microcentrifuge tubes,
- The samples were stained by adding 51  $\mu\text{l}$  of a 14.8  $\mu\text{M}$  propidium iodide working solution (see protocol 3.2) to each 1.5 ml sample; the final concentration was 0.5  $\mu\text{M}$ . Samples were allowed to stain for at least 15 minutes, so the dye could equilibrate.
- Samples were analyzed with the flow cytometer, with excitation at 488 nm, 44 mWatts, with light-mode power regulation. For each of 32,000 GMDs, 90° red fluorescence was measured, integrated, and stored using the Data Acquisition System, triggered on 90° blue scatter. The PMT gains were: 90° red: 2.0 and 90° blue: 1.65.
- Histograms of  $\log_{10} \text{RF}$  were computed off-line on our data analysis system, and are shown below.

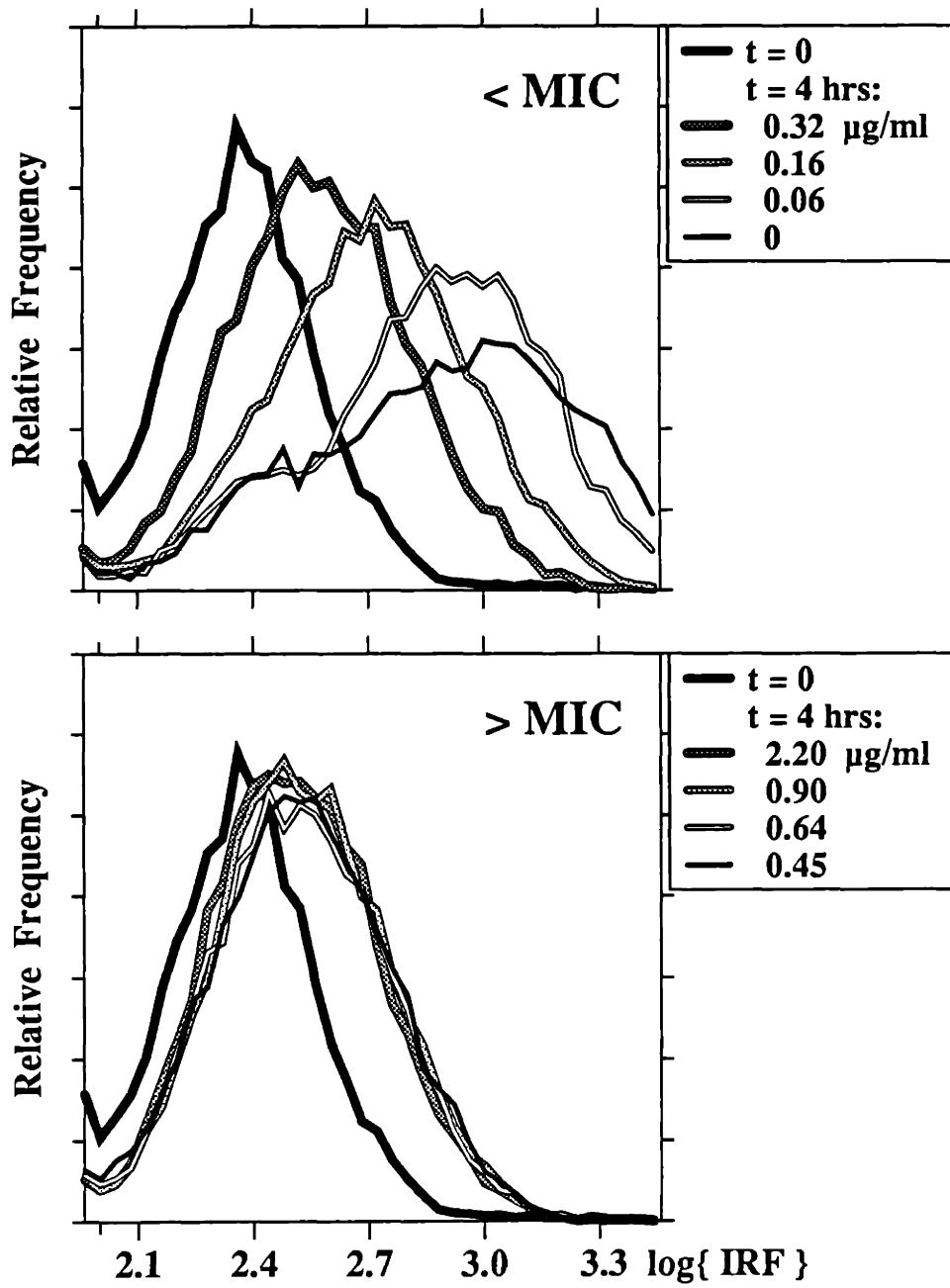


Figure 4.2: Susceptibility assay: GMD-based assay

## Results

Histograms of  $\log_{10}RF$  are shown in Figure 4.2. For clarity, I have elected to group the log histograms by their drug concentration, relative to the macroscopically derived MIC. The supra-MIC histograms are overlaid in the top panel, and the sub-MIC histograms in the lower panel; both panels include the  $t=0$  sample for reference. I will begin with some general observations about these results, and then present a more detailed look.

- In the top panel, each sample exhibits a shift in the RF distribution, relative to the control. The RF shift exhibited between the two drug-free samples, at  $t=0$  and  $t=4$  hours, indicates the maximum RF shift over the incubation period. Qualitatively, it is evident that adding drug to the sample decreased the extent of the RF shift, by an amount which increased with drug concentration.
- In the bottom panel, each sample exhibits a shift in the RF distribution, as above. However, the amount of the shift appears to be about the same in each case.

## Discussion

As usual, the RF shift evident in each of these samples is interpreted as increased biomass, *i.e.* growth, over the incubation period. Apparently, there is a graded response of this growth to the presence of drug. At low concentrations, there is a small but measurable decrease in the amount of net growth; as the drug concentration is increased, the amount of net growth decreases accordingly. At drug concentrations above some threshold, the amount of growth is apparently the same, and is equivalent to less than a doubling in biomass. Comparison to the results of Chapter 3, reveals this increase to be qualitatively the same as the 'initial growth' seen in earlier experiments. Thus, the tentative conclusion is reached that long

term growth has been inhibited in each of these samples, consistent with the macroscopic, reference MIC results.

#### 4.2.1: The Dose-Response Curve: Deriving an MIC

It is very encouraging that the log histograms are consistent with the macroscopic MICs; next we must consider going the other way: *i.e.* deriving an MIC from the log histograms. Although visual inspection seems adequate in this case, a more quantitative approach is preferred. In addition, relying on visual inspection of histograms invites inter- and intra-operator variability, and is to be avoided.

My approach is to plot a dose-response curve, plotting the mean integrated red fluorescence, (IRF) for each of the GMD samples *vs.* the log of the Amphotericin-B concentration. There is no underlying theory supporting this choice of variables; they seem intuitive, however, given the interpretation of mean RF as average biomass, and given a geometric progression of drug concentrations. The dose-response curve for the previous set of log histograms is shown in Figure 4.3. For comparison, on the curve, I have labeled the reference MIC, as determined by broth macrodilution.

For this curve, the following comments and observations apply:

- On the left side of the curve, the response of the control samples is shown; their abscissa is arbitrary, since  $\log(0)$  is not defined. The increase in RF is approximately 3.2-fold, indicating rapid growth with little or no lag over the incubation period.
- The remaining points depict the dose-response of this system. Supporting our qualitative results, there appear to be two distinct regions. For concentrations less than 0.45  $\mu\text{g/ml}$ , we see a linear segment of negative slope. For concentrations greater or equal to 0.45  $\mu\text{g/ml}$ , we see a linear segment of zero slope; these all have a vertical displacement from the  $t=0$

point, quantifying the initial growth discussed previously as about 40% of the initial value.

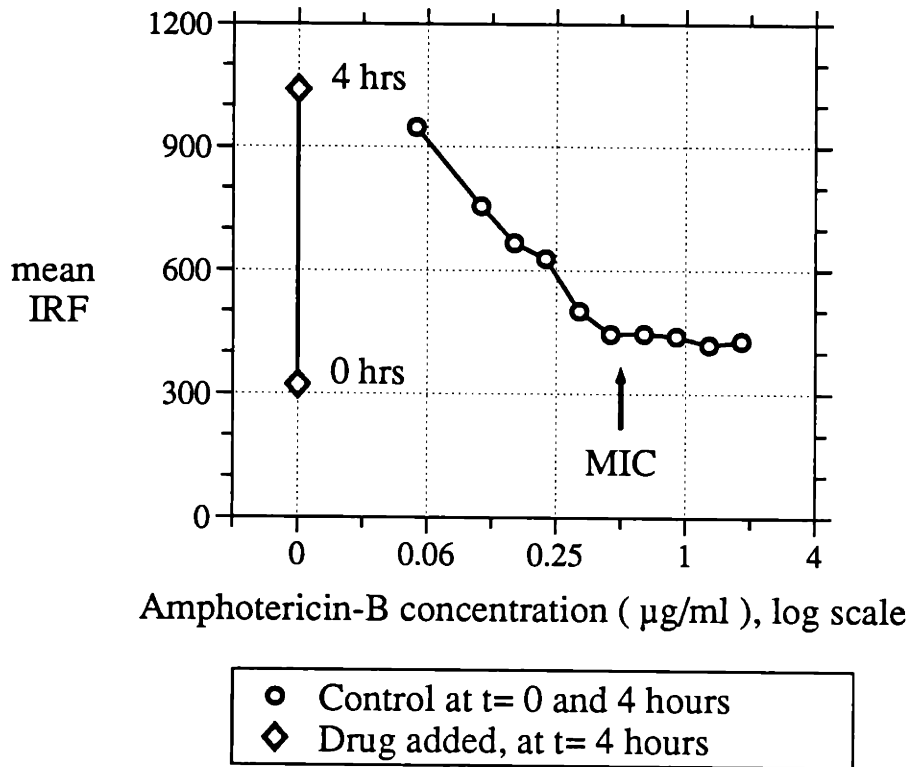


Figure 4.3: Dose-response curve for GMD-based MIC assay

From the curve shown, it is fairly straightforward to conclude that for concentrations less than 0.45 μg/ml, long-term growth is inhibited; thus, by definition, for the GMD-based assay, the MIC = 0.45 μg/ml.

This is in excellent agreement with the reference MIC of 0.5 μg/ml; of course, these experiments should be repeated with identical drug concentration profiles. On the other hand, the difference between 0.5 and 0.45 μg/ml is less than ½ a dilution step, *i.e.* less than a factor of  $\sqrt{2}$ , which is completely insignificant from a clinical perspective.

### Optical Density Dose-Response Curve: 4 Hours

For the purpose of comparison, as well as looking at a competing technology, I have computed a dose-response curve for the optical density method, after the same amount of incubation time. This curve, depicting the OD signal *vs.* log concentration, is shown in Figure 4.4. Again, I have labeled the reference MIC, as determined by broth macrodilution.

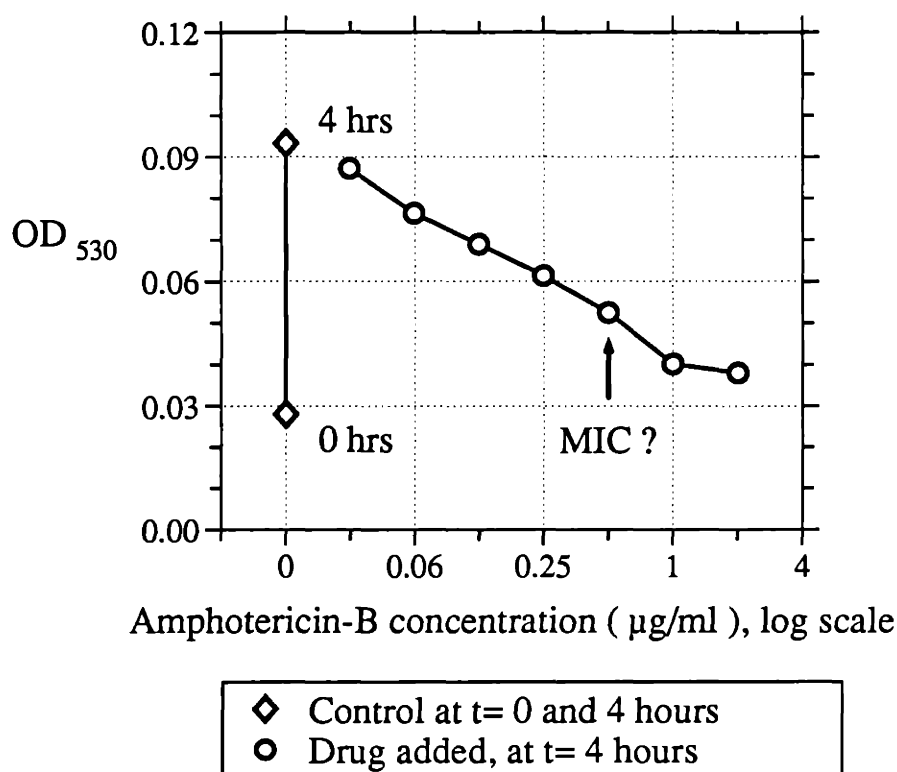


*Figure 4.4: Dose-response curve for OD-based MIC assay, at 4 hours*

Qualitatively, the curve looks similar to the GMD-assay dose response curve. Once again, the two control samples are presented on the left. For each of the drug added samples, it is possible to measure a difference in OD, relative to the control, as we saw for the GMD assay. And, as before, we observe an approximately straight-line relationship between these two variables.

The significant difference is in the MIC determination. There is not a clear choice in MIC, based on looking at this curve. Forced to pick an MIC, 1.0  $\mu\text{g/ml}$  would seem the best estimate, since the largest discontinuity in the curve occurs there. More samples in this region of the curve might help support this conclusion. However, what is clear is that the MIC determined from the long term OD measurements, *i.e.* 0.5  $\mu\text{g/ml}$ , is *not* suggested by this data.

### Optical Density Dose-Response Curve: Evolution

To help clarify this seeming discrepancy between the GMD and OD assay results, I have plotted dose-response curves for later times, in Figure 4.5.

In the top panel, I have overlaid the dose-response curves for OD readings taken at  $t=20$  hours with those of 4.2 hours, *i.e.* the same early data shown in the previous figure. At 24 hours, we see the same result shown in the raw OD plots:

- for concentrations of 0.125  $\mu\text{g/ml}$  or less, overnight growth led to very turbid growth, probably to the point of exhausting the medium, since the OD endpoints were all approximately the same.
- at 0.25  $\mu\text{g/ml}$ , incubation led to turbid growth, but not quite as much as for the lower concentrations.
- for 0.5  $\mu\text{g/ml}$ , there is essentially no change in OD, especially in contrast to the other tubes.

The dose-response curve shows a clear breakpoint, and the MIC is easily identified as 0.5  $\mu\text{g/ml}$ . This of course, is the same as the reference MIC.



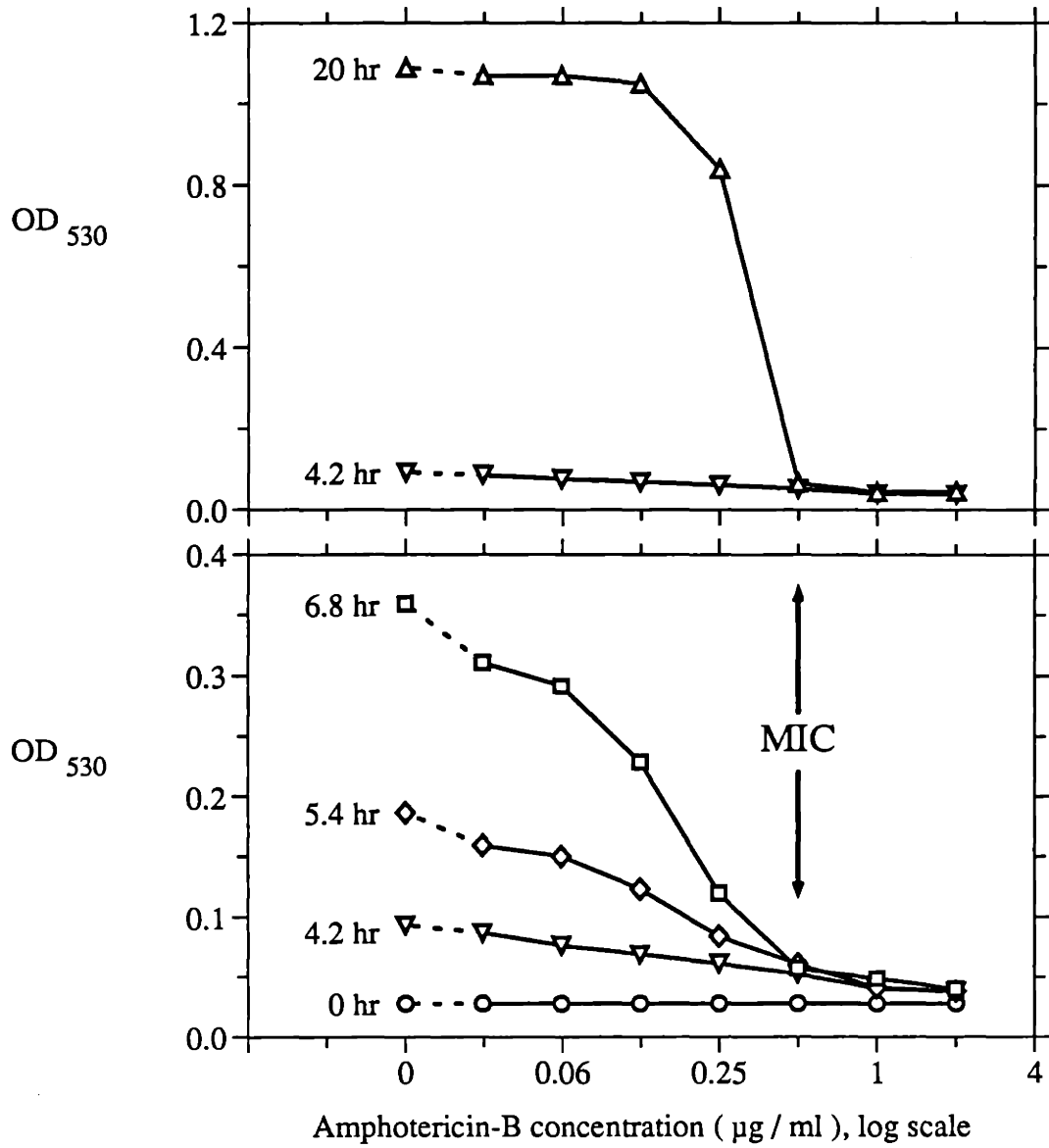


Figure 4.5: Evolution of Dose-response curve for OD-based MIC assay

In the bottom panel, I have overlaid dose-response curves for intermediate times,  $t=4.2, 5.4,$  and  $6.8$  hours. These curves are seen to be intermediate with respect to the  $4.2$  and  $20$  hour curves. Although the straight-line characteristic changes to a sigmoidal shape, there is still a clearly graded, monotonic response, *i.e.* a decrease in net OD change, as the drug concentration increases. Presented with only *one* of these curves, along with the  $t=0$  readings, I would find it very hard to pick an MIC. Again, forced to pick, an MIC of  $1 \mu\text{g/ml}$  would seem the best estimate. Presented with two or more curves, *e.g.* the  $4.2$  and  $7$  hour readings, an MIC of  $0.5 \mu\text{g/ml}$  becomes more apparent. This finding is in part a result of the early growth phase demonstrated and discussed earlier. Apparently, the initial increase in OD for the  $0.5 \mu\text{g/ml}$  sample was significantly greater than the initial increase at higher drug levels. With only an initial reading for reference, it is not possible to distinguish a difference in initial growth, from a difference in long-term growth.

This *caveat* also applies to the GMD-based assay. In particular, although there was a nice, clean breakpoint in the dose-response curve at  $0.45 \mu\text{g/ml}$ , it is not at all possible to predict the response at the next lowest concentration,  $0.32 \mu\text{g/ml}$ . In the dose-response curve, we see a measurably larger increase in mean RF at  $0.32 \mu\text{g/ml}$  with respect to  $0.45 \mu\text{g/ml}$ , but we cannot know for sure whether this represents true long term growth, or just a slight increase in short-term growth. In order to make a conclusion in this matter, RF measurements at a second, preferably later time point are necessary.

### **The Effect of Inoculation Density**

The previous data indicate excellent agreement between the short-term GMD results and the long-term OD results. The short term OD and GMD results differ slightly.

It should be pointed out that this is consistent with a slight difference in inoculation density between the two experiments.

- For the OD experiments, the inoculum was set so that the initial OD would be at about the lowest usable value, *i.e.* sufficiently large with respect to the measurement noise; a value of 0.025 was used. By haemocytometer count, this was found to correspond to a density of  $5.2 \times 10^6$  cells/ml.
- For the GMD experiments, the inoculation density was set to achieve a reasonable occupancy rate in the GMDs: aiming for about a 30% rate, a density of  $2 \times 10^7$  was used. After transfer of the GMDs into aqueous phase, the cells were effectively diluted to a density of  $2.4 \times 10^6$  cells/ml.

As noted in Chapter 1, the standard methods do require standardization of the inoculation density, since the results of these methods are sensitive to the inoculation density. Highly quantitative standardization is apparently not required, since all standard methods recommend visual comparison of the cell suspension to a  $\frac{1}{2}$  McFarland turbidity standard, for which there is an acknowledged order-of-magnitude inter-species variation in the corresponding cell concentration, for bacteria.

One might infer, then, that a difference of a factor of two, as we have here, should not affect the overall results of the test; indeed, the agreement was excellent. However, it is quite plausible that a measurable short-term difference be found in the dose responses, due to a difference in initial density. In particular, for the OD experiments, we have twice the initial cell density, and we are apparently seeing a difference in the early growth of the 0.25 and 0.5  $\mu\text{g/ml}$  samples.

Finally, it should be noted that the OD measurements are sensitive to a number of physical parameters that the GMD method would not be sensitive too. For instance, in the presence of membrane pores resulting from the drug action, it is almost certain that ions and small molecules will traverse the membrane, changing osmotic

forces, and inducing shrinkage or swelling. This would change the net light scatter, and thus bulk optical density measurement. Thus, while optical density appears to be a robust method for tracking the normal growth of cells in suspension, there may be some confounding factors which make it less robust in this situation, where the state of the cell is highly altered. In particular, in the vicinity of the MIC, where the cell state may be somewhat unstable, OD measurements may not be very reliable indicators of biomass. This, of course, is in contrast to the GMD assay, which should be relatively insensitive to such changes, unless they induce some compensatory measures by the cell which affect the amount of indicator biomaterial.

### Section 4.3: Summary

In this chapter, I presented experimental evidence that the GMD-based susceptibility assay does in fact work, for the yeast *C. utilis* and the antifungal Amphotericin-B. Of particular interest:

- Qualitatively, there is an obvious graded response in the shift of the log RF histogram which typifies microcolony growth, as the drug concentration is increased.
- At drug levels above the reference MIC, as determined by broth dilution, all GMD samples exhibit the same response, a small RF shift which is those same in all cases. This is interpreted as an initial growth phase, as seen in Chapter 3, with no apparent long-term growth.
- A GMD dose-response curve was constructed by plotting the mean RF *vs.* log drug concentration; from this, we were easily able to identify an MIC, which was in excellent agreement with the reference MIC.
- An optical density dose-response curve was derived by plotting OD *vs.* log drug concentration, over the same time interval used for the GMD assay. The MIC was *not* readily apparent, and the most likely candidate was a factor of 2 higher than the reference MIC. The significant confounding factor was the initial growth phase, which results in a change in *all* the

samples, above the initial baseline; in theory, taking two sets of early optical density readings, spaced by a few hours, would be required to give the same MIC as the correct, 20-hour reading.

- The underlying principles suggest that the GMD method is relatively insensitive to some processes, such as shrinkage or swelling, that might confound the OD method. However, it is possible that the ambiguities introduced by the initial growth phase may generally affect the GMD assay as well; if true, this would indicate the need for making GMD measurements at two or more time points, if the most rapid results are needed.

These results support the conclusion that GMD-based susceptibility is a feasible technology. However, as discussed in the next chapter, these experiments can only be considered the first steps, not a definitive study; much further work is both required and reasonable. Moreover, in order to realize the potential of the method, especially the use of mixed-species inocula, additional technology is required. These topics will be the focus of the final chapter.

---

*Chapter 5***Discussion & Conclusion**

---

In this final chapter, I plan to revisit and discuss some of the subjects raised previously, and introduce a few new ones. Along the way, I will suggest directions for future work, identify apparent, current limitations, and discuss some of the issues that I feel need to be addressed in order to bring this technology into the clinic.

**Section 5.1: Statistical Inoculation**

Historically, development of gel immobilization techniques, *e.g.* for bio-reactor design, has focussed on preparing droplets which contain a large number of cells. One of the distinguishing features of the methods proposed here, implicit in the discussion of the GMD-based assays, is the ability to form GMDs which contain single cells, or colony-forming units.

For single-species inocula, such as used in this thesis, single-cell occupancy is not critical. As suggested by the discussion of the GMD growth assay in Chapter 1, allowing multiply-occupied GMDs, *i.e.* GMDs which initially contain more than one CFU, merely affects the initial statistical distribution of biomass,  $M(0)$ . The exponential growth model still applies, and predicts that microcolony growth will result in the same characteristic shift of the log biomass signal with time. Some additional increase in the variance of the distribution would be expected if the initial CFUs grew at different rates. From a practical perspective, though, single occupancy is highly desired. If multiple occupancy is allowed, fewer cell divisions will be

possible before cell break-out occurs. In the experiments shown here, in which almost all GMDs were singly occupied. the limit seemed to be about 3-4 divisions; a decrease to 1-2 divisions would make the method much less useful. Going to a larger GMD size is a possible strategy, although by the analysis of Chapter 2, at sizes much above 100  $\mu\text{m}$  in diameter, diffusional limits may start to be significant; in addition, diffusional limits will become more significant when there are twice as many 'consumers' in the gel to be fed as in the case of single occupancy.

For multiple-species inocula, single-CFU occupancy of the GMDs is critical. This feature is one of the key motivations of the GMD method, as it makes it possible to isolate strains at the time of GMD formation, rather than requiring a pre-culture step.

The ability to isolate single CFUs from a suspension has as its basis, the principle of statistical inoculation; put simply, the idea is that if a macroscopic volume is subdivided into volume elements that are small enough, then probabilistic models predict that with very high likelihood, the elements will contain either 'zero or one' CFU. Under certain assumptions (*v.i.*), this concept is appropriately modeled by the Poisson distribution, which states:

$$P(n,V) = (1/n!) (\rho V)^n e^{-\rho V}$$

where:  $P(n,V)$  = probability that a GMD contains exactly  $n$  CFUs.  
 $V$  = GMD volume  
 $\rho$  = CFU density (CFU/ml)

For this distribution, it also well known that the mean number of CFUs per GMD (*i.e.* arrival rate), equals  $\rho V$ . As a point of reference, when  $\rho V = \frac{1}{2}$ , this equation predicts:

$P(0, V)$	= 0.61 = probability of unoccupied GMD
$P(1, V)$	= 0.30 = probability of singly-occupied GMD
$P(>1, V)$	= 0.09 = probability of multiply-occupied GMD

This makes explicit the intuitive notion that, in order to obtain a high probability of singly-occupied GMDs, a large fraction of the GMDs must be unoccupied; in fact a 2:1 ratio is suggested. Similar calculations can be used to adjust the inoculation density to get predominantly singly-occupied GMDs, for any desired GMD size.

Using the dispersion method for GMD formation complicates matters somewhat, since a range of GMD sizes results. Moreover, the GMD sizes are statistically distributed, and the exact distribution is a function of many factors including: oil viscosity (and hence, temperature), agarose viscosity (hence type, concentration and temperature), vortex speed, test tube diameter, presence and concentration of medium components with surfactant properties, *etc.*

Other methods for GMD preparation, *e.g.* using a vibrating orifice method, can deliver GMDs of very uniform size<sup>76</sup>. However, in a recent embodiment of this method which produced agarose droplets in the range of 10 to 40  $\mu\text{m}$ , decreased cell viability was observed<sup>101</sup>. For the bacterial strains where viability was assessed, the viability was less than 40% in all cases. It is unclear at this point whether this is a response to the high mechanical stresses associated with passing through the orifice, which vibrates at 30 to 130 kHz, or is due to other factors such as the rapid evaporation and shrinkage of the droplet in mid-flight. Dispersion methods seem to be kinder and gentler to the cells; a dispersion method which delivered a well-controlled and tight distribution of GMD sizes would be of great use here.



### 5.1.1: Cell Density From Occupation Statistics

Another possibly attractive aspect of statistical inoculation is that, if one measures the statistical distribution of GMD occupancy, and knows the GMD size, the density of CFUs in the inoculum can be estimated. Using the numbers from the example above, if measurement reveals that 39% of the GMD sample is occupied, we can infer that  $\rho V = \frac{1}{2}$ , from which we can estimate  $\rho$ , assuming we know  $V$ . Again, when the GMD size is statistically distributed, we either have to know the distribution beforehand, or make simultaneous measurements of GMD size and occupancy, which is technically feasible.

Of course, as a method of estimating cell density, this proposed method is unnecessarily cumbersome, expensive, and probably not very accurate. Using a Coulter counter would be a much saner approach, although Coulter technology does not distinguish between dead and viable cells. On the other hand, the GMD-based counting method may be an important adjunct to the antimicrobial susceptibility testing protocol. As discussed in Chapter 1, standard methods call for the preparation of a standard inoculum of known cell density; the motivation is a well-recognized sensitivity of the test results to the initial inoculum. Aside from the labor involved, and chance for technical error, this step tends to further delay testing. As discussed in Chapter 1, visual comparison to the  $\frac{1}{2}$  McFarland turbidity standard requires  $5\text{-}50 \times 10^7$  bacterial CFUs/ml. Optical density methods could reduce this by about an order of magnitude, but either method generally requires culture of the isolated organism, at least overnight, to get a sufficient cell number. By contrast, by measuring occupancy statistics, the GMD method may be able to provide a cell count and susceptibility results simultaneously, and compensate the susceptibility results for variable inoculation density. This would of course, require demonstration that such compensation is possible, and acceptable to the community of users.

### 5.1.2: Poisson Assumptions: Modified Poisson Statistics

The derivation of the Poisson model hinges on two assumptions which, using traditional terminology, are stated as:

- independent 'arrivals': the probability of having a CFU in any incremental volume element is independent of the presence or absence of cells in any other incremental volume.
- At most one 'arrival' per incremental volume, and the probability of having an arrival is proportional to the volume, with the CFU density,  $\rho$ , being the constant of proportionality.

For the GMD method, the first assumption is not going to be strictly true, and will affect the occupation statistics.

First, this assumption will be violated if there is not perfect mixing of the inoculum into the molten agarose, at the time of GMD formation. Failing this, there will be a correlation in the spatial locations of the CFUs that violates independence. In practice, perfect mixing is nearly impossible to obtain, largely due to the viscosity of the agarose. This problem is lessened somewhat by using low agarose concentrations, and performing the mixing at warm temperatures. Clearly, mixing can be improved by vortexing the preparation at highest intensity and for longer times; however, the requirement to preserve cell viability speaks against mixing too aggressively. In practice, to effect the isolation of CFUs from the suspension, we only need sufficient mixing to get a high probability of 'zero or one' occupation; on the other hand, the ability to obtain a highly accurate cell density from occupation statistics will be compromised by poor or variable mixing.

Secondly, this assumption is violated because CFUs have finite size. As a result, a steric inhibition phenomenon is possible; the presence of one or more CFUs in a GMD may exclude others, thus violating independence. For example, only one 4  $\mu\text{m}$  yeast cell can fit into a GMD less than 8  $\mu\text{m}$  in diameter. The full treatment of this

reality leads to a modified Poisson model. Its derivation invokes geometric arguments to decompose the volume of each GMD into regions where either (i) CFUs are excluded, *i.e.*  $P(n,V)=0$ , due to the presence of other CFUs, and (ii) CFUs are allowed, and independent arrivals are assumed. Qualitatively, the net effect on the model is to favor fewer CFUs per GMD than predicted by the Poisson model; the presence of a CFU in a GMD effectively reduces the volume  $V$  available for further occupation. A full development of this model was deemed beyond the scope of this thesis. The geometric complexity involved suggests a Monte Carlo approach may be appropriate. Given the number of physical factors which can affect droplet formation and cell immobilization, a more practically useful approach might well be to just measure a large number of GMDs and empirically derive a calibration distribution. Finally, for typical bacterial sizes (0.5 - 2  $\mu\text{m}$ ), and for GMDs of the sizes used here, ( $> 20 \mu\text{m}$ ), one would not expect a significant deviation from the Poisson model. This was recently verified<sup>101</sup>.

## Section 5.2: A Demonstration of Strain Isolation: Photomicroscopy

In this section, I will present and describe a few photomicrographs which demonstrate the principle of statistical inoculation, and support the notion of strain isolation.

### Method

- A GMD sample was prepared in the usual manner, as described in Appendix 1. With respect to the other experiments in this thesis, the only difference was that the inoculum was a 1:1 mixture of *C. utilis* and another yeast, *Schizosaccharomyces pombe* (ATCC# 26189). *S.pombe* was chosen because it has a characteristic rod shape, making it easily distinguishable from *C. utilis*, which is much closer to spherical (*v.i.*).
- After preparation, the sample was incubated, with rotation, at 26°C, for about 4.5 hours. The cells were fixed in 50% methanol, sieved (20 to 44

$\mu\text{m}$ ), washed, and suspended in 10mM phosphate buffer. Propidium iodide was added, to a final concentration of  $\sim 1 \mu\text{M}$ , and left to equilibrate for 10 minutes.

- Photomicrographs were taken using an Olympus 35mm camera, mounted on an Olympus fluorescence microscope, under conditions noted below. Kodak Ektachrome film, ASA 200, was used, with typical exposure times of  $\frac{1}{2}$  to 4 seconds. These black & white prints were made from 2x2 internegatives.

### Plate 1

This plate, (labeled 22 10 33), depicts the GMD preparation as viewed with the 10x lens. A special configuration was used to approximate dark-field illumination over the central part of the viewing field. Simultaneous blue light excitation was provided, in order to visualize PI uptake. Points of interest include:

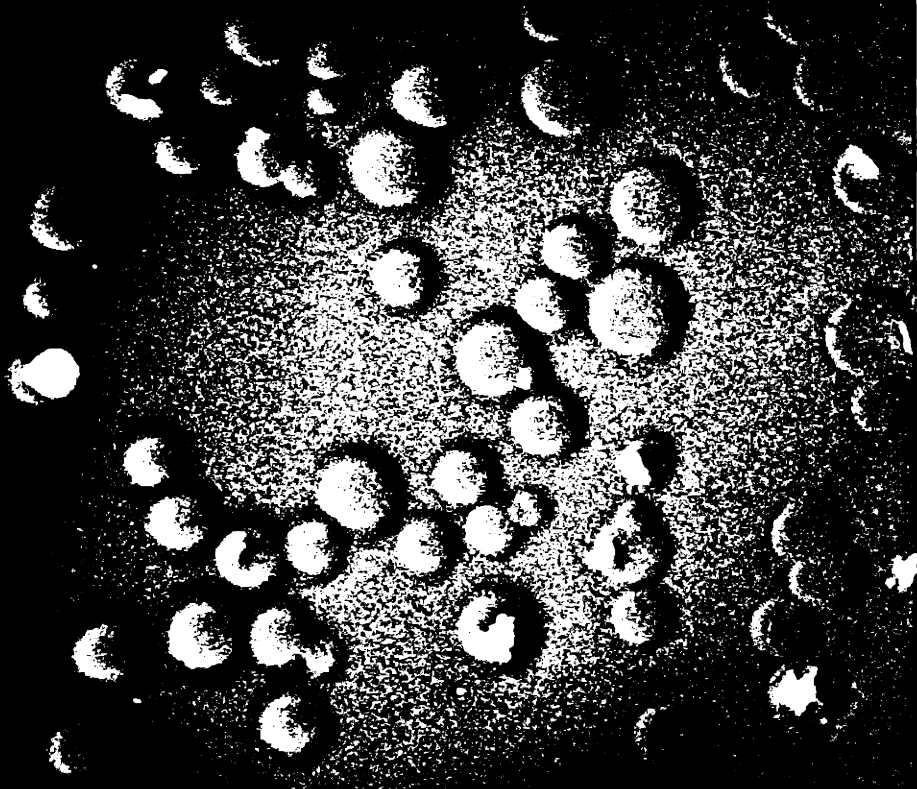
- Since GMDs are mostly water, they are normally almost invisible under normal microscopy. The dark-field approximation allowed good visualization of the GMDs. As pointed out by Shapiro<sup>22</sup>, light scatter measurements in flow cytometry are ideally under dark-field conditions; this picture provides a hint of what the flow cytometer sees when GMDs pass through the flow cell. As noted above, these GMDs are in the size range 20 to 44  $\mu\text{m}$ .
- The occasional bright white splotches in the picture are microcolonies stained with propidium iodide, emitting red fluorescence in response to blue excitation.
- A quick survey of the field of view demonstrates the concept of statistical inoculation described above. In particular: (i) most of the GMDs are empty (ii) the frequency-of-occupation is higher for larger GMDs than smaller GMDs, (iii) the occupied GMDs appear to contain only one microcolony each, except for one (NNW of center), which contains two CFUs.

- It is admittedly hard to tell from this photo, but one can also observe the isolation of species here. The large, clumpy microcolonies, *e.g.* the one due west of center, are *C. utilis*. The smaller microcolonies of rod-shaped cells are *S.pombe*; the microcolonies are smaller because the division time for *S.pombe* is longer than that of *C. utilis*.

## Plate 2

This plate, (labeled 22 11 24), depicts the GMD preparation as viewed with the 100x oil immersion lens. Normal incandescent illumination was used. The horizontal lines (grid lines on a haemocytometer) are 50  $\mu\text{m}$  apart. Here, we see an approximately 40  $\mu\text{m}$  GMD which contains a *C. utilis* microcolony. There appear to be about 12 to 16 cells in this microcolony. This is consistent with the incubation time, which was about 3 nominal division times (4.5 hours), though it seems likely that the initial CFU either had two cells, or was in the process of dividing. One also gets the sense that continued microcolony growth would soon lead to cell break-out, as described in Chapter 3.

EE 01 22



42

11



05 01 22



**Plate 3**

This plate, (labeled 22 10 50), is taken under the same conditions as Plate 2. Here, we see two occupied GMDs, in the range 25 to 30  $\mu\text{m}$ . This plate shows the isolation and culture of the two organisms; at the bottom, we see a microcolony of the round and plump *C. utilis*, and the top, four rod-shaped *S.pombe*. Incubation has resulted in the formation of microcolonies as usual. Had suitable levels of Amphotericin-B been present, we might have observed a differential response in microcolony growth of the two organisms. Finally, if we had a fluorescent signal for identity, e.g. a fluorescently-labeled antibody for one of the organisms, we could have run the sample in the flow cytometer, and obtained that information in 4.5 hours, *vs.* the 48 hours or more required by traditional methods.

It should be noted that the time elapsed from the point just prior to GMD formation to transferral of the GMDs from oil phase to aqueous nutrient is less than 20 minutes; about 5 minutes are required to disperse and gel the GMDs, and 15 minutes or less is sufficient to perform the transferral by the method of Appendix 1. This compares favorably to the 24 to 48 hours required for strain isolation by conventional, plating methods.

**Section 5.3: Sample Size Requirements for GMD Assays**

In previous sections, I have presented the recommended inocula for various standard methods, and discussed some of the consequences of same. Of particular interest has been the need to pre-culture the isolated strains in order to get enough cells to set up and run the tests. In this section, I will explore the sample size requirements for the GMD method.

Unlike other methods, there really is no lower limit for the sample size; since the flow cytometer measures one microcolony at a time, the allowable sample size range starts at 1, and increases indefinitely. Of course, a sample size of one microcolony,

while technically feasible, is statistically unsound. We have expected and seen a wide variation in the initial biomass contained in each occupied GMD; therefore drawing conclusions regarding growth over an incubation period on the basis of examining only a few microcolonies is intuitively dangerous. Statistical methods quantify the danger, or conversely indicate the number of microcolonies that must be measured to reduce the danger to an acceptable level.

The key question is as follows: if flow cytometric analysis of two GMD samples results in two different values of mean red fluorescence (RF), with what confidence can we conclude that their *true* values of mean RF really are different? In particular, if the two samples were incubated in the presence of two different drug concentrations, with what confidence can we assert that a true difference in drug-response exists? Referring to the dose-response curve for the GMD based assay, Figure 4.3, we are most interested in the region in the vicinity of the MIC, where the question becomes: at what concentration is there a statistically significant difference in mean RF with respect to the growth-inhibited samples above the MIC?

Statistical methods provide the tools to address this issue. It is recognized that the sample means derived by measuring a finite number of microcolonies is only an estimate the true mean of the RF distribution; of course, the same is true of the *difference* in sample means. Assuming the sample measurements are statistically independent, the goodness of the estimated means depends on:

- the variance of the parameter being measured, in this case integrated RF. As this variance increases, the variance of the sample mean increases.
- the number of samples measured; as the sample size increases the variance of the sample mean decreases.

In similar fashion, the significance of a difference in sample means depends on the same factors. For the GMD application, the message is clear. The required sample size depends on the variance of the indicator biomaterial signal, and the degree of

confidence we require in declaring two sample means, *e.g.* two drug-responses, different.

Under certain assumptions, the relationship between these factors is quantified by the two-sample Student t-test. Along with the requirement for statistically independent samples, the two-sample t-test is strictly applicable only for comparison of two quantities which are described by normal (Gaussian) distributions, and for which the variances are the same. Here we will use the t-test, not seeking a highly precise result, but a rather a general sense of the relationship between sample size and statistical significance of the assay results.

As discussed in Chapter 1, we have no particular justification for claiming a Gaussian distribution for biomass. However, the histograms shown in Figure 4.2, depicting the distribution of  $\log\{\text{integrated RF}\}$  for different drug levels, suggest that the Gaussian assumption is a reasonable approximation in the vicinity of the MIC. Also, as discussed Chapter 1, under the conditions of exponential growth with uniform rates, the variance of the  $\log\{\text{biomass}\}$  distribution is expected to remain constant, as the mean of the distribution increases with time. Of course, we have anticipated and observed several factors which result in departure from this model, such as cell-break out, non-uniform lag and growth rates, *etc.*, but again we hope to minimize these effects by comparing very similar distributions, near the MIC. In addition, the possible effects that high drug levels may have on the distribution must be acknowledged, although nothing drastic was suggested by the results of Chapter 4, for this particular model system. Overall, we would expect the quantitative validity of the t-test to decrease markedly when comparing two samples of greatly different conditions, such as incubation times, drug levels, *etc.* However, here our objective is to compare two samples in the vicinity of the MIC breakpoint, for which the distributions are qualitatively similar.

The statistic of interest is  $t$ , defined as:

$$t = \frac{\text{MLRF}_2 - \text{MLRF}_1}{s_p \{1/n + 1/m\}^{1/2}}$$

where:

MLRF = mean log (red fluorescence)

$s_p$  = pooled sample standard deviation from the two combined samples.

$n, m$  = the number of points in each of the two samples.

A one-sided  $t$ -test is called for, since we are looking for an increase in Mean LRF as the drug dose decreases, so the hypothesis under test is stated formally as:

$$H_0 : \text{MLRF}_2 = \text{MLRF}_1 \quad \text{and the } t\text{-test asserts: reject } H_0 \text{ when } t \geq t_{\alpha, n+m-2}.$$

The values for  $t_{\alpha, k}$  are taken from published tables. The  $\alpha$ -level, or level-of-significance, is the probability that we will incorrectly conclude that two Mean LRF values are significantly different from each other, and thus obtain an incorrect MIC, on the basis of the test results. The other critical question, which is the probability of incorrectly concluding that the Mean LRF values are *not* significantly different, which will also result in an incorrect MIC, is analytically much less tractable, and will not be addressed here.

Here, I present numbers needed to proceed, derived from the flow cytometric data set acquired in the MIC experiment of Chapter 4.

drug conc ( $\mu\text{g/ml}$ )	mean log{RF}	std. dev. log{RF}	No. of microcolonies measured
0.45	2.6481	0.2289	10042
0.32	2.6987	0.2350	9928

Next, I present the computed t-statistic for this data set, and the values that would result for various, smaller sample sizes. In each case, I present also the  $\alpha$ -level, *i.e.* the false-positive rate, for rejecting the null hypothesis, based on the computed t-statistic and tabulated values of  $t_{\alpha,k}$ .

N:	10000	1000	300
t:	10.9	3.45	1.88
$\alpha$ :	< 0.005	< 0.005	< 0.05

The conclusion is that, despite the seemingly large variance of the indicator biomaterial signal, as we have seen in all the log histograms in this thesis, in actuality a rather small number of microcolony measurements will suffice to detect a statistical significant difference in drug response. Some further points to consider include:

- In the clinical testing scenario, the drug-level resolution is less; *i.e.* concentrations would be varied by a factor of 2, whereas here the steps are a factor of  $\sqrt{2}$ . From the drug-response curve, we observe that increasing the drug-concentration step size will increase the 'signal' that we are trying to measure, *i.e.* the difference in means. From the perspective of the table above, this will increase the confidence level of the conclusion, or alternatively allow an even smaller number of measurements to achieve the same confidence level.
- Instead of labeling both RNA and DNA as we have here, we could label only DNA as an indicator of biomaterial; for example, we could treat the samples with an RNase to digest the RNA, or use a dye such as Hoechst 33258 and 33342, which specifically bind only to DNA<sup>94</sup>. This would have the advantage of a much smaller signal variance, and consequent decrease in the required sample size. The major technical problem to be overcome is that the DNA signal from bacteria is so small that it would be overpowered by the non-specific staining of the gel by any of the

fluorescent dyes tried to date. As discussed in Chapter 2, the fundamental issue is the size of the *integrated* non-specific fluorescence *i.e.* over the volume of the GMD, with respect to the integrated fluorescence of the biomaterial indicator. Thus, some relief can be obtained by using smaller GMDs, *i.e.* for which the volume is less. This approach is limited, however, by the need for sufficient volume and droplet strength to allow for growth and expansion of the microcolony. In short, it would be worth the effort to perform a survey of DNA dyes and protocols in search of one for which the non-specific staining of the gel was not prohibitive.

- Of course, this entire discussion addresses only the issue of variance of the indicator biomaterial measurement, and to some degree only applies to the methods and instruments used here. There is no consideration of other technical errors which can affect the reliability of the result, *e.g.* errors in sample preparation and handling, drug concentrations, staining protocols, *etc.* Also, it is anticipated that a clinically acceptable (*i.e.* reasonably priced) flow cytometer may not have the same measurement performance as the Ortho system used in this research. A system with larger measurement noise will result in a higher  $\log(\text{RF})$  variance, thus requiring a larger sample size to obtain the same overall performance.

### 5.3.1: A Glimpse of a Clinical Instrument

Let us assume for the moment that, on the basis of continued evaluation, a sample size of 1000 microcolonies per drug level was deemed reasonable. Based on the observations of Chapter 4, we might need to make measurements at two different time points, and would then postulate measuring 500 microcolonies at each time. Using these numbers allows us to reach some useful, if tentative conclusions about the specific embodiment of the GMD method in a clinical testing scenario. Of particular interest is the expected overall sample size needed, and the overall test time.

For comparison purposes, we recall that the Vitek technology, currently in place, allows routine testing of 11 drugs at a total of 30 drug concentrations. In Chapter 1, we saw that rather large number of CFUs needed to inoculate each Vitek card, about  $2.5\text{-}25 \times 10^6$  CFUs per drug-level, requiring a lengthy pre-culture step. After incubation, the Vitek reads its cards at a maximum rate of 2 per minute.

Assuming the desire to offer technology comparable to that presently in place, *i.e.* 30 total drug-dose combinations, a GMD test would need to start with 30,000 immobilized CFUs. This number of CFUs is easy to obtain in some cases; for example, by definition a clinically significant a urinary infection implies  $1\text{-}10 \times 10^4$  CFU/ml in the urine sample. In other cases, *e.g.* septicemia, infection is significant at 1 organism /ml. A blood sample might yield 10 organisms, but further incubation would be required; a 3,000-fold amplification would require about 12 division times, or at least 4-6 hours for the fastest growing organisms. Although this time might be shortened by a policy decision to test fewer drug-dose combinations, this pre-incubation is likely to delay the result beyond the time of initial drug choice.

The number of CFUs needed is greatly affected by the efficiency of the GMD formation step, *i.e.* the fraction of CFUs in the inoculum which actually end up immobilized in GMDs of appropriate size. The method used in this thesis has an overall efficiency of only 1 to 2%. Thus, requiring  $3 \times 10^4$  immobilized CFUs as indicated above would dictate an initial need for  $3 \times 10^6$  CFUs in the inoculum. This would still be possible from urine infected at a level of  $1 \times 10^5$  CFU/ml; for the case of septicemia, the pre-incubation would be increased by another 7 division times, at least 3.5 hours. Experience of other workers has shown that the efficiency can be greatly improved by the addition of materials with surfactant properties, such as fetal calf serum<sup>78</sup>, or by improved dispersion methods (G.Williams, personal communication). As discussed above, vibrating orifice methods, which can theoretically approach 100% efficiency, may be fundamentally limited by a cell viability problem, and cannot be recommended at this time.

### **Incubation Time**

Once the GMDs have been formed, the results of this thesis suggest that yeast susceptibility results might be available in as little as 4 hours. Based on work to date in our laboratory, bacterial results may be obtainable in about 2 hours, (G.Harrison, personal communication). An extremely important *caveat* is that in many cases resistance is present but not expressed until incubation for some time in the presence of an antibiotic; the induction of  $\beta$ -lactamases is a classic and well-known example. This fact commonly subverts currently available rapid methods, since the incubation period used is not long enough for the resistance to be expressed; of course the same fact must be addressed in the GMD assay. This is just a specific example of a general requirement, *i.e.* that a systematic validation process must demonstrate agreement of short-term MIC results derived from the GMD method with those obtained from long-term (24 hour) standard methods, and ultimately, with the clinical course of the patients.

### **Test Result Reading Time**

An additional factor to consider is the time and effort required by a specific technology to 'read' the results, *i.e.* to make measurements on each of the drug-dosage samples, and reach an MIC decision. This is especially relevant to a flow cytometer based technology which makes fundamentally serial measurements. As discussed above, due to Poisson occupation, 1000 singly-occupied GMDs requires a total sample of 3000 GMDs, per drug level. At a reasonable flow cytometer event rate of 1000 per second, a reading time of 3 seconds is obtained. Assuming 30 total drug-dose combinations, the net reading time is 90 seconds, using the GMD flow cytometry method. Of course, this assumes a method of sequentially delivering the different GMD samples to the flow cytometer, without a delay between samples. To my knowledge, this technology does not yet exist, but seems realistically feasible. Finally, it should be clear at this point that reading the test results is not the rate-limiting step in the process; assuming the GMD method can eliminate a 24-hour in-



cubation step, adding 60 seconds to the reading time, or even 300 seconds, would seem to be reasonable.

## Section 5.4: Conclusion

The ultimate goal of this work is to develop a new clinical technology for antibiotic testing, distinguished from all available methods by an ability to provide results at the time of the physician's initial choice of antibiotic therapy. In this thesis, I have taken the first, exploratory steps in this process, striving to demonstrate the fundamental ability to isolate, culture, and test individual colony-forming units, and to obtain the same susceptibility results, *i.e.* MIC, as obtained by a gold-standard method. I feel comfortable in claiming a modicum of success in this endeavor, certainly sufficient to warrant further development of the technology.

Of course, at this point, any success claimed can only be applied to the organism-drug combination I have chosen here. Nevertheless, on the basis of the results presented in this thesis, the following conclusions are reasonable:

- *C. utilis* can be readily isolated, immobilized and cultured in agarose GMDs (2½% ULMP, 20 to 44 µm). The subsequent growth of microcolonies, as assessed by flow cytometric measurements of fluorescently labeled double-stranded nucleic acids (DSNA), was seen to conform to the exponential growth model. Moreover, the rate of measured biomaterial increase speaks strongly against any growth inhibition, due for example to mechanical squeezing or molecular transport limitations. This was assessed out to 3 division times, and the maximum colony size seen was about 16 cells.
- The growth of *C. utilis* microcolonies was inhibited by the presence of Amphotericin-B in the growth medium, indicating that the drug was able to reach the immobilized cells. Growth inhibition, as inferred from flow cytometric measurements of microcolony DSNA was consistent, both

qualitatively and quantitatively, with optical density measurements of *C. utilis* in suspension culture, which was used as a reference method.

- Quantitative assessment of microcolony growth in the presence of Amphotericin-B enabled us to derive a minimum inhibitory concentration (MIC) of 0.45  $\mu\text{g/ml}$ , after 4 hours of incubation. This was in excellent agreement with reference MIC of 0.5  $\mu\text{g/ml}$ , derived by the gold-standard method of broth macrodilution, with visual scoring of turbidity after a 20 hour incubation. This was also in agreement with the long-term MIC of 0.5  $\mu\text{g/ml}$  derived by optical density measurements after 20 hours of incubation.
- Attempts to derive an MIC from optical density measurements at 4 hours were not successful, but rather were confounded by an initial growth period common to all drug levels. It was found that making OD measurements at two or more time points allowed a correct MIC determination within 7 hours, and suggested that a similar strategy might be ultimately required for GMD-based methods.
- Microscopic examination of a GMD preparation inoculated with two species, *C. utilis* and *S.pombe*, demonstrated the principle of statistical inoculation, and verified that strain isolation is possible in 20 minutes or less. Strain isolation by traditional methods (plating) is known to required 24 to 48 hours for yeast.

#### 5.4.1: Towards a Clinically Useful Technology

In a status report of DNA probe technology for clinical medicine, the Chief of the Microbiology Laboratory at a VA Medical Center offered the following set of criteria for judging a new clinical technology<sup>19</sup>. Here, I quote the list; clearly, the more questions that are answered in the affirmative, the better.

- Does it open new doors to allow the routine laboratory to diagnose diseases that previously could be detected only by a few research or reference laboratories ?
- Does it provide quicker results ?

- Is it less expensive than the current methods ?
- Is it easier to perform than present procedures ?
- Is less technologists' time involved ?
- Is it more sensitive and/or more specific ?
- Is the reagent shelf-life long enough to meet the demands of the laboratory?
- Is it readily available ?
- Have the published evaluations been conducted in a clinical setting as opposed to a research environment ?

By inference, and as shown by history, the success of a clinical technology can have as much to do with convenience and low total cost (especially labor costs) as with getting the most accurate result.

As is appropriate for this stage of development, for GMD-based susceptibility testing the answers to all of these questions, possibly excepting the shelf-life issue, is currently 'No'. However, on the basis of this thesis work, my opinion is that upon further development, these questions can be answered either 'Yes', or 'the same as accepted methods'. This assertion is based on the overall philosophy of the technology, which is to miniaturize standard methods to the single CFU level, with the expectation that susceptibility results can be obtained significantly faster, as evidenced by the results of this thesis. Thus, I feel that most of the issues raised by this checklist can be addressed to the satisfaction of the intended users, and will require primarily time, money, much more research and development, and ultimately, the interest of the community.

With the ultimate goals in mind, I see three major directions for future work:

- The first goal should be to validate the method with the large numbers of pathogens and antimicrobials of interest. Already, more than 10 common pathogens have been shown to survive with detectable metabolic activity

in GMDs surrounded by oil<sup>102</sup>. This is a promising result, but demonstration of normal growth and drug susceptibility in aqueous suspension is still required. Preliminary results in our laboratory with a penicillin-sensitive strain of *E.coli* shows good agreement between GMD and turbidity-based methods (G.Harrison, personal communication); again, extension to pathogens is called for.

- The second goal, which can and should be addressed in parallel, is the development of a simple, low-cost embodiment of the technology for the clinical market. From the perspective of acceptance, this is critically important, and will require, in my estimation, a significant engineering effort. On the other hand, there is precedent for the acceptance of fairly sophisticated technology in the clinical setting, such flow cytometers, blood chemistry analyzers, *etc.* The key, I suppose, will be to hide the sophistication behind a friendly user-interface. Aside from ease of use issues, an improvement in yield of appropriately-sized GMDs is critical. As discussed above, the cost of continued low yield would be the need for more CFUs from the clinical specimen, which would add a highly undesirable pre-incubation requirement in some cases.
- The third goal is the demonstration of at least one strain identification method amenable to the GMD-based assay, either antibody-based or with fluorescently-labeled gene probes. As explained at length in this thesis, a breakthrough in antimicrobial susceptibility testing will require the elimination or drastic shortening of the pre-culture step. I have demonstrated the ability of GMDs to isolate strains in this thesis; the feasibility of strain identification in GMDs remains as the key point to be proven. Previous work in our laboratory has demonstrated the ability to diffuse antibodies in and out of GMDs of this type, and to perform a GMD-based sandwich assay<sup>103</sup>. Monoclonal (murine) antibodies are commercially available for such clinically interesting pathogens as *C.albicans*, *N.gonorrhoea*, *M.tuberculosis*, and *E.coli*, as well as Streptococci Group A and B.<sup>104</sup> The application of recently developed fluorescently-labeled DNA probes<sup>7</sup> should be investigated as soon as possible.

GMDs may be the enabling technology which sparks a breakthrough in clinical susceptibility testing. When the first two goals listed above are met, an evolutionary step in clinical testing will be possible. The miniaturization and automation of standard methods, in combination with a smaller inoculum requirement and the fundamental rapidity of the method, will be able to provide more rapid test results than currently available methods. When *all* of these goals are convincingly met, it will become possible to obtain susceptibility results, directly from (at least some) clinical specimens, and early enough to guide the physician's initial choice of antibiotic therapy. At that time, a revolutionary change in clinical antimicrobial susceptibility testing will be made possible, based on gel microdroplets and flow cytometry.

*Appendix A***Protocol for GMD Preparation**

---

**Section A.1: Introduction**

In this appendix, I will present the protocol by which GMDs were made and inoculated, for all of the experiments in this thesis. This protocol has evolved over a few years, with the ultimate goal of maximizing predictability and yield, and minimizing cell trauma and experimental hassle. Experience has shown that every member of this laboratory who starts using GMD methods develops his or her own GMD method, which is to say that the basis of the dispersion method is robust enough to tolerate considerable variation. Indeed, this protocol includes those elements of the protocols of others which I found best suited the needs of this problem, plus many twists of my own.

Ultimately, of course, it would be completely inappropriate to propose such a labor intensive protocol for the clinical setting. However, it has served well in helping to achieve the goals of this thesis, and due to its simplicity and generality, serves as a starting place for other researchers to evaluate the suitability of GMD methods for their own work; indeed, such a process is ongoing at this time,

The GMD protocol has these parts:

- preparation of gel
- inoculation of gel
- formation of emulsion
- gelation of droplets
- recovery of droplets from oil phase
- fixation and staining of cells, typically after an incubation period
- recovery of desired droplets from aqueous phase

In the following sections, I will discuss each of these sections with a combination of explicit step-by-step instructions, and comments on such topics as alternate methods.

## Section A.2: Overview of Protocol

A tube refers to one test-tube (16x100 mm) sample of GMDs. Each tube starts with a 100 $\mu$ l aliquot of the cell suspension, typically  $1.2 \times 10^7$  total cells. Usual yield per tube is about 80 to 100,000 GMDs in the size range 20-44 $\mu$ , of which about 30% (25 to 30,000) are occupied by colony-forming units. In general, I use one tube per sample, *i.e.* per time-point, or per drug concentration.

The recipe for making one tube of emulsion is:

- 0.5 ml Type IX Agarose (2.5 % in YPD)
- 0.1 ml cell suspension at:  $1.2 \times 10^8$  cells/ml.  
Final concentration:  $2.0 \times 10^7$  cells/ml.
- 5 ml mineral oil

And its formation, central to the dispersion method, is summarized in Figure A.6.

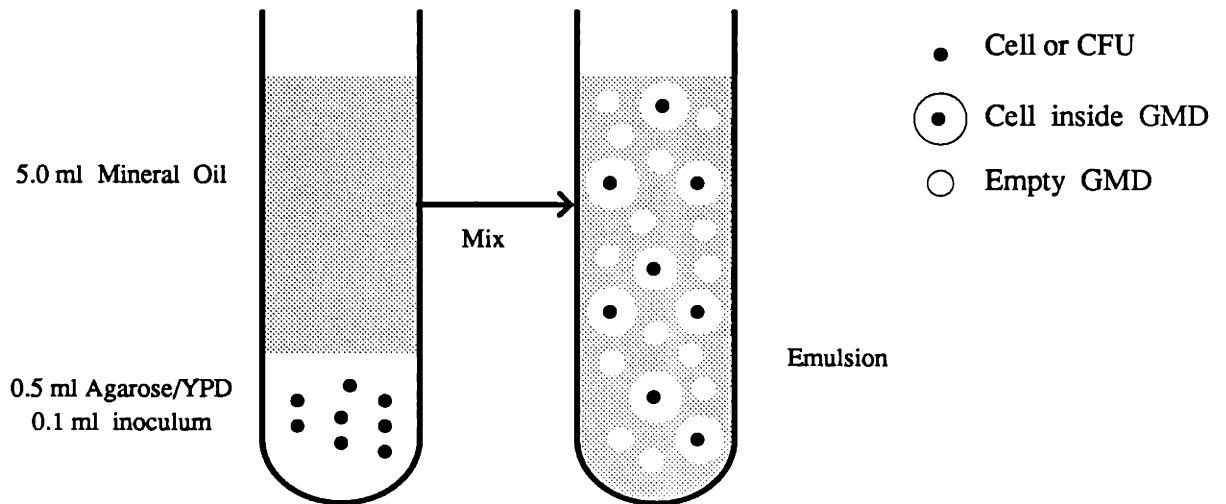


*Figure A.1: Schematic view of dispersion protocol for GMDs*

## Section A.3: Detailed GMD protocol

### A.3.1: General Preparation

- preheat 50 ml water in a 150 ml beaker to 70-80°C.
- preheat 50 ml water in another 150 ml beaker to 37°C.
- preheat 5 ml mineral oil per tube, to 37°C.
- prepare icebath
- prepare 5.5 ml YPD per tube. YPD = 1% Yeast Extract (Difco), 2% Peptone (Difco), 2% Dextrose, in DIW.
- of this, measure 5 ml YPD into a 15 ml culture tube, per tube
- prepare 10 ml 75% (v:v) methanol:water per tube



### A.3.2: Preparation of Gel

- In test-tube, measure 6 ml of YPD medium. While vigorously mixing YPD, *i.e.* with a vortexer, slowly add 0.16 g of Agarose IX. Great care must be taken, so that the agarose does not clump. When done correctly, a slurry will result.
- To each of (up to) 12 test-tubes, measure 0.5 ml of agarose slurry. This is difficult to do with great accuracy or precision. I use a Rainin "pipet-man" with a 1 ml tip (blue-tip), and trim the end so that the minimum opening size is about 3 mm diameter; moreover, I also use a volume setting of 0.52 ml. The slurry should be revortexed as needed to prevent settling during this dispensation.
- Melt the agarose by placing the test-tubes into a water bath, preheated to 70 to 80°C, for 5 minutes. The resulting sol should be translucent, with no graininess, clumps, or foam. If the water temperature is too hot, or the tubes left in too long, evaporation will cause the agarose concentration to rise unacceptably. In general, this step sterilizes the gel sufficiently for my work. In cases where absolute sterility is required, the gel can be autoclaved in bulk, maintained in sol form at 37°C, and dispensed to the tubes<sup>103</sup>.
- Reduce the agarose temperature by placing the test-tubes in a water bath preheated to 37°C for 5 minutes. Evaporation is less of a problem here, but if the tubes are going to be left for more than 10 minutes, I cover them with foil.

The medium used here matters. In particular, the surfactant properties of the medium greatly affect the size distribution of GMDs formed upon mixing. The YPD medium used (yeast extract, peptone, dextrose) has enough surfactant activity to provide a good yield of the small GMD sizes used in this work. In contrast, the medium YNB, a minimal medium for yeast, is noticeably poorer in this regard. It is likely that one or more polypeptide components of peptone (a peptic digest of pro-

tein), or of the yeast extract, carries the surfactant activity; YNB is protein free. Similarly, Powell reported that adding 5% fetal bovine serum dramatically improved GMD yield in his work.<sup>103</sup> And there has been reported initial success with a protein-enhanced medium used in malarial parasite research (D. Kyle, personal communication).

Of course, there are several surfactants commonly used in biological research, which may be applicable here. The caveat of course is that nothing should be used which might traumatize the cells, or affect the outcome of the antibiotic susceptibility tests. Also, it may be the case that some surfactants are "too good". After gelation, we will need to separate the aqueous and oil phases for further incubation; there is some evidence that if the surfactant used stabilizes the emulsion too well, the phase separation will have a lower yield.

### **A.3.3: Inoculation of Gel**

- Using a pipetman and 100 $\mu$ l tip (yellow-tip), add 100 $\mu$ l of inoculum to YPD/agarose; inject at the bottom of the test-tube and draw the tip up during injection to promote mixing. Vortex immediately, speed 10, for 5 seconds, or until well mixed.

The key to everything is good mixing; without uniform mixing, statistical inoculation is meaningless. The concentration (cells/ml) and volume of inoculum depends on the desired inoculation statistics, (*i.e.* Poisson statistics) as described elsewhere. I prefer a largish inoculum volume, in this case 100 $\mu$ l, to promote good mixing. For the same reason, the YPD/Agarose should be kept in the 37°C bath just up to the point of inoculation. I also warm my cell suspension to 37°C before injection, as injecting cold cells can be expected to cause clumping.

#### **A.3.4: Formation and Gelation of Liquid Microdroplets**

- Immediately add 5 ml of pre-warmed (37 °C) mineral oil with a 10 ml pipet, and vortex for 15-20 seconds. Again, the key is mixing. I find that repeated up and down motions (*i.e.* to stop and restart the vortexer) are helpful in this regard.
- Immediately place the test-tube into the ice bath. Each tube should remain in the ice bath about 5 minutes in order for gelation to occur. To prevent settling and clumping, the tube should be revortexed for about 5 seconds every 2 minutes or so.

#### **A.3.5: Recovery of Gel Microdroplets**

- After gelation, pour the contents of the tube into a 15 ml culture tube (orange-cap), into which 5 ml of YPD has been pre-measured. Then place the tube into the rotator, rotating at about 1-2 rpm at 27°C. (This temperature is not sacred, I use it because yeast like it; for bacterial work, 37°C should be ok)
- After 15-20 minutes of rotation, remove the tube from the rotator. The aqueous phase should now contain the majority of the GMDs, and the oil phase should be predominantly clear. Using an 18 gauge needle, punch a hole in the bottom of the tube. It helps to loosen the cap, pre-compress the tube and tighten the cap to create a slight negative pressure in the tube before making the hole. This prevents sample from squirting out the hole when the needle is removed. Remove the needle and drain the aqueous phase only from the bottom of the tube into a clean 15 ml tube (sterile technique); the oil layer on top will act as a piston to push the aqueous phase out the bottom. Stop draining about 0.5 cm before the aqueous/oil interface reaches the hole, to be sure that no oil is transferred with the aqueous sample.

- Once the separation is completed, place the tube back into the rotator immediately to resume incubation of the cells.

The transfer of GMDs back to aqueous phase is effected by the interaction of the two phases at their interface, and depends on the action of a detergent component in the YPD medium. Substitution of other media can be expected to work to an extent which depends on the specific media formulation. In cases where a specific medium is required which does not promote good transfer, the GMDs can be recovered by centrifuging, as per Powell and Weaver (Bio/Technology, April 1990). I find however that the small GMDs that I use for microbiology tend to clump upon centrifugation.

It is crucial that there is minimal mixing of the oil and YPD phases, *i.e.* the tube should not be shaken, inverted, mixed, or any similar thing. If shaken, oil droplets will form, and be suspended in the aqueous phase. This has not been seen to effect growth in our work, but it would almost certainly effect the derived MICs for any drug which partitions into the oil phase. I have found that aspirating the oil from the top of the tube (rather than draining the aqueous phase from the bottom) to be less satisfactory in terms of completeness of oil removal.

GMD transfer from oil to aqueous phase starts immediately, and a large fraction will have transferred within 5 minutes. I usually use a 15-20 minute rotation, after which the oil phase is observed to be clear. Of course, there is a tradeoff here between maximizing yield and getting access to the GMDs as quickly as possible, *i.e.* for purposes of getting a "time 0" sample.

Also of interest is that the transfer is sensitive to the type of tube used in the rotator, in particular to the material the tube is made of, and possibly the tube diameter. I have found the Corning polypropylene 15 ml ("orange-cap") tubes to be by far superior to glass, polystyrene, or even polypropylene 50 ml tubes ("blue cap") from Becton-Dickinson.

I find it easiest to drain the first tube through the needle-hole, rather than through the needle itself. Experience has suggested that the GMDs don't appreciate the shear involved with being sucked through a needle. In cases where drawing through needle is preferred, *e.g.* to protect sterility, draw gently.

### **A.3.6: Fixing Samples**

- After the incubation period expires, fix the cells in the tube by adding 10 ml of 75% methanol; the tube should contain 5 ml of YPD and GMDs, so the final concentration is 50% methanol. Fix for 5-10 minutes. I have left samples as long as 24 hours in 50% methanol:YPD with no obvious deleterious effects. On the other hand, experiments have shown a gradual decrease in stainable DNA-RNA with time, in fixed cells, so it is probably not wise to store samples like this indefinitely.

At noted times in the protocol, GMD samples are taken, and fixed to (1) stop growth and (2) prepare for flow cytometry - *i.e.* permeabilize the cell membrane to fluorescent dyes. The goal of fixation is to get the cell(s) to stay together long enough for analysis, but not in such a manner that important structures for fluorescent labeling (*e.g.* surface antigens) are disturbed. For our work, I have used the simplest method that works, methanol fixation. My experience is that the GMD acts to hold the cell together sufficiently, and that further fixation, *e.g.* with formaldehyde or glutaraldehyde, is not only unnecessary, but known to disturb markers.

### **A.3.7: GMD sieving**

Flow cytometry requires that large GMDs be removed from the GMD preparation. In addition, one wants to remove small GMDs, which are plentiful and very rarely occupied. And for most work, we are interested in GMDs of a limited size class, for which the vast majority of GMDs are occupied by at most one cell.

I use a sieving device, shown in Figure A.2, that uses nylon mesh of three sizes. The first has a large area, and is used to remove very large particles. The second has a smaller area, and establishes the upper size limit. The last also has a small area, and establishes the lower size limit. The meshes are supported by various plastic components, appropriately modified with hacksaws and knives; these include: funnels, beakers, filter supports and chromatography columns. To my knowledge, the specifics are not sacred, and commercially available sieves are probably adaptable.

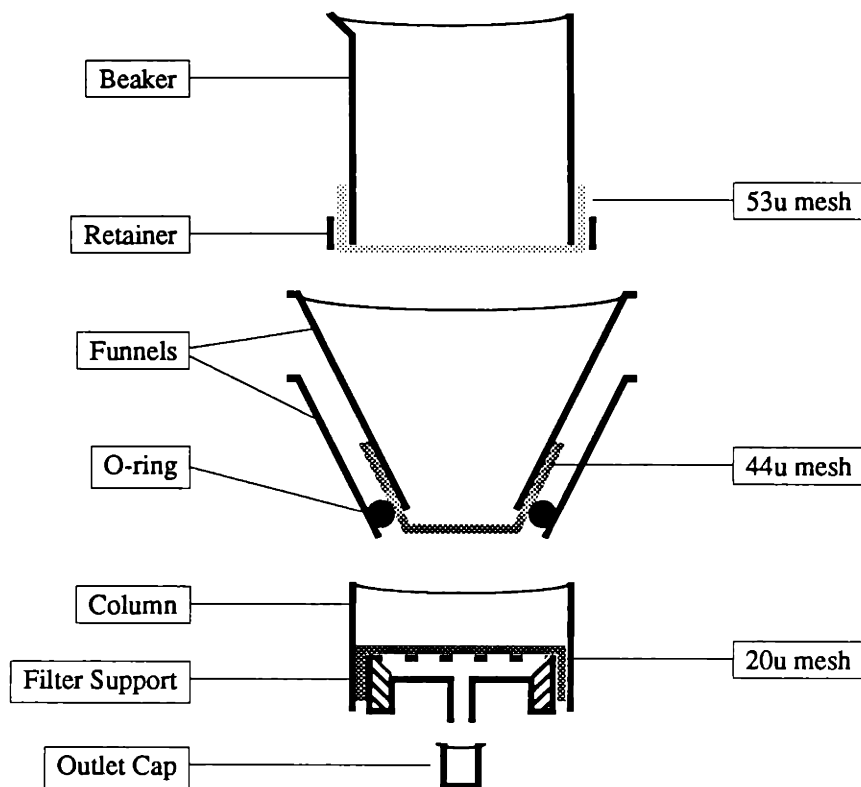


*Figure A.2: Sieve device to recover GMDs (20 $\mu$  to 44 $\mu$ )*

After fixation, the GMD sample is poured into this device, and washed thoroughly with several volumes of DI water. The desired GMDs are captured by the small mesh in the bottom cup. Wash the GMDs in the cup with 5 ml or so of phosphate buffer (10 mM, pH 7.0). Cap the cup outlet drain, and add about 0.8 ml phosphate buffer. Swirl the phosphate buffer around a few times, and pour the GMDs

into a microcentrifuge tube. Repeat with another 0.8 ml, for a total of about 1.5 ml recovered.

## Section A.4: Materials

- Agarose, type IX. (# A-5030, Sigma, St. Louis, MO)
- Mineral Oil, light weight. (# M-111, Package Chemical, Boston, MA) Almost any weight should work, but the lighter oil is easier to pipet, promotes quicker transfer, etc. The downside is a tendency for larger GMDs to settle out, thus requiring occasional remixing during gelation step.
- Test tube, borosilicate, 16x100 mm, (# 60825-957, VWR, Bridgeport NJ)
- Culture tube 15 ml polypropylene (orange-cap). (# 25319, Corning, Corning NY)
- Microcentrifuge tube, polypropylene. (# USA 505, USA/Scientific, Ocala, FL)
- Micropipettor Tips, 1ml (Blue tips) and 100 $\mu$ l (Yellow tips). (# RT-200, RT-20, Rainin, Woburn MA)
- Pipets, 10/5/1 ml, Falcon sero, (# 7551, 7543, 7521, Becton-Dickinson, Lincoln Park, NJ)

### A.4.1: Sieve Apparatus

- Filter support, 25mm, Acetal, (# 4320, Gelman, Ann Arbor, MI). Remove the metal screen with a pair of pliers. Keep the O-ring for use with funnel assembly. The top half (internally threaded) part of the support is not used.
- Column. A polypropylene tube, 1 inch inner diameter by about 0.75 inches vertically. I use the reservoir from a 2.5 cm "Econo-column"

chromatography column (# 737-2510, Bio-Rad, Richmond, CA), cut to 0.75 inches for ease of sample recovery. Many substitutes are possible; the critical feature is that it should fit snugly over threaded part of filter support with the mesh in place, to prevent loss of sample out the sides.

- Outlet cap. Filter support has a Luer-style fitting, so many things will work. I use a chromatography column cap.
- Funnel, (2), polypropylene, 80mm, Nalgene (Rochester, NY) Cut the spout from one funnel, and cut the second so that the first will "nest" inside it. The complete assembly (funnels, mesh and O-ring) are held together with a document binding clip.
- Mesh, Nylon, 20 $\mu$ , 44 $\mu$ , 53 $\mu$ . (# CMN-20, CMN-44, CMN-53, Small Parts, Miami, FL)
- Beaker, polypropylene, 50 ml, Mallinckrodt (Paris, KY). Nalgene equivalent would probably be OK. Cut the bottom off, then cut the next 0.25 to 0.35 inch off to use as a retaining ring for the large mesh.

#### A.4.2: Other Devices

- Vortexer: "Vortex-Genie", (# 12-812, Fisher Scientific, Springfield NJ).  
(in reality: # K-550-G, Scientific Industries, Bohemia, NY).
- Rotator: Rollerdrum, 14 inch diameter drum. (# TC-7, New Brunswick Scientific, Edison NJ)
- Incubator: IsoTemp, model 255D, (Fisher Scientific)



*Appendix B***DAS: The Data Acquisition System**

---

**Section B.1: Introduction**

As described in Chapter 2, for each GMD passing through the interrogation volume, the opto-electronic subsystem of the flow cytometer delivers a set of (up to) five pulses which describe some of the physical properties of the GMD and the microcolony it contains, if any. The Ortho flow cytometer contains circuitry to perform limited analysis and display of up to two channels of this data at a time. Hardcopy is limited to Polaroid pictures of histograms and scatter plots. In order to collect, analyze, display and compare data sets, as well as to generate more informative plots, a computer-based data acquisition system is necessary.

This chapter will describe the data acquisition system which I designed, constructed and used for the experiments presented in this thesis. I will begin with a general, functional overview, intending to describe some of the design considerations, and the limits of measurement performance of the design. Then, I will proceed with a more detailed, technical description of the hardware and software which comprise the DAS.

### **B.1.1: DAS Functional Specification**

For the work presented in this thesis, we ultimately want a measurement of pulse area, since this is expected to be a good measure of the total biomaterial in the GMD, as was discussed in Chapter 2. In addition, for this work, two channels are sufficient to obtain the desired results: one for microcolony biomass and one for GMD size or possibly cell identity via fluorescently-labeled antibody. Finally, the ability to trigger off a third independent channel is desired. Thus, the functional specification of the DAS is as follows:

- accept three channels of input, from (up to) three PMT pre-amplifier outputs,
- detect a voltage pulse in one channel,
- measure the areas of the corresponding pulses appearing in two other channels,
- digitize and display these two measurements, and store them for subsequent analysis.

There were also several design objectives which guided and constrained the current implementation. In particular, the DAS was designed to be:

- simple enough to deliver the needed measurements, but no simpler
- easily expandable, up to 5 channels
- easily debuggable, when some component inevitably fails
- inexpensive

## Section B.2: Functional Description

### B.2.1: Pulse Feature Sampling

With the understanding that the input to the DAS is a set of analog voltages, and the output a set of digital numbers, the only question is where in the signal path to perform the analog-to-digital conversion. There is a strong argument that one should just sample the output of the pre-amplifiers, and do all the pulse measurement operations inside the computer. Ultimately, this will be the best approach, inasmuch as there is valuable information, such as pulse morphology, that would be preserved by this method. Unfortunately, sampling the raw signal requires some high-performance circuitry. Typical pulse widths for small cells such as bacteria are in the 2  $\mu$ sec range. Due to the sampling theorem, a sampling rate in excess of 1 MHz per channel, *i.e.* 1 million 12-bit analog-to-digital conversions per second, and realistically more like 5 to 10 MHz per channel would be required. At the time the DAS was built, the cost and complexity to sample at these rates was prohibitive; as of 1990, at least the cost would be more moderate.

The DAS employs an alternate approach to sampling the raw signal, which is termed pulse feature sampling. By this method, various features of each pulse, such as area, height or width, are measured in the analog domain, and the results are sampled and converted to digital form. In this manner the sampling rate is reduced to the product of maximum event rate and the number of channels. In particular, with a two-channel system, and a maximum event rate of 2,000 GMDs per second, a 4 kHz sampling rate is required. This rate is not only easy to obtain, but easy to extend as well, in particular, to 5 channels times 10,000 GMDs/second, which is the maximum obtainable performance from the Ortho flow cytometer.

### B.2.2: Pulse Detection and Integrator Control

In the DAS, pulse areas are measured with a gated integrator circuit, which:

- integrates its input over some time interval, *i.e.* over the duration of the pulse,
- holds the result briefly during the analog-to-digital conversion,
- is reset to zero, in anticipation of the next pulse.

Clearly, the key to operation is the signals telling the integrator when to integrate, hold and reset. In this section, I will discuss the method by which the DAS derives the "integrate" signal, and the implications related to measurement error.

As implied by the functional specification, the integrate signal is derived from a pulse detection operation; *i.e.* whenever a pulse is detected in the trigger input, the DAS should be integrating the two data inputs. The simplest approach would be to continuously compare the instantaneous trigger input,  $V_T$ , to a threshold voltage; when a pulse occurs, sending  $V_T$  above the threshold, the integrators are turned on. However, this simple scheme is inadequate for this application because of the unavoidable presence of noise on the trigger input. The appearance of pulses at the trigger input signals not only things of interest, such as GMDs, but also:

- opto-electronic noise, contributed by the PMTs and pre-amplifiers
- unavoidable small particles such as cellular debris or dust in the sheath or sample fluid which give rise to a small scatter or fluorescence signals
- mechanical artifacts, *e.g.* small vibrations of the flow cell which are transduced into optical signals, especially if the flow cell is at all dirty

These noise components at the trigger input force one to set the threshold voltage sufficiently high that the probability of a false trigger due to a noise pulse is acceptably low. This approach leads, however, to a problem which is illustrated in Figure B.3.

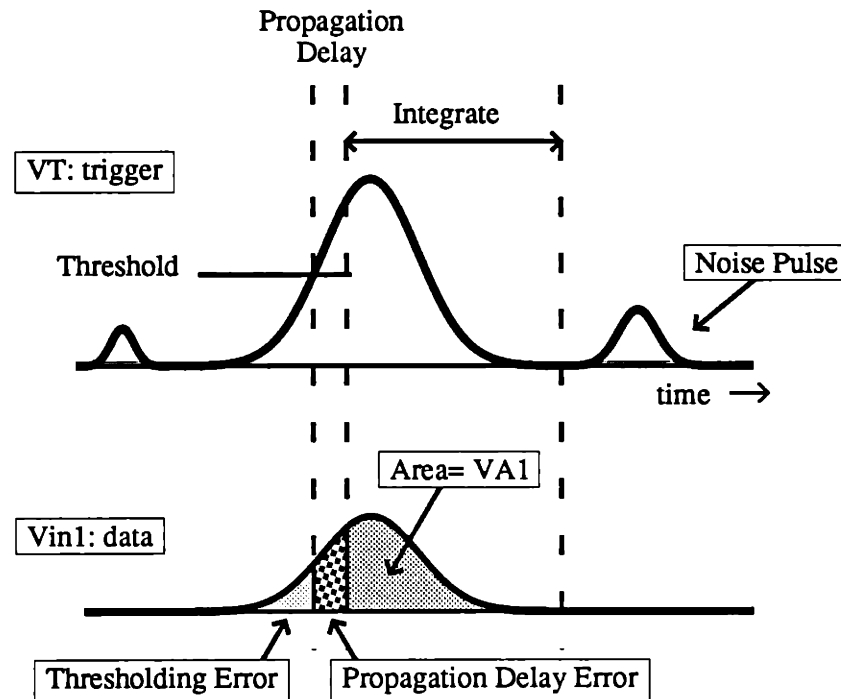


Figure B.1: Single-threshold triggering scheme

By setting the threshold moderately high, the pulse is not detected until some time after the pulse has actually started. In addition, there is an unavoidable time delay while the fact that the trigger voltage has crossed the threshold propagates through the circuits to turn on the integrators. The net result is that the integrators will unavoidably miss the beginning fraction of the pulse, and the "pulse area" thus measured will be low, by an error amount equaling the sum of the threshold error and the propagation delay error, depicted in Figure B.1. An additional thresholding error is added if the second threshold crossing (*i.e.* when VT is on the downside of the pulse) is used to turn off the integrator, though in this case the propagation delay diminishes the size of this error. Some sort of timing mechanism, such as a monostable multivibrator can be used to delay turning off the integrators until some time  $\Delta t$  after the pulse has ended.

The circuits internal to the Ortho flow cytometer deal with this whole problem by inserting a delay-line in the data channels, so that by the time the pulse detector has changed state and turned on the integrators, the pulse is "just arriving" at the integrator inputs, and the entire pulse is integrated.

### **B.2.3: Dual-threshold Trigger Scheme**

Rather than using delay-lines, the DAS employs a dual-threshold trigger circuit, whose function is depicted in Figure B.2, and summarized here:

- A low threshold is used to generate the "integrate" signal: the data inputs are integrated during the time interval delimited by the two low-threshold crossings.
- A high threshold is used to "validate" the pulse. If, and only if, the pulse crosses the high threshold, the integrator outputs are held, digitized and stored. Otherwise the integrators are reset immediately after the end of the pulse.

The low threshold can be set very low, to minimize the "threshold" error discussed previously, but with the expectation of high probability of false triggers due to noise spikes. However, at the end of the noise pulse, the integrators are reset very quickly, and will be ready (with high probability) for a valid pulse when it comes along. In addition, as is evident by comparing Figure B.2 and Figure B.1, using a lower threshold also decreases the propagation delay error, by shifting the propagation delay interval closer to the beginning of the pulse.

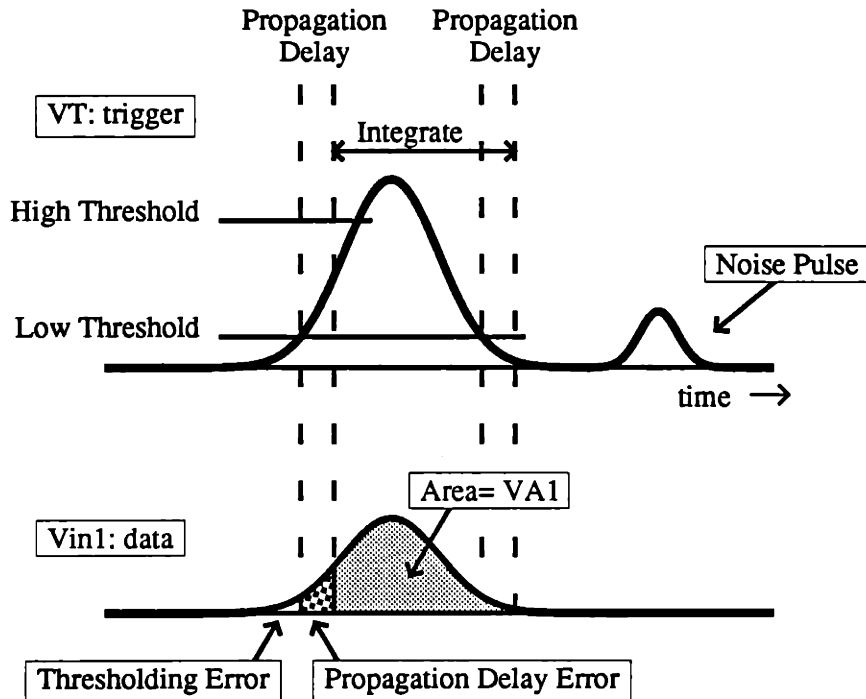


Figure B.2: Dual threshold triggering scheme

As before, some sort of timing device *could* be used to delay turning off the integrators at the end of the pulse, to preclude a trailing-edge thresholding error. However, using this triggering scheme, the product of a moderately high false-trigger rate and the fixed time delay interval could result in a significant increase in the system deadtime (*v.i.*). Conversely, the combination of a lower threshold to delimit the pulse, and the propagation delay of the logic circuits, serve to make the trailing-edge error negligible for this work, and obviates the need for such a timing device.

In my implementation, the effect of the threshold and propagation delay is that the integrators are turned on about 0.2  $\mu\text{sec}$  after the beginning of the pulse. This could obviously be significant if the DAS were used to measure single small cells such as bacteria, for which a 2  $\mu\text{sec}$  pulse width is typical. However, for larger cells such as yeast and mammalian cells, and for bacterial microcolonies, this error has not been seen to be significant. Moreover, in almost all protocols, I trigger off the light scat-

tered by the GMDs, which are at least 20 times larger in diameter than bacteria. By providing a big signal to trigger from, while measuring small things like bacteria, the GMDs greatly relax the performance requirements of the DAS.

**B.2.4: DAS Hardware Overview**

The data acquisition system is a standalone instrument. It is based on the Slicer microcomputer system (Slicer Systems, Minneapolis, MN), which in turn is based on the Intel 80186 microprocessor, and runs the CP/M operating system. To the Slicer system, I have added an interface unit which accepts input from the flow cytometer pre-amplifiers, and which contains the analog processing circuits, the analog-to-digital converter, and requisite control logic. The DAS uses a Graphon GO-140 (Graphon Inc., San Jose, CA) graphics terminal for user interface, and uses a 5¼ inch floppy disk for program and data storage. This configuration is illustrated in Figure B.3:

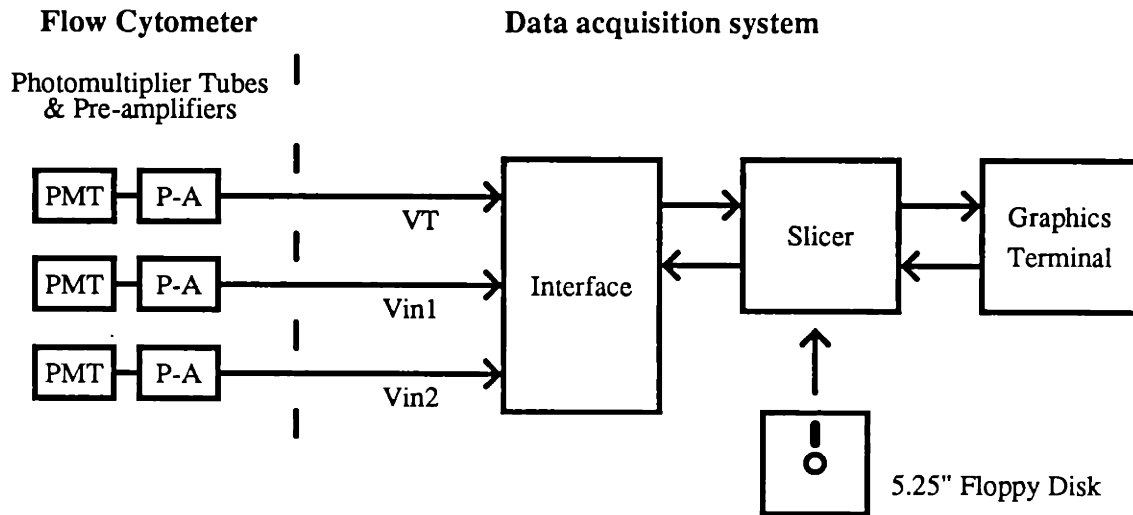


*Figure B.3: Overview of DAS Hardware*

A functional description of the interface box, as well as detailed circuit schematics of its various submodules will be presented in Section B.3.



### **B.2.5: DAS Software Overview: AQ**

The data acquisition process is ultimately controlled by a program running on the Slicer, called AQ. The functionality of the program can be summarized as:

- **data acquisition:** initializing and controlling the DAS interface, and accepting data, *i.e.* digitized pulse areas, from the interface, via direct-memory-access.
- **data display:** histogram displays of the data collected from the two channels, updated in "real-time" so the operator can verify that acquisition is proceeding as expected
- **data storage:** on 5¼ inch floppy disks, for transport to more a powerful system where data analysis programs reside.

A functional description of the software, as well as flow-charts and source code which relate to the data acquisition module will be presented in Section B.4.

## **Section B.3: DAS Interface Details**

In this section, further details of the DAS interface hardware will be presented, first with a block diagram indicating the relation of the interface submodules, and then with fairly detailed schematics of each of the submodules.

The DAS interface box is comprised of four subcircuits, as shown in Figure B.4, which closely follow the functional specification of Section B.1. The submodules of the interface are:

- **trigger and control circuit:** detects pulses at the trigger input, and generates control signals for the integrators, multiplexer and analog-to-digital converter (ADC) circuits.
- **two (identical) integrator circuits:** compute pulse areas by integrating their respective inputs during the interval specified by the trigger

- analog multiplexer and analog-to-digital converter: digitizes the integrator outputs, and signals the microprocessor to collect and store them.

Each of these modules, as well as the signals which are passed between them, will be presented in detail in the next sections.

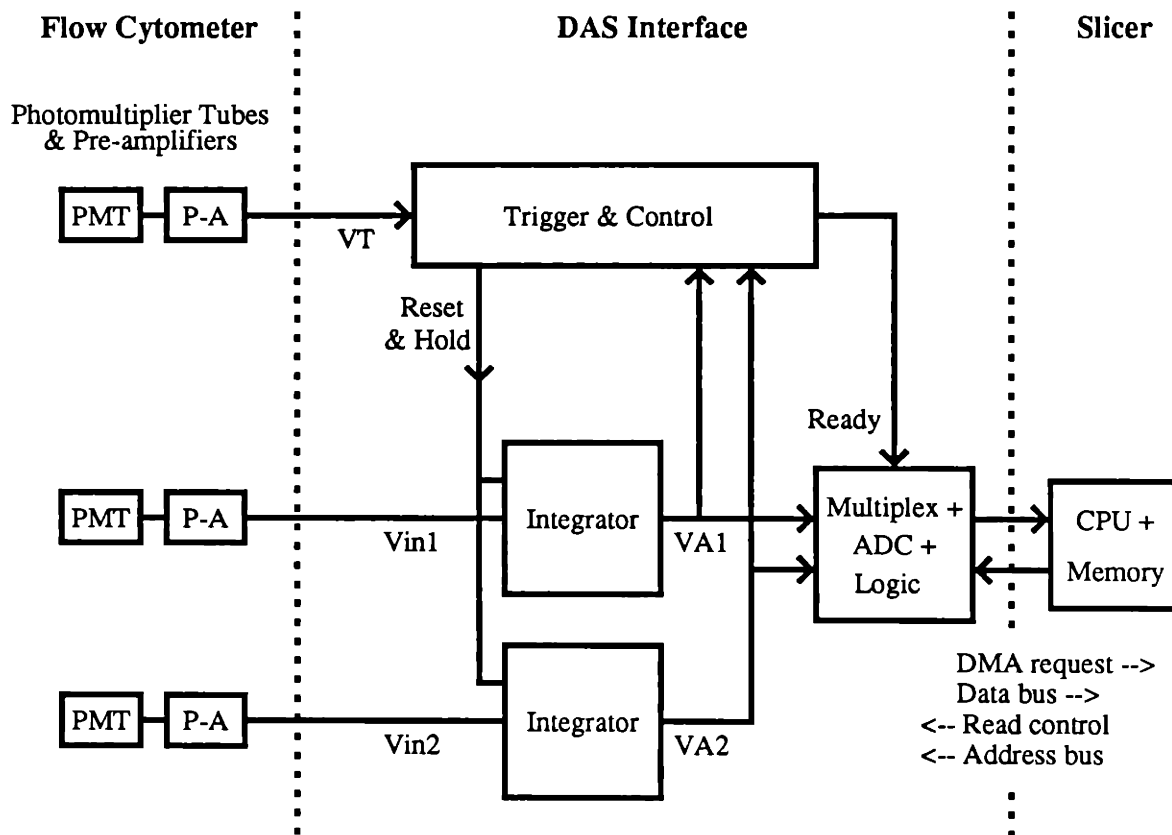


Figure B.4: Functional schematic of DAS interface

### B.3.1: Trigger and Control Circuit

This section describes the operation of the trigger and control circuit; Figure B.5 is the schematic diagram for this circuit:



crossings have occurred for a given pulse.

- comparators, **C3** and **C4**, (each  $\frac{1}{4}$  LM339). Examine the state of the integrators, and prevent the trigger circuit from being armed until the integrators have been reset to zero. Open-collector outputs allow wired-nor configuration, easily expandable to more channels.
- comparator threshold inputs bypassed by  $0.1 \mu\text{F}$  capacitors to ground.
- power to comparators and integrated circuits bypassed by  $0.1 \mu\text{F}$  capacitors to ground.

### Signals Received

- $\overline{\text{DReset}}$  ("not digital reset"), from the ADC circuit. Goes low when all channels have been digitized and stored, and initiates reset of the trigger circuit.
- VA1 and VA2, the integrator outputs. Used to ensure that the trigger circuit is re-armed only when the integrators have been reset.

### Signals Generated

- AReset (analog reset). Set high to reset the integrators.
- Ready. Set high at the end of a valid pulse, to cause the analog-to-digital converter to start digitizing the integrator outputs.

### Trigger Operation: Valid Pulse

When a valid pulse (*i.e.* one which is higher than the high threshold) occurs, the trigger circuit operates in the following manner.

- All flip-flops are reset, so for each, Q output is low
- when the trigger input, VT, crosses the low threshold, the output of C1

goes high; this propagates through logic and causes AReset to go low, which causes integrators to start integrating their inputs.

- the trigger input crosses the high threshold, causing C2's output to go high, thus setting F2.
- the trigger input, now decreasing, crosses the low threshold from above, setting F3, which asserts the "Ready" signal, thus starting the process by which the integrator outputs are digitized and stored by the computer.
- when both channels have been digitized and stored,  $\overline{\text{DReset}}$  goes low, resetting F2 and F3; resetting F2 causes AReset to go high, causing the integrators to reset.
- When the integrators have fully reset, the outputs of C3 and C4 go low, causing their wired-nor output configuration to go high. Assuming the trigger input is less than the low threshold, this causes F1 to be reset, thus re-arming the trigger.
- In cases when the trigger input is *greater* than the low threshold, *i.e.* if another pulse comes along before the conversion/storage process is completed, the trigger circuit waits for its input to fall below the threshold; when that happens, F1 is reset as above. This prevents the trigger from being re-armed in the middle of the second pulse, which if allowed, would lead to a meaningless area measurement for the second pulse.

### Trigger Operation: Noise Pulse

In the event that a "sub-threshold pulse" occurs, *e.g.* due to noise, the sequence of events is similar, with important exceptions:

- As above, all flip-flops start in the reset state
- As above, when VT crosses the low threshold, C1 goes high, causing AReset to go low, and the integrators to start integrating.

- The trigger input, now decreasing, crosses the low threshold from above. However, since the high threshold was never crossed, F2 was never set. F3 is clocked by the threshold crossing, and reads in F2's output, thus remaining reset. Thus, the "Ready" signal is not activated, and no analog-to-digital conversions take place.
- In addition, since F2 was never set, when VT falls below the threshold, AReset goes high, causing the integrators to reset.
- As above, when the integrators have fully reset, the wired-nor configuration of C3 and C4 goes high, and the trigger is re-armed.

### System Dead-time

As shown in the circuit diagram, the outputs of the comparators C1 and C2 are gated by F1; *i.e.* when F1 is set, the comparator outputs are effectively disconnected from the rest of the circuit. F1 is set when the trigger input crosses the low threshold from above, *i.e.* at the end of the pulse, and reset only when the integrators have fully reset, whether or not the pulse was valid. As a result, the system ignores any pulses which may occur during the conversion/storage process, and this period is deadtime for the DAS. For this implementation, each conversion and storage requires 50  $\mu$ sec. This is dominated by the rather slow ADC used which has a 35  $\mu$ sec conversion time, maximum rating. For this 2-channel system, each event requires two such cycles, for a total of 100  $\mu$ sec deadtime, and a maximum rate of 10,000 events per second. For experiments presented in this thesis, typical event rates are less than 500 per second, so this is not a problem. In the event that more channels were added, or higher event rates, the speed of the converter could be limiting.

The other source of dead-time is the time it takes to reset the integrators after the system is triggered by noise pulses. As discussed in Section B.3.1, the discharging time-constant for the integrators is on the order of 0.01  $\mu$ sec, so the system will be

dead for less than  $0.05 \mu\text{sec}$  after a noise pulse, using the  $5\tau$  rule. Thus, the seriousness of noise-induced dead-time is determined by the low threshold; it must be high enough that the false trigger rate is suitably low, *i.e.* so that only a small fraction of the time is spent resetting after an invalid pulse. For the experiments in this thesis, I used a low threshold of 100 mV, which was found to easily meet this criterion; indeed, decreasing this threshold to 30 to 40 mV should be no problem in this regard.

### Propagation Delay

The key performance issue for the trigger circuit is to turn on the integrators as fast as possible at the beginning of each pulse. As demonstrated in Section B.3.1, the integrators are turned on by turning off the AReset signal. The propagation time for this circuit, for the AReset transition is:

LM311: low to high = 200 nanoseconds

74LS08: low to high = 8/15 ns (typical/maximum ratings)

74LS04: high to low = 10/15 ns

74LS08: high to low = 10/20 ns

for a total of 250 nanoseconds, worst case. This could certainly result in a significant propagation delay error for a  $2 \mu\text{sec}$  pulse size, as expected for bacteria. However, for the work in this thesis, the pulses are significantly longer (10  $\mu\text{sec}$  minimum), due to the strategy of triggering off optical signals arising from GMDs, and no evidence of a major measurement error was observed.

For work where this propagation error is unacceptable, there are a few options open:

- combine logic: the and-or-and can be replaced by other logic in such a way that only a single transition is required, thus saving 35 ns (maximum).
- use a faster comparator: *e.g.* LM319 (80 nanosecond transition) or Signetics 521 (12 nsec). This is clearly the place where significant gains can be made. However, there is a practical limit. Roman found that the

highest-speed comparators tended to oscillate under certain conditions, making them unacceptable here<sup>105</sup>. Also, the faster comparators have a tendency to respond more to high frequency noise at their inputs, giving rise to more false triggers. The 80 nsec LM319 would seem a good compromise for future designs.

### B.3.2: Integrate and Hold Circuit

This section describes the operation of the DAS analog circuits which compute pulse areas, whose function is most accurately described as "integrate and hold". The circuit diagram for each of these channels is as shown here:

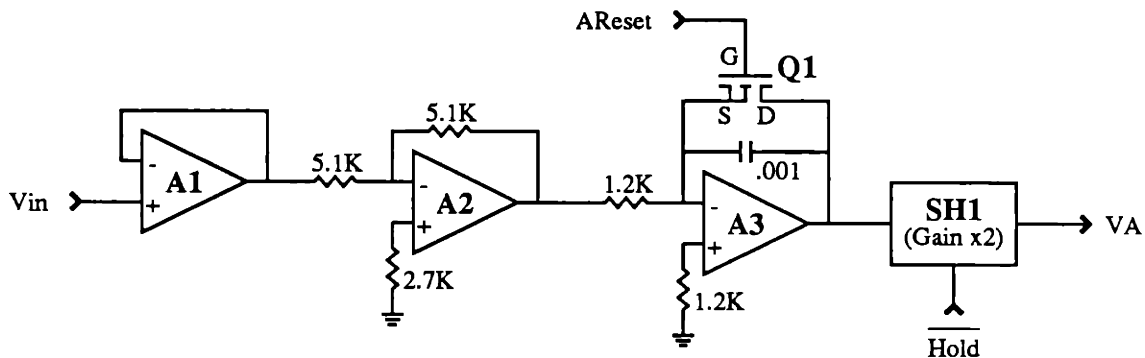


Figure B.6: DAS integrate-and-hold circuit

#### Components

- isolation buffer, **A1**, (LM310): provides a high-impedance connection to the pre-amplifier card; unity gain.
- inverting amplifier, **A2**, (LM318), gets the signal polarity right for the rest of the circuit; gain = -1.
- integrator, **A3**, (LM318), described below
- sample-and-hold, **SH1**, (AD585, Analog Devices) Samples the integrator



output and holds it during analog-to-digital conversion; gain=2.

- FET switch, Q1, (VN10-KM, Siliconix). Resets the integrator when AReset is high.
- Power to each op-amp is supplied through by a  $22\Omega$  resistor, and bypassed by a  $0.1\ \mu\text{F}$  capacitor to ground.

### Signals Received

- $V_{in}$  from a flow cytometer pre-amplifier card.
- AReset (analog reset) from the trigger circuit. When high, resets the integrator.
- $\overline{\text{Hold}}$  - from the trigger circuit. When low, the sample-and-hold holds its output constant.

### Signals Generated

- $V_A$ , the integral of  $V_{in}$  over the period of integration. Goes to the ADC circuit for conversion, and also to the trigger circuit to signal the integrator state.

### Integrator Operation: Valid Pulse

When a valid pulse (*i.e.* one which is higher than the high threshold) occurs, the integrator operates in the following manner.

- AReset starts out high, which keeps the FET switch on, and the capacitor discharged.  $\overline{\text{Hold}}$  starts low.
- When the trigger input crosses its low threshold (going up) the trigger circuit causes AReset to go low, and the circuit begins integrating the input voltage,  $V_{in}$ . At the same time, the trigger circuit sends  $\overline{\text{Hold}}$  high, causing the sample-and-hold to track the output of the integrator.

- When the trigger input crosses its low threshold, (coming down) the trigger circuit causes  $\overline{\text{Hold}}$  to go low, causing the sample-and-hold to hold the output of the integrator.  $\text{AReset}$  remains low.
- When the analog-to-digital conversions are completed, the trigger circuit causes  $\text{AReset}$  to go high, closing the FET switch and discharging the capacitor.

### **Integrator Operation: Noise Pulse**

In the event that a "sub-threshold pulse" occurs, *e.g.* due to noise, the sequence of events is similar, with one important exception; at the end of the pulse, the trigger circuit immediately causes  $\text{AReset}$  to go high, closing the FET switch and discharging the capacitor.

### **Integrator Performance**

The output of the integrator is  $-1/RC$  times the integral of its input, over the integration period. In this case, with  $R= 1.2 \text{ K}\Omega$  and  $C= 0.001 \text{ }\mu\text{F}$ , the gain factor is  $8.3 \times 10^5$ . For the shortest-duration pulse of interest,  $2 \text{ }\mu\text{sec}$ , a 1-Volt (peak amplitude) pulse would give an output of about 0.83 Volts, and a 10-Volt pulse would produce an 8.3 Volt output. For yeast cells, a more typical pulse width is  $4 \text{ }\mu\text{sec}$ , which would double these output values, except that the op-amp saturates, and cannot deliver more than about 10 V. In addition, the sample-and-hold circuit has a gain of 2, so to prevent it from saturating, the integrator output must be kept less than 5 Volts. In practice, this is done by doing a few brief test runs on the flow cytometer, and adjusting the PMT gains to prevent saturation. This particular gain configuration was chosen so that small entities such as bacteria and yeast could be examined; for larger cells, *e.g.* mammalian cells, the signals are sufficiently large and wide that a lower integrator gain must be used.

### Integrator Droop

Unfortunately, the low capacitor value required for high gain results in a moderately high integrator droop. When the input to the integrator is zero, its output should ideally remain constant; in reality its output droops, *i.e.* it slowly decreases with time. Droop is caused primarily by various current sources and sinks in the circuit discharging the capacitor; an excellent example of this is the input bias current of the integrator op-amp A3. Using a low C value makes matters worse because of the physics of capacitors, which dictates that the time derivative of the capacitor voltage equals  $(1/C)$  times the capacitor current, explicitly indicating that for smaller values of C, the capacitor voltage is more sensitive to these current sources. Leaky capacitors can also droop by virtue of their relatively low shunt resistance, but the capacitor used here is a low-leakage variety.

To be specific, for the LM318, the input bias current is rated at 0.5  $\mu\text{A}$  maximum. With  $C=0.001 \mu\text{F}$ , this results in a droop of  $i/C = 500 \mu\text{V}/\mu\text{sec}$ . The ADC is rated at 35  $\mu\text{sec}$  per conversion, maximum, giving a worst-case droop of 17.5 mV, more than 7 bits. (The ADC is 12 bits and 10 Volts full-scale, a resolution of 2.44 mV per bit.)

Droop is merely bothersome from an instrumentation point of view. Assuming that the output is held the same amount of time for each conversion, the value would be expected to droop by about the same amount also; thus suitable calibration should make it possible to get an accurate value for pulse area. However, droop is practically intolerable for this application, because the analog-to-digital converter used is *very* sensitive to changes in its input during the actual conversion. This is a consequence of the "successive approximation" algorithm used by the converter, and the result is that a small change in its input voltage can result in large, and non-monotonic changes in the digitized value.

### Sample and Hold

To accommodate the droop in the integrator, designers often use higher performance op-amps. In particular, use of FET-input op-amps, such as the LF356, have drastically lower input bias currents than bipolar-input op-amps such as the LM318 used here. I have chosen instead to separate the integration and hold functions by using a commercial sample-and-hold circuit, SH1, to hold the integrator's final value during the analog-to-digital conversion. The particular device, AD585 (Analog Devices), has a droop rate of  $1 \mu\text{V}/\mu\text{sec}$ , 1/500 as large as that of the integrator. Over the maximum conversion time of the ADC, we expect a worst case droop of  $35 \mu\text{V}$ , substantially less than  $\frac{1}{2}$  an ADC bit.

The sample-and-hold, as directed by the trigger circuit, tracks the integrator output during the integration period, and switches to "hold" mode at the end of the integration period. Each integrator has its own sample-and-hold, and their outputs are multiplexed later. To save money (25 dollars), one could use just one sample-and-hold, at the input to the ADC, and multiplex the integrator outputs; this would have the disadvantage that the second channel would droop during the time the first channel is being digitized.

Another advantage of using a sample-and-hold in this configuration is that it obviates the need for a "series switch" between the input,  $V_{in}$ , and the integrator. Typically, a gated integrator uses a series switch to turn its input on and off, at the beginning and end of the integration period. When the input is off, *i.e.* 0 Volts, the integrator ideally holds its value until reset; by this means, the integrator value is held until the analog-to-digital conversion is done. Since this circuit has no series switch, as shown in Figure B.6,  $V_{in}$  (inverted) is always present at the input to the integrator. However, when  $A_{Reset}$  is high and the FET turned on, no significant charge is stored in the integrator's capacitor in response to variations in  $V_{in}$ . (With the FET on, and assuming an on-resistance of 20 integrator becomes a low-pass filter with a DC gain of 20/1200 and a cutoff-frequency  $> 300 \text{ MHz}$ .) Only as  $A_{Reset}$

goes low and the FET starts to turn off, does charge accumulate and integration begin. One could propose modifying this circuit by adding a switch, *e.g.* a DG271 (Siliconix) between A1 and A2, which would be closed at all times except when holding the integrator value for the ADC; of course, attempting to close the switch at the beginning of the pulse would only worsen the propagation delay error. However, having decided to use the sample-and-hold to address the droop issue, its use makes the use of a series switch unnecessary.

### FET Reset Switch

The use of a FET switch to reset the integrator was chosen to minimize the propagation error component due to switch transition times<sup>106</sup>. Of special importance is the turn-off time, since we want the switch to turn off rapidly at the beginning of the pulse. Commercially available FET-switch-and-driver packages, such as the DG271 (Siliconix), have turn-on times on order of 80 nsec, maximum. The VN10-KM FET, by comparison, has a 10 nsec turn-on/off time, maximum rating. In practice, the achievable turn-off time is governed by the FET's load resistance and capacitance, and the performance the circuit driving the FET; in this implementation a turn-off time of about 40 nsec was achieved.

The FET, an N-channel enhancement MOSFET, begins to conduct when the gate-source voltage,  $V_{gs}$ , goes above its threshold of 2.5 volts. In the circuit shown, the source is at a virtual ground, so the FET turns on when  $V_g > 2.5$  volts. The on-resistance of the FET depends on both the difference between  $V_g$  and the threshold, and the FET drain current,  $I_d$ , but is typically on order of  $10\Omega$  or less, giving a discharging time constant (RC) of 0.01  $\mu$ sec for the integrator.

### FET Drive Circuit

In more general switching applications, one would typically shift the AReset signal from TTL levels, 0 to +5V, to a higher range, *e.g.* 0 to +10V<sup>107</sup>. This has the principle advantage of reducing the on-resistance of the FET, often by a factor of 2. Level-shifting is usually done by using an open-collector driver (*e.g.* 74LS07), with a pull-up resistor.

I have chosen instead to drive the FET directly from the TTL output that generates AReset. The TTL output guarantees at least 3.5 V when high, and this is adequate for turning on the FET. The key performance issue is that the FET must be turned off rapidly, at the beginning of the pulse. This requirement is actually better met by making AReset slew from +5 to 0 Volts, rather than +10 to 0 Volts. The cost of using 3.5 Volts instead of 10 Volts to turn on the FET is an increase in the on-resistance from about 3  $\Omega$  to about 15  $\Omega$ , increasing the discharge time constant from 0.003  $\mu\text{sec}$  to 0.015  $\mu\text{sec}$ ; this is not significant for this application. The design of the trigger circuit ensures that the capacitor will be fully discharged before the trigger is re-armed.

### Charge Dumping

The major disadvantage of the FET configuration shown is that when the FET is turned off, charge is dumped from the FET (specifically, from the gate-source capacitance) into the integrator's feedback capacitor. This results in an offset voltage of size  $\Delta V = \Delta Q/C$ . Various approaches can be used to correct for this, such as using dummy devices, but I chose a computational method. Since the amount of charge dumped is about the same for each event, the error offset can be subtracted from the raw data when it is transferred to the computer. For this circuit, the offset is about 50 bins (of 4096 full-scale).

**B.3.3: Multiplex and Digital Converter Circuit**

This section describes the operation of the DAS analog multiplexer and analog-to-digital converter circuit, whose circuit diagram is shown here:

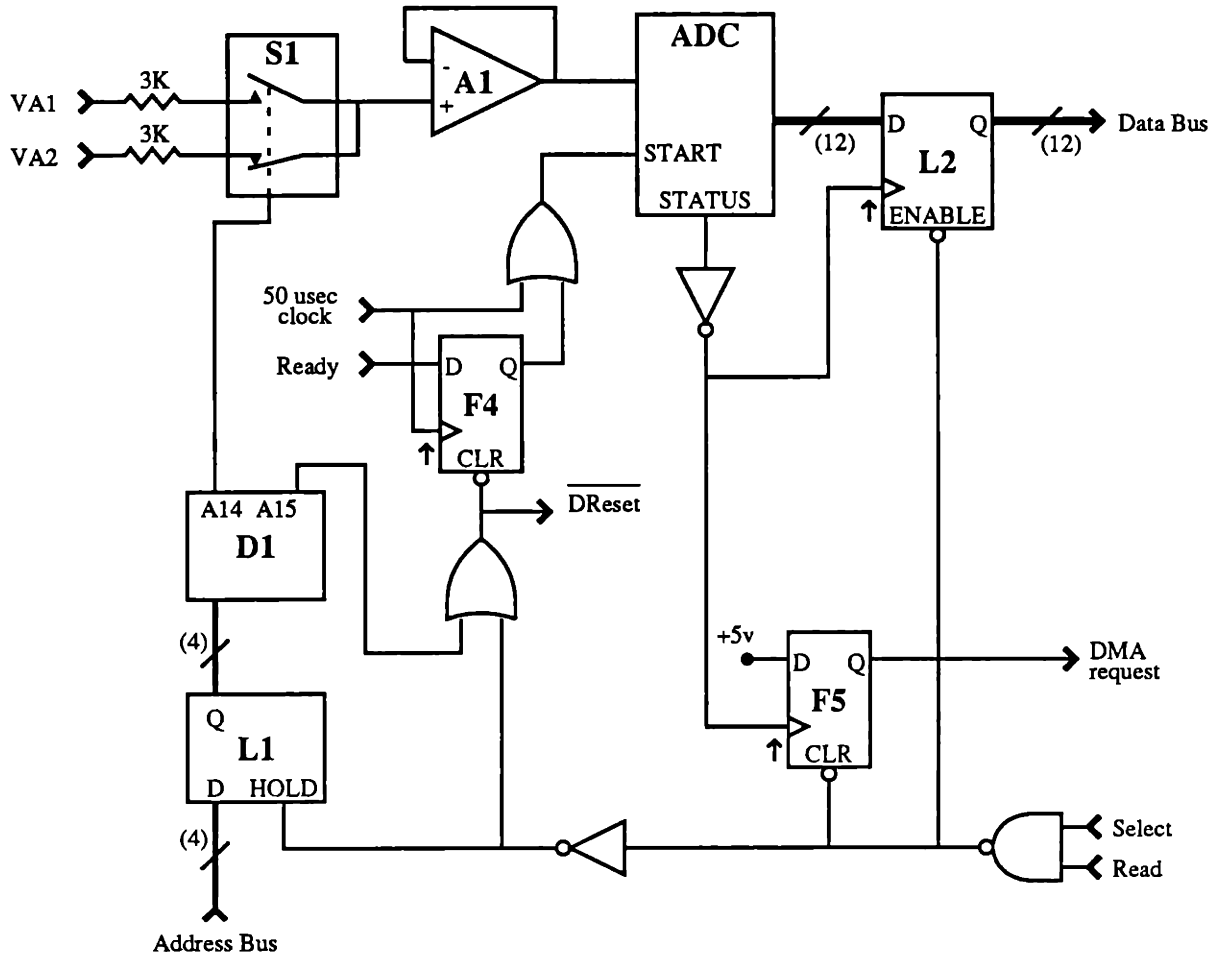


*Figure B.7: DAS multiplexer and digital converter circuit*

### Components

- analog switch, **S1**, ( $\frac{1}{2}$  DG303, Siliconix). Double-pole double-throw; switches ADC signal input between the two integrate-and-hold outputs.
- analog-to-digital converter, **ADC**, (AD584, Analog Devices). 12 bits, 10 Volt full-scale, 35  $\mu$ sec, maximum rating.
- address latch, **L1** and decoder, **D1** (74LS75 and 74LS154 respectively). Latches four bits from the address bus of the Slicer, and decodes them into switch control signals. Address 15 is reserved to generate the **DReset** signal.
- data latch, **L2**, (2x 74LS363). Latches digitized result from ADC. Three-state output makes it invisible to data bus (high-impedance output) except when the "enable" input is low.
- flip-flop, **F4**, ( $\frac{1}{2}$  74LS74). Latches "Ready" signal
- flip-flop, **F5**, ( $\frac{1}{2}$  74LS74). Latches DMA request signal
- Other logic, (74LS00, 74LS02, 74LS04). Especially Nand gate to decode "read interface" signal, which goes low when the Slicer is trying to read the DAS interface. Select is the "peripheral chip select 4" output from the 80186.
- Power to each integrated circuit bypassed by 0.1  $\mu$ F capacitor to ground.

### Signals Received

- Analog inputs, **VA1** and **VA2**, from the integrate-and-hold circuits.
- **Ready**, from the trigger circuit. Signals that a valid pulse has been detected and integrated, and that analog-to-digital conversion should proceed.
- 50  $\mu$ sec clock, from the 80186 integrated timer. Gated by "Ready" to start ADC conversion cycles.



- Select and Read, from the Slicer. Signal that the interface device is being selected, and that a read operation is requested.

### Signals Generated

- DMA request : goes high when the ADC has finished a conversion, *i.e.* when a digitized result is available for storage. Signals the 80186 to execute a direct-memory-access cycle to transfer the digitized result from the data latches to Slicer memory.
- $\overline{\text{DReset}}$  ("not digital reset") : sent to the trigger and control circuit after all conversions have been done, to initiate trigger circuit reset.
- Data out : 12 bits which are placed on the data bus in response to a "read interface" command.

### Multiplexer and Digitizer Circuit: Operation

Prior to arming the trigger circuit, the DAS program

- initializes the 80186's DMA controller, so that in response to DMA requests, the controller will execute "read" commands in that part of the address space corresponding to the DAS analog multiplexer.
- executes a read instruction, at an address that selects, via the decoder and analog switch, the output from the first integrate-and-hold circuit as the input to the ADC. (*i.e.* the read instruction is used only to set up the address; no data is actually read)

When a valid pulse (*i.e.* one which is higher than the high threshold) occurs, the multiplexer and digitize circuit operates in the following manner.

- During the pulse, the integrate-and-hold circuits integrate, so at the end of the pulse, VA1 and VA2 signal the pulse areas obtained from channels

1 and 2 respectively.

- At the end of the pulse, the trigger sets "Ready" high, which is clocked in to F4 by the 50  $\mu$ sec clock, thus enabling the 50  $\mu$ sec clock to trigger the ADC start input.
- At the end of the conversion, the ADC status line goes high. This causes the data latch, L2, to latch the output of the ADC, and also clocks F5, setting the "DMA request" line.
- At the earliest possible time, the Slicer responds to the DMA request by executing a "read interface" command, which strobes the output enable of L2, putting the data latched by L2 on the data bus from whence it is read into the Slicer's memory. This "read interface" signal also causes the address latch, L2, to latch the address from the address bus which, via the decoder and analog switch, selects the output from the second integrate-and-hold circuit as the input to the ADC. Thus, on any given read command, the interface latches in the current read address, but puts on the data bus the result of the *previous* read command. This simplifies the interface timing and maximizes throughput.
- The cycle is repeated to digitize and store the pulse area from the second channel. When the second "read interface" command occurs, the address latched in is decoded to generate the  $\overline{\text{DReset}}$  signal, which initiates resetting the trigger circuit. The decoder output must be gated by the "read interface" signal to eliminate glitches that occur while the decoder changes states, and which otherwise would lead to a false DReset.
- The DAS program detects when all channels have been digitized and stored by inspecting the DMA controller registers. When this has occurred, the DAS program updates its graphics and writes data to its floppy disk (if its internal buffer is full), and then re-initializes the DMA controller and waits for the next pulse.

### ADC Performance

The analog-to-digital converter used, the AD584 (Analog Devices), is a 12-bit, successive approximation converter. It is relatively slow, with a 35  $\mu$ sec conversion time, maximum rating. As indicated elsewhere, this is sufficiently fast for the event rates encountered in these experiments. The major shortcoming is that the converter is very sensitive to changes at its signal input during the conversion, which result in dropped codes and non-monotonic conversion errors. To a large extent, this is helped by using a sample-and-hold upstream from the converter, but I have found an unavoidable presence of noise at the input which degrades performance. As a result of this noise, this 12-bit converter is really only delivering 9 or 10 good bits.

In many cases, 9 bits is sufficient; indeed many commercial instruments use 8 bits converters. The case where more bits is important is in doing logarithmic transformations of data. Many commercial systems use logarithmic amplifiers to transform the data *before* conversion. For this thesis work, I have collected data in linear mode, and done the log transformations *post facto*, on the computer. Doing this requires at least 9 good bits, and preferably 12 or more, to get reasonable results in the low log-channel numbers.

My suspicion is that a faster conversion time would help get more useful bits from the converter, by minimizing the time over which the input needs to be held constant, and thus recommend *e.g.* a AD578 (4.5  $\mu$ sec) or AD684A (15  $\mu$ sec, AD584 pin-compatible) as replacements.

### DMA performance

The use of DMA for data transfer seems a bit excessive, for the data rates expected here. The Slicer, running at 6 MHz, can achieve data transfer rates of one million words per second using DMA, whereas we are expecting data at a rate of 10,000 words/second maximum. The use of DMA does permit easy expansion to more chan-

### B.4.1: Data Acquisition Module

The function of the acquisition modules is to setup and co-ordinate the 80186 and DAS interface to acquire data from the flow cytometer. The data acquisition is done in segments of 2048 events; *i.e.* after 2048 events have been detected, digitized and stored in the Slicer's memory, AQ pauses to write the data out to the floppy disk. This is intended to guard against possible crises which might otherwise result in data loss.

Data transfer from the DAS interface to Slicer memory is done via direct memory access (DMA), so the job of this portion of AQ is to setup and arm the 80186 DMA controller, arm the DAS trigger circuit, and wait for an indication that the DMA has finished. This is all inside a loop that fills a buffer big enough for 2048 events, writes the buffer and starts over, and finishes when a specified number of events has been acquired. This will be presented in more detail momentarily.

### B.4.2: Data Display Module

The function of the display module is to provide some feedback to the operator, to verify that acquisition is proceeding at a reasonable rate, to verify that the PMT gain settings are appropriate, etc. To this end, commercial flow cytometers typically provide continuously updated histograms of the data collected by one or more channels; for the sake of user familiarity, I decided to include the same functionality in AQ. In particular, this module functions as follows:

- As each datum is acquired, each of two internal histogram buffers is updated; this is easy and rapid enough to do on the fly.
- In order to draw the each histogram bin, AQ generates a corresponding eight-byte graphics command (x and y coordinates of bin top and bottom), and sends the bytes to the graphics terminal via the serial port.
- During the acquisition, the user may type 'u' (up) or 'd' (down), to change the vertical scale of the histogram displays, and redraw the histograms.

nels, and once the DMA controller is set up, is easier to interface to, in both hardware and software, than a polling system.

### **Multiplexer Performance**

For two channels, a very simple multiplexer scheme is adequate. The only complication is that these switches, which are FET-based, dump charge on transitions. This is particularly onerous since they tend to dump charge upstream into the internal capacitors of the sample-and-hold circuits, thus providing a path for very strong cross-channel contamination. To prevent this, series resistors were used to slow down the rate at which charge is dumped, and to give the sample-and-hold output circuits a chance to sink the charge, rather than forcing it into the capacitors.

The method of using FET switches and an external decoder was used to make expansion easy. One can be easily add more channels by adding more switches; the address latch and decoder have a capacity for 15 channels total. However, I would recommend using a commercially packaged analog multiplexer, such as the AD7506 (Analog Devices) 8 to 1 analog multiplexer. Even though they tend to be slower (700 nsec for the 7506 *vs* 80 nsec for a DG271 switch), speed is not an issue here, and the design objective of simplicity dominates.

### **Section B.4: DAS Software Overview**

As mentioned previously, the data acquisition process is controlled by a program running on the Slicer, called AQ. In this section, I will describe the three modules of AQ: acquisition, display and storage. I will begin with a functional description of each module, followed by a detailed description of the acquisition module. Although each of the modules has its own interesting aspects, the display and storage modules are not directly related to the problem of measurements in GMDs, and are somewhat more hardware specific.

A difficulty arises because the graphics display is operated via a serial interface, and even at 9600 baud, cannot update the histogram displays fast enough to keep up with typical event rates encountered. Therefore, I implemented an interrupt-driven histogram display spooler, which updates the display as fast as the display can go. In particular, this works as follows:

- When the graphics terminal is idle, it generates an interrupt request
- AQ handles terminal interrupts by sending one byte of the current eight-byte graphics command to the terminal. When the terminal has received and processed the byte, it generates another interrupt request, and is sent the next byte, etc. When all eight bytes of the command have been sent, AQ reads the value in the next histogram bin, and generates a new eight-byte command.
- The display interrupt is disabled just before arming the DAS trigger, and re-enabled after an event has been detected, digitized and stored. This was done to preclude being interrupted during an acquisition cycle, which could worsen the droop problem.
- Event rates *can* be very slow in some cases, and in particular, could unacceptably rate-limit the histogram display update rate. As an escape from this, AQ checks the keyboard input buffer *during* the acquisition cycle for one-letter commands; notably for this situation, typing a 'p' during the acquisition cycle causes an immediate update of both histogram displays on the screen.

### B.4.3: Data Storage Module

The function of the storage module is to write the contents of the DMA buffer onto a floppy disk, when the buffer is full. For the sake of speed and programming simplicity, I chose to bypass the CP/M file system, and instead write the data directly on

the disk, in sequential blocks. This implies that each experiment requires its own disk for storage, until the floppy is off-loaded onto another computer.

The "other computer" for these experiments is a 80386-based system, running AT&T Unix. I wrote a companion program, RFD (read floppy disk), which resides there and which knows the data format used by AQ. RFD performs the job of reading, verifying, and transferring the data from each floppy disk to a file on the Unix system. These files are then input to data analysis programs.

The disk data format used by AQ had to be compatible, of course, with what is available on the 386 system. Fortunately, the double-sided, double-density format of 512-bytes sectors, 8 sectors per track, (an older IBM disk format) is available on both machines. This gives a capacity of 340 kilobyte (kb) per disk, whereas a typical experiment uses less than 150 kbytes.

## **Section B.5: DAS Software - Details**

Rather than present the entire program listing for AQ, I will present an overview of the system via flow-charts, and discuss those portions that are intimately involved with the data acquisition process. The entire program is about 40 pages of 80186 assembly language, which could be included here for completeness, but would not be very illuminating.

### **B.5.1: AQ Top-level**

The flow-chart for the AQ top-level routine is shown in Figure B.8. Each line of the flow-chart specifies a specific action, that is typically performed by a separate subroutine. The items in the flow-chart specifically demonstrate the interaction of the acquisition, display and storage modules. As described above, the job of the top-level routine is to set up the various internal controllers of the 80186, and loop until the requested number of events have been detected, digitized and stored. Once the

controllers have been set up, AQ is fundamentally event-driven; in particular, is driven by DMA requests emanating from the DAS interface.

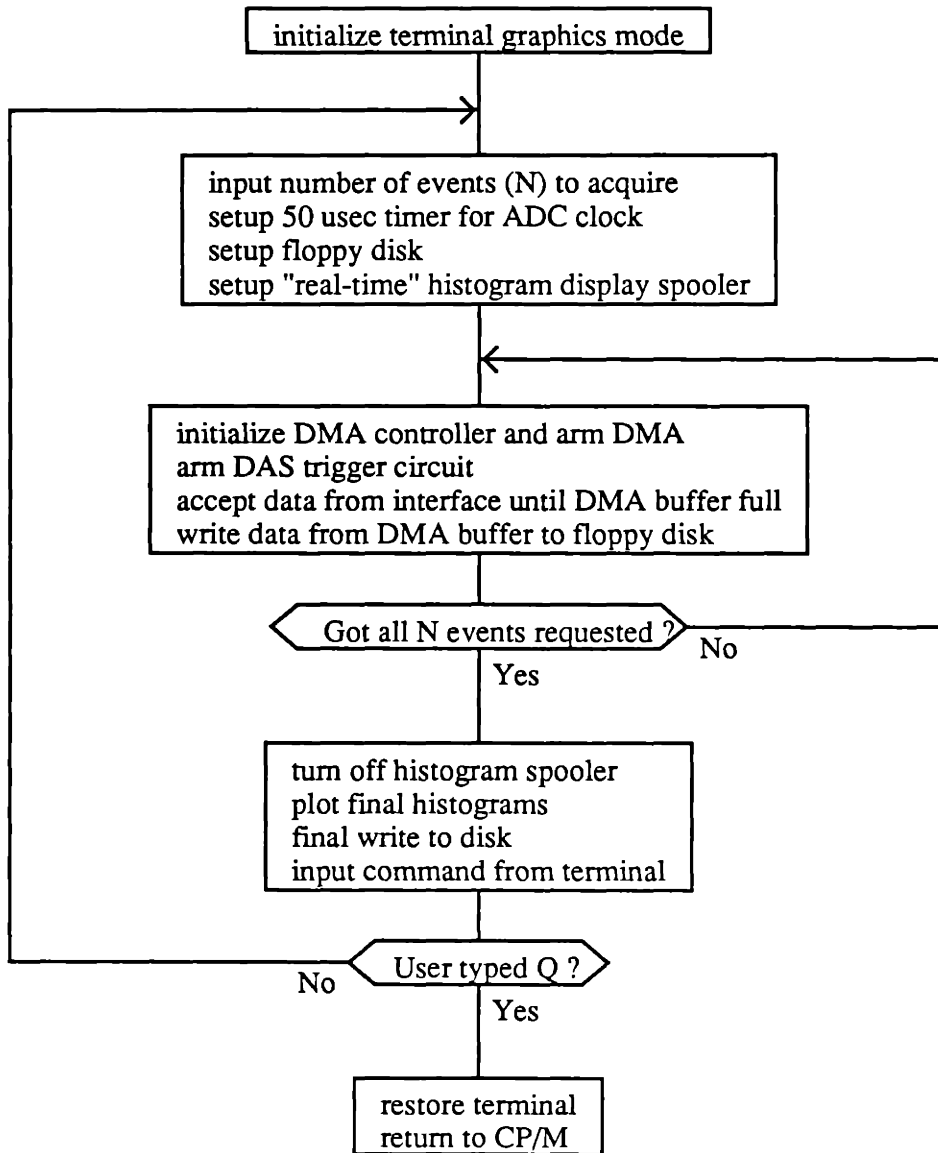


Figure B.8: AQ top-level software control



### B.5.2: AQ Interaction with DMA

Of the items listed in the top-level flow-chart, I will focus on the those in the acquisition module, *i.e.* those which interact with the DAS interface. With one exception, this interaction is centered around the DMA channel.

DMA transfers are controlled by one of the the 80186 integrated DMA controllers. Interface to the controller is accomplished by reading and writing to a set of four registers, listed here:

- source address register: address pointing to where data transferred from. In this case, the address of the DAS interface.
- destination address register: address pointing to where data transferred to. In this case, the DMA buffer, in Slicer memory.
- transfer count: initially contains the number of transfers to be performed, in this case 2 (2 channels). The counter decrements after each transfer.
- control word: 16 bits which select particular transfer mode. In this case, specify that both the source and destination addresses should increment after each transfer, and that no further DMA requests should be honored once the transfer count has decremented to zero.

Within AQ, there are three distinct cases in which these registers are accessed:

- initially, to set up the appropriate registers
- for each event, *i.e.* GMD, setting up the source address to read the first channel of the DAS interface
- for each 2048 events, setting up the destination address to the beginning of the "DMA buffer", which is emptied onto the floppy disk when full.

The initial setup occurs in the top-level routine presented above. The remaining steps occur in the subroutine "accept data from interface ..", which is presented in more detail in Figure B.9.

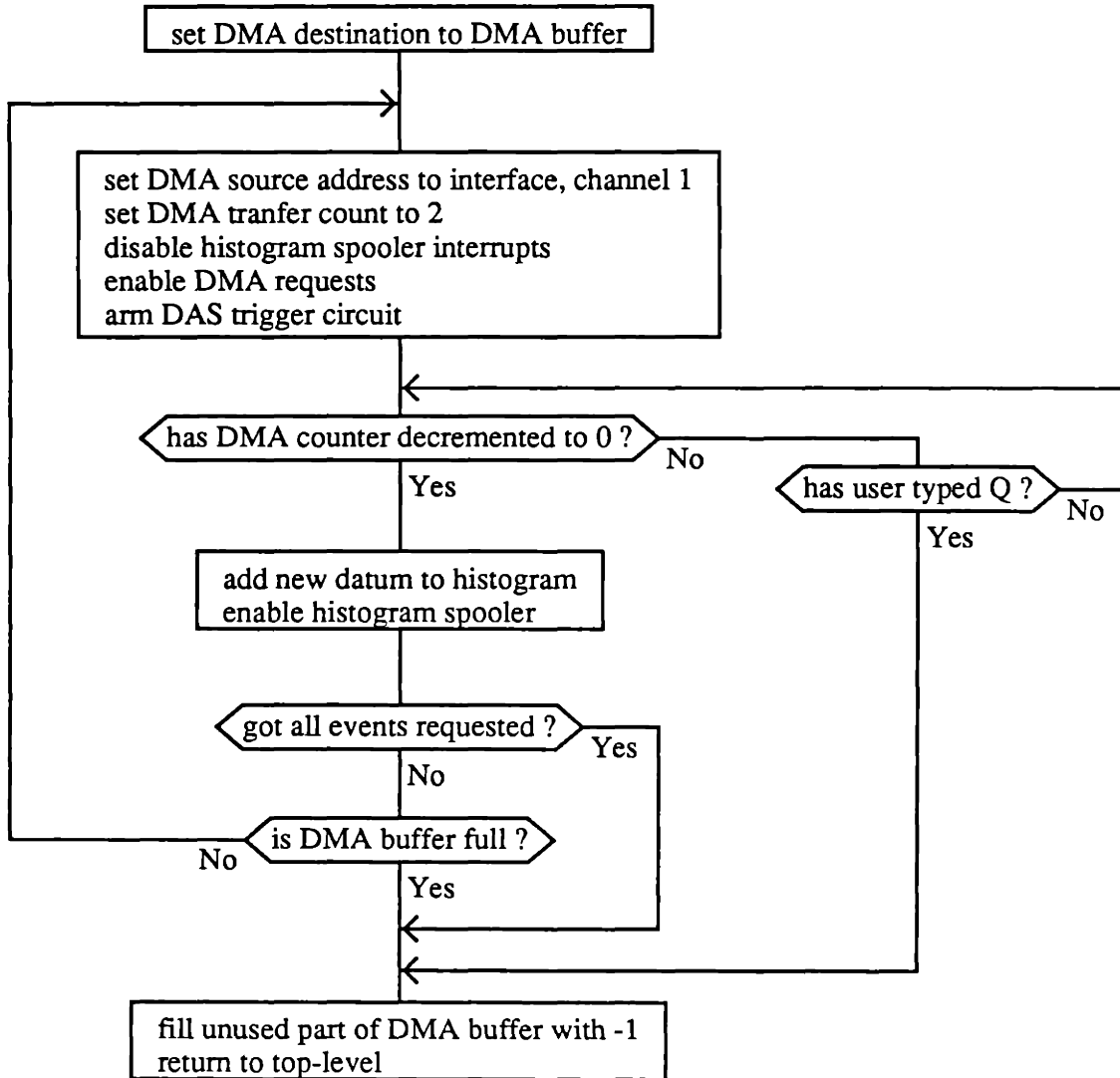


Figure B.9: DAS interface to DMA controller

### B.5.3: AQ Source Code

In this section, I present portions of AQ source code, to indicate to the steps needed to set up and run the 80186 DMA controller. First, Figure B.10 lists definitions for the location of the DMA control block which contains the registers listed above, and for the particular bits used to set up the control word. The most application specific definitions are the initial value for the transfer count (2), and for the source address initialization.

As stated, the source is the DAS interface, which I have located at addresses 200h through 20Eh. Accessing these addresses activates the "peripheral chip select 4" line of the 80186, which is 'and'ed with the "read" signal to generate the "read interface" signal discussed in the multiplexer/ADC circuit description. Among other things, "read interface" causes the contents of the address bus, which in this case equals the contents of the DMA source address register, to be latched into the interface's address latch. The source address increments after every DMA, until address 20Eh is reached, which is decoded in the multiplexer/ADC circuit to generate the DReset signal. Thus the source pointer is initialized to 20Eh minus the transfer count (multiplied by two, since each DMA transfer is 2 bytes in this case).

```

;; DMA control block base address & offsets

DMA1_CB_BASE          equ      0ffd0h    ; DAS interface uses DMA #1

DCBO_SRC_PTR_LO       equ      0        ; source address (two bytes)
DCBO_SRC_PTR_HI       equ      2
DCBO_DEST_PTR_LO      equ      4        ; destination address (two bytes)
DCBO_DEST_PTR_HI      equ      6
DCBO_XFR_COUNT        equ      8        ; # of DMAs to perform
DCBO_CW               equ      10       ; control word

; DMA control word bits

DCWB_DEST_M           equ      8000h    ; destination = memory
DCWB_DEST_INC         equ      2000h    ; increment dest addr after each DMA
DCWB_SRC_INC          equ      400h     ; increment src addr after each DMA
DCWB_TC               equ      200h     ; no more DMAa after count -> 0
DCWB_SRC_SYN         equ      40h      ; synchronize to source
DCWB_CHG              equ      4        ; enable changes to START
DCWB_START            equ      2        ; set this to arm DMA
DCWB_WORD             equ      1        ; word mode (2-byte) transfers

D1CWB_SRC             equ      DCWB_SRC_SYN + DCWB_SRC_INC
D1CWB_DEST            equ      DCWB_DEST_M + DCWB_DEST_INC
D1CWB_MODE            equ      DCWB_TC + DCWB_CHG + DCWB_WORD

DMA1_CW               equ      D1CWB_SRC + D1CWB_DEST + D1CWB_MODE

;; DMA source is the DAS interface - see text for details

DMA1_XFR_COUNT        equ      2        ; 2 channels = 2 ADCs = 2 DMAs
DMA1_SRC_PTR_HI       equ      0
DMA1_SRC_PTR_LO       equ      20Eh - DMA1_XFR_COUNT shl 1

```

*Figure B.10: AQ definitions for DMA controller use*

Figure B.11 is the source code used to initialize the DMA controller. Much of the initialization involves loading addresses and values from the definitions of Figure B.10, and stuffing the controller registers using the 'out' command. The exceptions is computing the address of the DMA buffer from its segment and offset values, and putting it in the form suitable for the DMA destination register. Finally, the DMA control word is loaded, but the DMA is not enabled until just prior to arming the DAS trigger, as shown in the flow-chart of Figure 8.

```

DMA1_DEST_PTR_HI      dw      0      ; computed below
DMA1_DEST_PTR_LO      dw      0

SETUP_DMA1:
  mov     ax, DMA1_XFR_COUNT      ; set # DMAs = # channels
  mov     dx, DMA1_CB_BASE + DCBO_XFR_COUNT
  out
  dx, ax

  mov     ax, DMA1_SRC_PTR_LO     ; set DMA source = interface
  mov     dx, DMA1_CB_BASE + DCBO_SRC_PTR_LO
  out
  dx, ax

  mov     ax, DMA1_SRC_PTR_HI
  mov     dx, DMA1_CB_BASE + DCBO_SRC_PTR_HI
  out
  dx, ax

;;      Compute DMA destination from segment and offset of DMA buffer

  mov     ax, seg DMA1_BUFFER
  SLR     ax, 12                  ; top four bits, hi-order 0's
  mov     DMA1_DEST_PTR_HI, ax

  mov     ax, seg DMA1_BUFFER
  SLL     ax, 4                  ; shift left 4, lo-order 0's
  add     ax, offset DMA1_BUFFER ; and add offset
  mov     DMA1_DEST_PTR_LO, ax

  mov     ax, DMA1_DEST_PTR_LO
  mov     dx, DMA1_CB_BASE + DCBO_DEST_PTR_LO
  out
  dx, ax

  mov     ax, DMA1_DEST_PTR_HI
  mov     dx, DMA1_CB_BASE + DCBO_DEST_PTR_HI
  out
  dx, ax

;;      load control word, but don't arm DMA

  mov     ax, DMA1_CW and not DCWB_START
  mov     dx, DMA1_CB_BASE + DCBO_CW
  out
  dx, ax

```

*Figure B.11: AQ code for initializing DMA controller*

Finally, Figure B.12 shows (part of) the source code which implements the acquisition control loop shown in flow-chart form above. This code collects data from the DAS interface until either the DMA buffer fills up, or the number of events requested by the user is reached.

```

FILL_DMA_BUFFER:
    mov     dx, DMA1_CB_BASE + DCBO_DEST_PTR_LO ; set dma destination
    mov     ax, DMA1_DEST_PTR_LO
    out     dx, ax

    mov     dx, DMA1_CB_BASE + DCBO_DEST_PTR_HI
    mov     ax, DMA1_DEST_PTR_HI
    out     dx, ax

    mov     cx, DMA_CYCLES_PER_BUFFER           ; 1 cycle = 2 DMA's
fidb0:    mov     dx, DMA1_CB_BASE + DCBO_SRC_PTR_LO ; set dma source reg
    mov     ax, DMA1_SRC_PTR_LO
    out     dx, ax

    mov     dx, DMA1_CB_BASE + DCBO_XFR_COUNT   ; set dma counter
    mov     ax, DMA1_XFR_COUNT
    out     dx, ax

    call    DISABLE_SPOOL_INT                   ; histograms off

    mov     dx, DMA1_CB_BASE + DCBO_CW
    mov     ax, DMA1_CW + DCWB_START           ; arm dma
    out     dx, ax

    mov     dx, DMA1_SRC_PTR_LO
    sub     dx, 2                               ; select channel 1 for 1st adc
    in      ax, dx                              ; and arm DAS trigger

    mov     dx, DMA1_CB_BASE + DCBO_XFR_COUNT
fidb1:    mov     bx, 869Ch                        ; keyboard input buffer

    in      ax, dx                              ; inspect DMA counter
    or     ax, ax                               ; loop until count => 0
    jz     fidb2

    mov     ax, es:[bx]                         ; inspect input buffer
    cmp    ax, es:2[bx]
    jz     fidb1                               ; no key pressed - loop again

    call    PARSE_KEY                           ; key pressed - handle it
    jmp    fidb1
fidb2:    call    ADD_HIST_PT                     ; count = zero. update hist
    call    ENABLE_SPOOL_INT                    ; re-enable histogram display

    dec    PULSE_CTR                           ; got requested # of pulses ?
    jz     fidbx                               ; if yes, then quit

    loop   fidb0                               ; dec cx, loop to 0 (buffer full)
fidbx:    ret

```

Figure B.12: AQ code for filling DMA buffer

The code begins by setting the DMA destination register to equal the beginning of the DMA buffer, and initializing a count register, `cx`, to the number of DMA cycles that will fill the buffer. This number is computed by dividing the buffer size by the number of bytes consumed by each DMA cycle; in this case 2 channels x 2 bytes.

The outer loop, `fdb0`, initializes the source address register, and DMA count register, then disables the histogram display interrupt, and arms the DMA controller. Then the DAS trigger is enabled by reading (using the 'in' command) from one of the locations assigned to the DAS interface; this sets up the DAS address register to select channel 1 for the first analog-to-digital conversion, and generates a "DReset" signal which arms the DAS.

The inner loop, `fdb1`, repeatedly examines the DMA count register to see if it has counted down to zero, which indicates that all channels have been digitized and stored. Then the keyboard input buffer is examined (a very hardware specific bit of code), to see if a key has been pressed; if so, it is acted upon, and the inner loop is resumed.

When the inner loop is finished, the new datum is used to update the internal histogram buffers, and the histogram display spooler re-enabled to continue updating the display. If either the number of requested events has been acquired, or if the DMA buffer is now full, the loop exits, and control is returned to top-level. I have omitted some code which does cleaning up before the return.

#### **B.5.4: 80186 Timer**

The 80186 has three integrated timer/event counters. As indicated elsewhere, I use one of these timers to generate the pulses which provide the analog-to-digital converter "start" signal for each event. Setting up the timer requires only setting a few registers as appropriate, as is shown in Figure B.13:

```

;; Timer control block base address & offsets

TIMER0_CB_BASE      equ    0ff50h

TCBO_HI_TIME        equ    2      ; when in alternate mode
TCBO_LO_TIME        equ    4
TCBO_CW              equ    6      ; control word

;; Timer control word bits

TCWB_EN              equ    8000h   ; enable timer
TCWB_NOT_INH         equ    4000h   ; enable change to EN
TCWB_ALT              equ    0002h   ; alternate mode
TCWB_CONT             equ    0001h   ; continuous run

TIMER0_CW            equ    TCWB_EN + TCWB_NOT_INH + TCWB_ALT + TCWB_CONT

;; Slicer clock is 6 Mhz; clock ticks are at 1/4 cpu rate
;; so each clock tick is 2/3 usec. 50 usec cycle = 75 clock ticks

TIMER0_LO_TIME       equ    22      ; 15 usec
TIMER0_HI_TIME       equ    53      ; 35 usec

        cseg    $          ; Code Segment

SETUP_TIMER0:
        mov     ax, TIMER0_LO_TIME
        mov     dx, TIMER0_CB_BASE + TCBO_LO_TIME
        out     dx, ax

        mov     ax, TIMER0_HI_TIME
        mov     dx, TIMER0_CB_BASE + TCBO_HI_TIME
        out     dx, ax

        mov     ax, TIMER0_CW
        mov     dx, TIMER0_CB_BASE + TCBO_CW
        out     dx, ax

        ret

```

*Figure B.13: AQ source code for setting up 50  $\mu$ sec clock*



*Appendix C***Media & Apparatus**

---

**DIW: De-Ionized Water**

Cambridge city tap water, pre-filter with Fulflo wound-cotton cartridge filter, and then processed by Nanopure II de-ionizer (Barnstead). Four treatment cartridges were used: (i) Organic/colloid removal (Barnstead #D0835), (ii) Hi-capacity de-ionizer (#D0803), and (iii & iv) Ultrapure de-ionizers (#D0809). A 0.2  $\mu\text{m}$  final filter (#D3749) was used to sterilize the water.

**PB: Phosphate Buffer 10mM, pH 7.0**

In a 2 L volumetric flask, dispense ~1.5 L DIW, then mix in:

1.40 g sodium phosphate, dibasic

1.40 g sodium phosphate, monobasic

Add DIW to 2.0 L, dispense to 150 ml medium bottles & autoclave.

**YNBD: Yeast Nitrogen Base Dextrose x10 concentrate**

In a 100 ml volumetric flask, dispense ~70 ml DIW, then mix in:

0.67 g YNB (Difco 0392-15-9)

0.50 g dextrose

Add DIW to 100 ml, gently warm to dissolve dextrose if needed. Filter sterilize with 0.2  $\mu\text{m}$  filter (Nalgene 120-0020), and dispense to six 15 ml sterile tubes, *e.g.* polystyrene centrifuge tubes. To use: mix 1 part YNBDx10 + 9 parts Phosphate Buffer.

**YPD: Yeast extract - Peptone - Dextrose**

In a 1 L Erlenmeyer flask, dispense ~800 ml DIW, then mix in:

10 g Yeast extract (Difco 0127-01)

20 g Peptone (Difco 0118-01-8)

20 g Dextrose

Add DIW to 1 L, gently stirring and heating if needed, to dissolve dextrose. Dispense to 150 ml medium bottles & autoclave for 15 min at 15psi (250°C); too hot or too long will caramelize the dextrose. For YPD agar plates, add 30 g/L agar (Difco 0140-01) and a magnetic stir bar to the Erlenmeyer flask. After autoclaving, stir *gently* with the stir bar, otherwise the YPD will froth and make it harder to pour plates. (This is due to the same surfactant that makes YPD good for GMD preparation.) While mixing, cool the flask with damp paper towels. When the flask is cool enough to handle, pour into plates, to a depth of about 0.5 to 1 mm.

**YM : Yeast Morphology broth**

In a 1 L Erlenmeyer flask, dispense ~800 ml DIW, then mix in 21 g YM (Difco 0711-01). Add DIW to 1 L, dispense to 150 ml medium bottles and autoclave. For YM agar plates, add 30 g/L agar (Difco), and proceed as indicated for YPD agar plates, above.

**Apparatus** - see also Appendix A (GMD protocol)

- Spectrophotometer: Bausch & Lomb Spectronic-20
- Glass test tube *cum* spectrophotometry cuvette: 13x100 mm borosilicate test tube, VWR# 60824-568
- Culture tube: 15 ml clear "orange-cap" polystyrene centrifuge tube (Corning) *or* 50 ml "blue-cap" polypropylene (Becton-Dickinson).

---

*Appendix D***The Diffusion Equation**

---

In this appendix, I will outline a solution for the diffusion equation for spherical geometries. The solutions presented here describe the graphs in Chapter 2 showing the evolution of the concentration profiles in gel slabs and droplets, in response to a step-change in concentration in the bathing medium. I include this derivation not because it is novel, but because it is non-obvious. Further I wish to promote analytic solutions where possible, and delay for a day or two the moment when numerical methods make them completely obsolete.

**Rectangular Geometry**

First, we consider the well known case of diffusion in rectangular coordinates, with the constraint that the concentration,  $c(x,y,z,t)$ , only varies in one dimension. This is illustrated in Chapter 2, Figure 2.1. The solution we seek is  $c(x,t)$ , and the diffusion equation simplifies, thus:

$$\frac{\partial c}{\partial t} = D \nabla^2 c(x,y,z,t) = D \frac{\partial^2 c}{\partial x^2}, \quad 0 < x < L$$

with the boundary conditions:

$$c(L,t) = C_0 \text{ (constant)}$$

$$\frac{\partial c}{\partial x} = 0 \text{ at } x = 0,$$

and the initial condition:

$$c(x,0) = 0$$

The well-known method for solving this equation is the method of separation of variables, which can be found in any differential equation text<sup>108</sup>. The strategy is to assume that  $c(x,t)$  has the form:

$$c(x,t) = X(x) T(t)$$

Upon substitution into the differential equation, and algebraic manipulation, one obtains two differential equations, related by a constant separation parameter,  $\sigma$ :

$$\begin{aligned} X'' - \sigma X &= 0 \\ T' - D\sigma T &= 0 \end{aligned}$$

The first equation is second order, so its solution has the form of a linear combination of sinusoids. However, the boundary conditions eliminate all terms except those having the form:  $\cos(n+1/2)\pi x/L$ . The second equation, being first order, has an exponential solution; the particular form is derived by applying the initial condition, and substituting for the separation parameter,  $\sigma$ .

A complete derivation is given by Carslaw and Jaeger<sup>109</sup>, unfortunately out of print. The analytic solution is:

$$\frac{c(\xi,\tau)}{C_0} = 1 - \frac{2}{\pi} \sum_{n=0}^{\infty} \frac{(-1)^n}{n+1/2} e^{-(n+1/2)^2 \pi^2 \tau} \cos(n+1/2)\pi \xi$$

$$\text{where: } \xi = \frac{x}{L} \quad \text{and: } \tau = \frac{L^2 t}{D}$$

This equation was used to generate the family of curves depicting the evolution of the concentration profile for rectangular geometry, in Chapter 2, Figure 2.1.

### Spherical Geometry

Next, we consider the case of diffusion in a spherical geometry. In particular, we consider the case shown in Chapter 2, Figure 2.1, where spherical symmetry is assumed. As expected, the approach is to solve the diffusion equation in spherical coordinates, *i.e.* solving for  $c(r, \phi, \theta, t)$ . Under the symmetry assumption, the concentration is assumed to be independent of the angular co-ordinates, and only vary radially. Thus, the solution we seek is  $c(r, t)$ , where  $r$  is the radial co-ordinate indicated in Figure 2.1. Of course, we must map the diffusion equation to spherical co-ordinates, but once again, it simplifies:

$$\frac{\partial c}{\partial t} = D \nabla^2 (r, \phi, \theta, t) = D \frac{1}{r^2} \frac{\partial}{\partial r} \left[ r^2 \frac{\partial c}{\partial r} \right] \quad 0 < r < R$$

with the boundary condition:

$$c(R, t) = C_0 \text{ (constant)}$$

and the initial condition:

$$c(r, 0) = 0$$

The method of separation of variables is also used here, but first a variable substitution is required:

$$u(r, t) = r c(r, t)$$

then the diffusion equation becomes:

$$\frac{\partial u}{\partial t} = D \frac{\partial^2 u}{\partial r^2}, \quad 0 < r < R$$

This, of course, has the same form as the rectangular case, and is solved in the same manner. We assume that  $u(r,t)$  has the form:

$$u(r,t) = R(r) T(t)$$

As before, substitution and algebraic manipulation yields a second order differential equations for  $R(r)$ , and a first order equation for  $T(t)$ . The boundary conditions on eliminate from  $R(r)$  all terms except those having the form:  $\sin(n\pi r/R)$ . The second equation has an exponential solution, again involving the the separation parameter,  $\sigma$ . The complete solution, as derived in Carslaw and Jaeger<sup>109</sup> (p233) is:

$$\frac{c(\rho,\tau)}{C_0} = 1 + \frac{2}{\pi} \sum_{n=1}^{\infty} \frac{(-1)^n}{n} e^{-n^2\pi^2\tau} \frac{\sin n\pi\rho}{R}$$

$$\text{where: } \rho = \frac{r}{R} \quad \text{and: } \tau = \frac{R^2 t}{D}$$

This equation was used to generate the family of curves depicting the evolution of the concentration profile for spherical geometry, in Chapter 2, Figure 2.1.

---

## REFERENCES

---

1. Wright, K., "The Policy Response: In Limbo," *Science* **249** p. 24 (1990).
2. Wright, K., "Bad News Bacteria," *Science* **249** pp. 22-24 (1990).
3. Finland, M., "Emergence of Antibiotic Resistance in Hospitals, 1935-1975," *Rev. Infectious Dis.* **1** pp. 4-21 (1979).
4. Wenzel, R. P., "Infection Control Priorities in Critical Care Medicine: Device-Associated Intravascular Infections," pp. 123-128 in *Manual of Clinical Microbiology, Fourth Edition*, ed. E. H. Lennette, American Society for Microbiology, Washington, D.C. (1985).
5. Musial, C. A., III, F. R. Cockerill, and Roberts, G. D., "Fungal Infections of the Immuno-compromised Host: Clinical and Laboratory Aspects," *Clin. Microbiol. Revs.* **1** pp. 349-364 (1988).
6. Thornsberry, C. and Sherris, J. C., "Laboratory Tests in Chemotherapy: General Considerations," pp. 959-966 in *Manual of Clinical Microbiology, Fourth Edition*, ed. E. H. Lennette, American Society for Microbiology, Washington (1985).
7. Tsien, H. C., Bratina, B. J., Tsuji, K., and Hanson, R. S., *App. Env. Microbiol.* 1990.
8. Halbert, D. N., "DNA Probes for the Detection of Antibiotic Resistance Genes," *Clin. Microbiol. Newsletter* **10** pp. 33-37 (1988).
9. "Laboratory Tests in Chemotherapy: Susceptibility Tests - Agar Dilution," pp. 967-971 in *Manual of Clinical Microbiology, Fourth Edition*, ed. E. H. Lennette, American Society for Microbiology, Washington, D.C. (1985).
10. Jones, R. N., Barry, A. L., Gavan, T. L., and II, J. A. Washington, "Susceptibility Tests: Microdilution and Macrodilution Broth Procedures," pp. 972-977 in *Manual of Clinical Microbiology, Fourth Edition*, ed. E. H. Lennette, American Society for Microbiology, Washington, D.C. (1985).
11. Lampe, M. F., Aitken, C. F., Dennis, P. G., Forsythe, P. S., Patrick, K. E., Schoen-necht, F. D., and Sherris, J. C., *Relationship of Early Readings of Minimum Inhibitory Concentrations to the Results of Overnight Tests Antimicrob. Agents Chemother.* 1975.
12. Barry, A. L. and Thornsberry, C., "Susceptibility Tests: Diffusion Test Procedure," pp. 978-987 in *Manual of Clinical Microbiology, Fourth Edition*, ed. E. H. Lennette, American Society for Microbiology, Washington, D.C. (1985).

## References

13. Hattori, T., *The Viable Count: Quantitative and Environmental Aspects*, Brock/Springer, Madison (1988).
14. Tawfik, O. W., Papasian, C. J., Dixon, A. Y., and Potter, L. M., "Saccharomyces cerevisiae Pneumonia in a Patient with Acquired Immune Deficiency Syndrome," *J. Clin. Microbiol.* **27** pp. 1689-1691 (1989).
15. Guinet, R., Chanas, J., Goullier, A., Bonnefoy, G., and Ambroise-Thomas, P., "Fatal septicemia due to Amphotericin-B resistant *Candida lusitanae*," *J. Clin. Microbiol.* **18** pp. 443-444 (1983).
16. Shadomy, S., Espinel-Ingroff, A., and Cartwright, R. Y., "Laboratory Studies with Antifungal Agents: Susceptibility Tests and Bioassays," pp. 991-999 in *Manual of Clinical Microbiology, 4th Ed.*, ed. E. H. Lennette, American Society for Microbiology, Washington, D.C. (1985).
17. Thornsberry, C., "Automated Procedures for Antimicrobial Susceptibility Tests," pp. 1015-1022 in *Manual of Clinical Microbiology, Fourth Edition*, ed. E. H. Lennette, American Society for Microbiology, Washington, D.C. (1985).
18. Fling, M. E., Walton, L., and Elwell, L. P., "Monitoring of Plasmid-Encoded, Trimethoprim-Resistant Dihydrofolate Reductase Genes; Detection of a New Resistant Enzyme," *Antimicrob. Agents Chemother.* **22** pp. 882-888 (1982).
19. Zwadyk, P., "DNA Probes: Reality or Glitter and Hype?," *Clin. Microbiol. Newslett.* **11** pp. 84-86 (1989).
20. Tenover, F. C., "Studies of Antimicrobial Resistance Genes using DNA Probes," *Antimicrob. Agents Chemother.* **29** pp. 721-725 (1986).
21. Bauer, A. W., Kirby, W. M. M., Sherris, J. C., and Turck, M., "Antibiotic Susceptibility Testing by a Standardized Single Disk Method," *Am. J. Clin. Pathol.* **45** pp. 493-496 (1966).
22. Shapiro, H. M., *Practical Flow Cytometry, Second Edition*, A. R. Liss, New York (1988).
23. Drake, A. W., "Transforms and Some Applications to Sums of Independent Random Variables," pp. 37-122 in *Fundamentals of Applied Probability Theory*, McGraw-Hill Inc, New York (1967).
24. Dean, A.C.R. and C., Hinshelwood, Sir, *Growth, Function and Regulation in Bacterial Cells*, Oxford at the Clarendon Press, Oxford (1966).
25. Kierstan, M. P. and Coughlan, M. P., "Immobilization of Cells and Enzymes by Gel Entrapment," in *Immobilised Cells and Enzymes, a Practical Approach*, ed. J. Woodward, IRL Press, Oxford (1985).
26. Mitenyi, S., Müller, W., Weichel, W., and Radbruch, A., "High Gradient Magnetic Cell Separation with MACS," *Cytometry* **11** pp. 231 - 238 (1990).



27. Rotman, B., "Measurement of Activity of Single Molecules of  $\beta$ -D-Galactosidase," *PNAS* 47 pp. 1981 - 1991 (1961).
28. Rotman, M. B., "Partial Loss of Activity of Individual Molecules of Aged Galactosidase," pp. 279 - 289 in *The Galactose Operon*, ed. J. R. Beckwith and D. Zipser, Cold Spring Harbor (1970).
29. Nilsson, K., Birnbaum, S., Flygare, S., Linse, L., Schroder, U., Jeppsson, U., Larsson, P.-O., Mosbach, K., and Brodelius, P., "A General Method for the Immobilization of Cells with Preserved Viability," *Eur. J. Appl. Microbiol. Biotechnol.* 17 pp. 319 - 326 (1983).
30. Scheirer, W., Nilsson, K., Meront, O. W., Katinger, H. W., and Mosbach, K., "Entrapment of Animal Cells for the Production of Biomolecules such as Monoclonal Antibodies," *Dev. Biol. Stand.* 55 pp. 155-161 (1984).
31. Rose, S., *Method for Isolating Cells*, European Patent Application, Application No. 83307144.2 Filed Nov. 22, 1983.
32. Rose, S., *Isolation and Culture of Mammalian Cells Secreting Acetylcholinesterase and Recovery of Acetylcholinesterase Therefrom*, European Patent Application, Application No. 8430036.3 Filed Jan. 20, 1984.
33. Lim, F. and Sun, A. M., "Microencapsulated Islets as Bioartificial Endocrine Pancreas," *Science* 210 pp. 908 - 910 (1980).
34. Lim, F., "Microencapsulation of Living Cells and Tissues: 1983 Review and Update," *Appl. Biochem Biotechnol.* 10 pp. 81-85 (1984).
35. Gin, H., Dupuy, B., and Baquey, C., and Aubertin, J., "Agarose Encapsulation of Islets of Langerhans: Reduced Toxicity in vitro," *J. Microencapsulation* 4 pp. 39-242 (1987).
36. Perlman, D., *Methods for Isolating Mutant Microorganisms from Parental Populations*, U.S. Patent, No. 4,649,109 March 10, 1987.
37. Brodelius, P., "Immobilized Plant Cells: Preparation and Biosynthetic Capacity," in *Immobilised Cells and Enzymes, a Practical Approach*, ed. J. Woodward, IRL Press, Oxford (1985).
38. Brodelius, P. and Nilsson, K., "Entrapment of Plant Cells in Different Matrices," *FEBS Let* 122 pp. 312-316 (1980).
39. Linsefors, L. and Brodelius, P., "Immobilization of Plant Protoplasts: Viability Studies," *Plant Cell Rep.* 4 pp. 23-27 (1985).
40. Christou, P., Murphy, J. E., and Swain, W. F., "Stable Transformation of Soybean by Electroporation and Root Formation From Transformed Callus," *Proc. Natl. Acad. Sci.*, pp. 3962-3966 (1987).

41. Lih, M. M.-S., "Biomedical Applications," pp. 184-283 in *Transport Phenomena in Medicine and Biology*, J. Wiley & Sons, New York (1975).
42. Cantor, C. R. and Schimmel, P. R., *Biophysical Chemistry*, W. H. Freeman and Company, San Francisco (1980).
43. Guiseley, K. B., "Chemical and Physical Properties of Algal Polysaccharides Used for Cell Immobilization," *Enzyme Microb. Technol.* 11 pp. 706-716 (1989).
44. Brodelius, P., *Ann. N.Y. Acad. Sci.* 434 pp. 382-393 (1984).
45. Dalili, M. and Chau, P. C., *Appl. Microbiol. Biotechnol.* 26 pp. 500-506 (1987).
46. Yeoman, M. M, Miedzybrodzka, M. B., Lindsey, K., and McLauchlan, W. R., pp. 327-343 in *Plant Cell Cultures: Results and Perspectives*, Elsevier, Amsterdam (1980).
47. Arnott, S., Fulmer, A., Scott, W. E., Dea, I. C. M., Moorehouse, R., and Rees, D. A., "The Agarose Double Helix and its Function in Agarose Gel Structure," *J. Mol. Biol.* 90 pp. 269-284 (1974).
48. Guiseley, K.B., "The Relationship Between Methoxyl Content and Gelling Temperature of Agarose," *Carbohydr. Res.* 13 pp. 247-256 (1970).
49. Guiseley, K.B., *Modified Agarose and Agar and Method of Making Same*, U. S. Patent 3,956,273 (1976).
50. Serwer, P., Allen, J. L., and Hayes, S. J., "Agarose Gel Electrophoresis of Bacteriophages and Related Particles, III. Dependence of Gel Sieving on the Agarose Preparation," *Electrophoresis* 4 pp. 232-236 (1983).
51. "Chemistry and Properties of Agarose," pp. 63,65 in *The Agarose Source Book*, FMC BioProducts, Rockland, ME (1988). Figures 10,11
52. "Applications of Agarose: Nucleic Acids," pp. 73 in *The Agarose Source Book*, FMC BioProducts, Rockland, ME (1988). Figure 1
53. "Low Gelling/Melting Temperature Agarose," pp. 26,29 in *The Agarose Source Book*, FMC BioProducts, Rockland, ME (1988).
54. FMC, personal communication
55. Rees, D. A., Morris, E. A., Thom, D., and Madden, J. K., in *The Polysaccharides, Vol 1*, ed. G. O. Aspinall, Academic Press, New York and London (1982).
56. Nakajima, H., Sonomoto, K., Usui, N., Sato, F., Yamada, Y., Tanaka, A., and Fukui, S., *J. Biotechnology* 2 pp. 107-117 (1985).
57. Brodelius, P. and Nilsson, K., *FEBS Let.* 122 pp. 312-316 (1986).

58. Nilsson, K., Scheirer, W., Katlinger, H. W. D., and Mosbach, K., "Entrapment of Animal Cells," pp. 399 - 410 in *Methods in Enzymology*, Academic Press, London (1987).
59. Blin, N., Gabain, A. V., and Bujard, H., "Isolation of large molecular weight DNA from agarose gels for further digestion by restriction enzymes," *FEBS Letters* **53** pp. 84-86 (1975).
60. Vogelstein, B. and Gillespie, D., "Preparative and analytical purification of DNA from agarose," *Proc. Natl. Acad. Sci.* **76** pp. 615-619 (1979).
61. "Matrix Preparations and Applications," in *Affinity Chromatography - a Practical Approach*, ed. P. D. G. Dean, W. S. Johnson and F. A. Middle, IRL Press, Oxford (1985).
62. Hansson, H. A. and Kagedal, D. L., *Medium for Isoelectric Focusing*, US Patent 4,312,739 1982.
63. Cook, R. B. and Witt, H. J., *Agarose Composition, Aqueous Gel and Method of Making Same*, US Patent 4,290,911 1981.
64. Tamponnet, C., Constantino, F., Barbotino, J., and Calvayrac, R., *Physiol. Plant.* **1963** pp. 277-283 (1985).
65. Bridson, E. Y., "Natural and Synthetic Culture Media for Bacteria," pp. 124-129 in *Culture Media for Microorganisms and Plants. CRC Handbook Series in Nutrition and Food, Section G, Vol. III*, ed. M. Rechigl, CRC Press, Cleveland OH (1978).
66. Hanus, F. J., Sands, J. G., and Bennett, E. O., "Antibiotic Activity in the Presence of Agar," *Appl. Microbiol.* **15** pp. 31-34 (1967).
67. Ho, W. C. and Ko, W. H., "Agarose Medium for Bioassay of Antimicrobial Substances," *Phytopathology* **70** pp. 764-766 (1980).
68. Stellwagen, N. C., "Effect of the Electric Field on the Apparent Mobility of Large DNA Fragments in Agarose Gels," *Biopolymers* **24** pp. 2243-2255 ( ).
69. Morris, E. R., Rees, D. A., and Robinson, G., *J. Mol. Biol.* **138** pp. 349-362 (1980).
70. Hulst, A. C. and Tramper, J., "Immobilized Plant Cells: A Literature Survey," *Enzyme Microb. Technol* **11** pp. 546-558 (1989).
71. Furuya, T., Yoshikawa, T., and Taira, M., *Phytochemistry* **23** pp. 999-1001 (1984).
72. Chevalier, P., Cosentino, G. P., Noue, J. de le, and Rakhit, S., *Biotechnol. Techniques* **18** pp. 189-196 (1983).
73. Hendrickx, M., Ooms, C., Engels, C., Pottelbergh, E. Van, and Tobback, P., *J. Food Sci* **52** pp. 1113-1114 (1987).
74. Hulst, A. C., Tramper, J., Riet, K. van't, and Westerbeek, J. M., *Biotechnol. Bioeng.* **27** pp. 870-876 (1985).

## References

75. Brodelius, P. and Mosbach, K., pp. 1-26 in *Advantage. Appl. Microbiology*, ed. A. I. Laskin, Academic Press, New York (1982).
76. Weaver, J. C., Seissler, P. E., Threefoot, S. A., Lorenz, J. W., Huie, T., Rodrigues, R., and Klivanov, A. M., "Microbiological Measurements by Immobilization of Cells within Small Volume Elements," *Ann. N.Y. Acad. Sci.* 434 pp. 363 - 372 (1984).
77. Sahar, E., Nir, R., and Lamed, R., *Flow Cytometric Analysis and Sorting of Bacterial Colonies*, (Late abstract for the XIV International Meeting of the Society for Analytical Cytology, March 18 - 23, Asheville, NC) 1990.
78. Powell, K. T., *Mammalian Cell Clonal Growth and Secretion Measurements Using Gel Microdroplets and Flow Cytometry*, Ph.D. Thesis, M.I.T. 1989.
79. Olson, R. J., Frankel, S. L., Chisholm, S. W., and Shapiro, H. M., "An Inexpensive Flow Cytometer for the Analysis of Fluorescence Signals in Phytoplankton: Chlorophyll and DNA Distributions," *J. Exp. Mar. Biol. Ecol.* 68 pp. 129 - 144 (1983).
80. Gray, M. L., *Negative Fluorescence: An Optical Flow Cytometric Technique for Cell Volume Determination*, M.S. Thesis, Massachusetts Institute of Technology 1981.
81. Kachel, V. and Menke, E., "Hydrodynamic Properties of Flow Cytometric Instruments," in *Flow Cytometry and Sorting*, ed. E. R. Melamed, P. F. Mullaney and M. L. Mendelsohn, Wiley, New York (1979).
82. Jett, J. H. and Alexander, R. G., "Droplet Sorting of Large Particles," *Cytometry* 6 pp. 484 - 486 (1985).
83. Freyer, J. P., Fillak, D., and Jett, J. H., "Use of Xantham Gum to Suspend Large Particles During Flow Cytometric Analysis and Sorting," *Cytometry* 10 pp. 803 - 806 (1989).
84. Steinkamp, J. A., Habbersett, R. C., and Martin, J. C., "Improved Method For Multicolor Fluorescence Detection Using Dichroic, Color-Separating Filters," *Cytometry Supp.* 4 p. 69 (1990). (Abstract) XIV International Meeting of the Society for Analytical Cytology
85. Hutter, K.-J. and Eipel, H. E., "Flow Cytometric Determinations of Cellular Substances in Algae, Bacteria, Moulds and Yeasts," *Antonie van Leeuwenhoek* 44 pp. 269-282 (1978).
86. Hutter, K.-J. and Eipel, H. E., "Microbial Determinations by Flow Cytometry," *J. General Microbiology* 113 pp. 369-375 (1979).
87. Sahar, E. and Cohen, C. Y., "Rapid Flow Cytometric Bacterial Detection and Determination of Susceptibility to Amikacin in Body Fluids and Exudates," *J. Clin. Microbiol.* 27 pp. 1250-1256 (1989).
88. Weaver, J. C., Williams, G. B., Powell, K. T., Bliss, J. G., and Harrison, G. I., *Gel Microdroplets with Enhanced Measurement Properties and Process for the Use Thereof*, (U.S. Patent Application; filed April 22, 1988)

89. Bartoletti, D. C., *Electroporative Uptake by Intact Yeast: pH Studies and Quantitative Measurement*, M.S. Thesis, Massachusetts Institute of Technology 1989.
90. Dillon, J. R., Nasim, A., and Nestmann, E. R., "Gel Electrophoresis," pp. 13-27 in *Recombinant DNA Methodology*, J. Wiley & Sons, New York (1985).
91. Gaugain, B., Barbet, J., Capelle, N., Roques, B. P., and Pecq, J-B. Le, "DNA Bifunctional Intercalators. 2. Fluorescence Properties and DNA Binding Interaction of an Ethidium Homodimer and an Acridine Ethidium Heterodimer," *Biochemistry* 17 pp. 5078 - 5088 (1978).
92. Laugaa, P. and al., et., "Comparative Binding of Ethidium and Three Azido Analogs to Dinucleotides: Affinity and Intercalation Geometry. A Proton NMR And Visible Spectroscopy Study," *Eur. J. Biochem.*, ().
93. Weaver, J. C., Bliss, J. G., Powell, K. T., Harrison, G. I., and Williams, G. B., *Clonal Growth Measurements at the Single-Cell Level Using Flow Cytometry and Gel Microdroplets*, (submitted)
94. Haugland, R. P., *Handbook of Fluorescent Probes and Research Chemicals*, Molecular Probes, Junction City, OR (1985).
95. Salzman, G., Mullaney, P. F., and Price, B. J., "Light-Scattering Approaches to Cell Characterization," in *Flow Cytometry and Sorting*, ed. E. R. Melamed, P. F. Mullaney and M. L. Mendelsohn, Wiley, New York (1979).
96. Edberg, S. C. and Berger, S. A., "The Photometric Analysis of Microbial Growth for the Identification and Antimicrobial Susceptibility Testing of Bacterial Pathogens," pp. 215 - 221 in *Rapid Methods and Automation in Microbiology and Immunology*, ed. K. O. Habermehl, Springer-Verlag, Berlin (1985).
97. Koch, A. L., "Turbidity Measurements in Microbiology," *ASM News* 50:10 pp. 473-477 (1984).
98. Davis, B. D., Dulbecco, R., Eisen, H. N., and Ginsberg, H. S., "Bacterial Growth and Nutrition," pp. 60-70 in *Microbiology, Third Edition*, Harper and Row, Hagerstown, MD (1980).
99. Gray, J. W., Dean, P. N., and Mendelsohn, M. L., "Quantitative Cell-Cycle Analysis," in *Flow Cytometry and Sorting*, ed. E. R. Melamed, P. F. Mullaney and M. L. Mendelsohn, Wiley, New York (1979).
100. Atlas, R. M., "Antifungal Agents," pp. 546-547 in *Microbiology: Fundamentals and Applications*, Macmillan, New York (1984).
101. Nir, R., Lamed, R., Gueta, L., and Sahar, E., "Single-Cell Entrapment and Microcolony Development Within Uniform Microspheres Amenable to Flow Cytometry," *Appl. Env. Microbiol.* 56 pp. 2870-2875 (1990).
102. Williams, G. B., Weaver, J. C., and Demain, A. L., "Rapid Microbial Detection and Enumeration Using Gel Microdroplets: Colorimetric versus Fluorescent Indicator Systems," *J. Clin. Microbiol.* 28 pp. 1002 - 1008 (1990).

## References

103. Powell, K. T. and Weaver, J. C., "Gel Microdroplets and Flow Cytometry: Rapid Determination of Antibody Secretion by Individual Cells within a Cell Population," *Bio/Technology* 8 pp. 333 - 337 (1990).
104. Monoclonal Antibodies and Immunological Reagents (Catalog). Chemicon International. Temecula, CA. (1990)
105. Roman, P. J., *A High-Speed Data Acquisition System for Multi-Station Flow Cytometry*, M.S. Thesis, Dept. of Electrical Engineering & Computer Science, MIT (unpublished) 1988.
106. *Don't Trade Off Analog Switch Specs. VMOS - A Solution to High Speed, High Current, Low resistance Analog Switches.*, Siliconix Application Note, AN77-2
107. *Using Power MOSFET Transistors to Interface From IC Logic to High Power Loads*, Siliconix Application Note, AN79-6
108. Boyce, W. E. and DiPrima, R. C., "Heat Conduction and Separation of Variables," pp. 453-460 in *Elementary Differential Equations and Boundary Value Problems, 3rd Edition*, John Wiley, New York (1977).
109. Carslaw, H. S. and Jaeger, J. C., *Conduction of Heat in Solids, 2nd Ed.*, Oxford Univ. Press (1959).